

AN OVERVIEW OF DETECTION IN MIMO RADAR

A THESIS SUBMITTED TO
THE GRADUATE SCHOOL OF NATURAL AND APPLIED SCIENCES
OF
MIDDLE EAST TECHNICAL UNIVERSITY

BY

ŞAFAK BİLGİ AKDEMİR

IN PARTIAL FULLFILMENT OF THE REQUIREMENTS
FOR
THE DEGREE OF MASTER OF SCIENCE
IN
ELECTRICAL AND ELECTRONICS ENGINEERING

SEPTEMBER 2010

Approval of the thesis:

AN OVERVIEW OF DETECTION IN MIMO RADAR

submitted by **ŞAFAK BİLGİ AKDEMİR** in partial fulfillment of the requirements for the degree of **Master Of Science in Electrical and Electronics Engineering Department, Middle East Technical University** by,

Prof. Dr. Canan Özgen
Dean, Graduate School of **Natural and Applied Sciences** _____

Prof. Dr. İsmet Erkmén
Head of Department, **Electrical and Electronics Eng. Dept.** _____

Assoc. Prof. Dr. Çağatay Candan
Supervisor, **Electrical and Electronics Eng. Dept., METU** _____

Examining Committee Members:

Prof. Dr. Mete Severcan
Electrical and Electronics Engineering Dept., METU _____

Assoc. Prof. Dr. Çağatay Candan
Electrical and Electronics Engineering Dept., METU _____

Prof. Dr. Buyurman Baykal
Electrical and Electronics Engineering Dept., METU _____

Assoc. Prof. Dr. Tolga Çilođlu
Electrical and Electronics Engineering Dept., METU _____

Dr. Alper Yıldırım
TÜBİTAK UEKAE / İLTAREN _____

Date: 17.09.2010

I hereby declare that all information in this document has been obtained and presented in accordance with academic rules and ethical conduct. I also declare that, as required by these rules and conduct, I have fully cited and referenced all material and results that are not original to this work.

Name, Last Name : Şafak BİLGİ AKDEMİR

Signature :

ABSTRACT

AN OVERVIEW OF DETECTION IN MIMO RADAR

Bilgi Akdemir, Şafak

M. Sc., Department Of Electrical and Electronics Engineering

Supervisor: Assoc. Prof. Dr. Çağatay Candan

September 2010, 96 pages

In this thesis study, an overview of MIMO radar is presented. The differences in radar cross section, channel and received signal models in different MIMO radar configurations are examined. The performance improvements that can be achieved by the use of waveform diversity in coherent MIMO radar and by the use of angular diversity in statistical MIMO radar are investigated. The optimal detector under Neyman-Pearson criterion for Coherent MIMO radar when the interfering signal is white Gaussian noise is developed. Detection performance of phased array radar, coherent MIMO radar and Statistical MIMO radar are compared through numerical simulations. A detector for MIMO radar that contains the space time codes explicitly is also examined.

Keywords: Multiple Input Multiple Output (MIMO) Radar, Waveform Diversity, Angular Diversity, Space Time Coded Signals, Target Detection

ÖZ

ÇGÇÇ RADARLARDA HEDEF TESPİTİNE GENEL BAKIŞ

Bilgi Akdemir, Şafak

Yüksek Lisans, Elektrik ve Elektronik Mühendisliği

Tez Yöneticisi : Doç. Dr. Çağatay Candan

Eylül 2010, 96 sayfa

Bu tezde ÇGÇÇ radar konusu genel hatlarıyla sunulmuştur. Farklı ÇGÇÇ radar yapıları, radar kesit alanı, kanal ve alınan sinyal modelleri açısından incelenmiştir. Dalga biçimi çeşitliliğinin, evreuyumlu ÇGÇÇ radarda, açısal çeşitliliğin de istatistiksel ÇGÇÇ radarda kullanımlarıyla elde edilebilecek başarımların iyileştirilmeleri araştırılmıştır. Evreuyumlu ÇGÇÇ radar için Neyman-Pearson ölçütü altında ve beyaz Gaussian gürültünün varlığında optimal detektör geliştirilmiştir. Faz dizili, evreuyumlu ve istatistiksel ÇGÇÇ radarın hedef tespit başarımları karşılaştırılmıştır. Uzay zaman kodlarını açıkça içeren bir ÇGÇÇ radar detektörü ayrıca incelenmiştir.

Anahtar Kelimeler: Çok Girdili Çok Çıktılı (ÇGÇÇ) Radar, Dalga Biçimi Çeşitliliği, Açısal Çeşitlilik, Uzay Zaman Kodlu İşaretler, Hedef Tespiti

To My Mum,
and
To My Ögü

ACKNOWLEDGEMENTS

I would like to express my gratitude to my supervisor, Assoc. Prof. Dr. Çağatay Candan, for his valuable guidance, suggestions and insight throughout this thesis study.

I wish to express my gratitude to my team leader, Dr. Alper Yıldırım, at TUBİTAK UEKAE / İLTAREN for his support and encouragement at all phases of my graduate study. I would also like to thank my colleagues at work for the friendly working environment which increases my working motivation at all times.

I am especially indebted to my mum, not only for making the completion of this thesis possible by her excellent effort to look after my daughter, but also for her endless love, constant support, encouragement and trust on me throughout my life. I am also grateful to my dad for providing me the best possible education and his love.

I wish to express my deepest gratitude to my husband, Özgür, without his love, support and tolerance my graduate study would not have been possible.

Finally I would like to thank to my little daughter, Zeynep Işık, for her sweetness and her mem mems.

TABLE OF CONTENTS

| | |
|---|------|
| ACKNOWLEDGEMENTS | vii |
| TABLE OF CONTENTS..... | viii |
| LIST OF FIGURES | xi |
| CHAPTERS | |
| 1 INTRODUCTION | 1 |
| 2 OVERVIEW OF MIMO RADAR..... | 4 |
| 2. 1 Preliminaries..... | 4 |
| 2. 2 Multistatic Radar Systems..... | 6 |
| 2. 3 Phased Array Radar..... | 10 |
| 2. 3. 1 Signal Model | 12 |
| 2. 3. 2 Detection In Phased Array Radar | 15 |
| 2. 4 MIMO Radar | 17 |
| 2. 4. 1 Coherent MIMO Radar (MIMO Radar With Colocated Antennas)..... | 19 |
| 2. 4. 1. 1 Signal Model..... | 20 |
| 2. 4. 1. 2 Improvements That Coherent MIMO Radar Systems Offer | 23 |
| 2. 4. 1. 2. 1 Higher Resolution | 23 |
| 2. 4. 1. 2. 2 Parameter Identifiability | 25 |
| 2. 4. 1. 2. 3 Transmit Beampattern Synthesis | 26 |
| 2. 4. 1. 2. 4 Direct Application Of Adaptive Array Techniques | 29 |
| 2. 4. 1. 3 Detection In Coherent MIMO Radar | 29 |
| 2. 4. 2 Statistical MIMO Radar (MIMO Radar with Widely Separated Antennas)..... | 34 |

| | |
|---|-----------|
| 2. 4. 2. 1 Signal Model..... | 36 |
| 2. 4. 2. 2 Improvements That Statistical MIMO Radar Systems Offer | 42 |
| 2. 4. 2. 2. 1 Direction of Arrival Estimation | 42 |
| 2. 4. 2. 2. 2 Detection Performance..... | 42 |
| 2. 4. 2. 2. 3 Detection Performance in Clutter | 43 |
| 2. 4. 2. 2. 4 Moving Target Detection Performance | 43 |
| 2. 4. 2. 3 Detection In Statistical MIMO Radar..... | 44 |
| 2. 4. 3 Phased-MIMO Radar [27]..... | 47 |
| 3 DETECTION IN MIMO RADAR USING SPACE TIME CODED WAVEFORMS | 51 |
| 3. 1 Signal Model [28]..... | 52 |
| 3. 2 Detection in MIMO Radar Using STC Waveforms..... | 55 |
| 3. 2. 1 Full Rank Code Matrix | 57 |
| 3. 2. 1. 1 Case 1: $N \geq Mt$:..... | 57 |
| 3. 2. 1. 2 Case 2: $N \leq Mt$ | 61 |
| 3. 2. 2 Rank 1 Code Matrix | 63 |
| 3. 2. 3 Detection of Moving Targets..... | 64 |
| 3. 3 Optimization of Space Time Codes [9],[28] | 67 |
| 4 SIMULATION RESULTS | 69 |
| 4. 1 Detection in Coherent MIMO Radar..... | 69 |
| 4. 2 Detection in Statistical MIMO Radar..... | 74 |
| 4. 3 Detection in STC MIMO Radar | 77 |
| 4. 3. 1 Simulations for Stationary Target | 78 |
| 4. 3. 1. 1 MISO System..... | 78 |
| 4. 3. 1. 1. 1 $N \geq Mt$ Case | 78 |
| 4. 3. 1. 1. 2 $N \leq Mt$ Case | 80 |

| | |
|---|----|
| 4. 3. 1. 2 MIMO System | 82 |
| 4. 3. 1. 2. 1 $N \geq Mt$ Case | 82 |
| 4. 3. 1. 2. 2 $N \leq Mt$ Case | 86 |
| 4. 3. 2 Simulations for Moving Target | 89 |
| 5 CONCLUSION AND FUTURE WORK..... | 91 |
| REFERENCES..... | 94 |

LIST OF FIGURES

FIGURES

| | |
|--|----|
| Figure 2-1 Multistatic Radar System Configuration 1 (Multiple Bistatic Case) | 7 |
| Figure 2-2 Multistatic Radar System Configuration 2 (Multiple Monostatic Case). 8 | |
| Figure 2-3 Multistatic Radar System Configuration 3 (Fully Multistatic Case)..... | 8 |
| Figure 2-4 Phased Array Radar Configuration | 11 |
| Figure 2-5 Receiver Structure of MIMO Radar | 18 |
| Figure 2-6 Coherent MIMO Radar Configuration | 19 |
| Figure 2-7 Virtual Receiver Array Configuration – The Worst Case [20] | 24 |
| Figure 2-8 Virtual Receiver Array Configuration – The Best Case [20]..... | 25 |
| Figure 2-9 Statistical MIMO Radar Configuration 1 | 35 |
| Figure 2-10 Statistical MIMO Radar Configuration 2 | 37 |
| Figure 2-11 Transmit Array Structure Of Phased-MIMO Radar | 48 |
| Figure 3-1 STC MIMO Radar Configuration [28]..... | 52 |
| Figure 3-2 The visualization of Equation (3-7)..... | 54 |
| Figure 4-1 Coherent MIMO Radar, Changing M_t | 70 |
| Figure 4-2 Phased Array Radar, Changing M_t | 71 |
| Figure 4-3 Coherent MIMO Radar, Changing M_r | 72 |
| Figure 4-4 Phased Array Radar, Changing M_r | 72 |
| Figure 4-5 ROC of Coherent MIMO and Phased Array Radar | 73 |
| Figure 4-6 Statistical MIMO Radar, Changing M_t | 74 |
| Figure 4-7 Statistical MIMO Radar, Changing M_r | 75 |
| Figure 4-8 ROC of Statistical MIMO and Phased Array Radar, $M_t=2$, $M_r=2$ | 76 |
| Figure 4-9 ROC of Statistical MIMO and Coherent MIMO Radar, $M_t=2$, $M_r=2$.. | 77 |
| Figure 4-10 MISO Case, Full Rank, Changing M_t , Detector (3-35) | 79 |
| Figure 4-11 MISO Case, Full Rank, Changing M_t , Detector (3-47) | 80 |
| Figure 4-12 MISO Case, Full Rank, Changing N , $N=M_t$ | 81 |
| Figure 4-13 MISO Case, Full Rank, Transmit Power is Constant, Changing N , $N=M_t$ | 82 |
| Figure 4-14 MIMO Case, Full Rank, Changing M_r , Detector (3-35)..... | 83 |

| | |
|---|----|
| Figure 4-15 MIMO Case, $N \geq Mt$, Changing M_r , Detector (3-47) | 84 |
| Figure 4-16 The Detector in (2-101) vs the Detector in (3-35)..... | 85 |
| Figure 4-17 The Detector in (2-101) vs the Detector in (3-35), Normalized Power | 85 |
| Figure 4-18 MIMO Case, Full Rank, Changing M_r , Detector (3-47)..... | 86 |
| Figure 4-19 The Detector in (2-101) vs the Detector in (3-47), Normalized Power, $M_t = 4$, $M_r = 4$, $N = 2$ | 87 |
| Figure 4-20 The Detector in (2-101) vs the Detector in (3-47), Normalized Power, $M_t = 4$, $M_r = 4$, $N = 4$ | 88 |
| Figure 4-21 Detection Performance of Coded and Uncoded Signals | 88 |
| Figure 4-22 Moving Target, Changing N , $M_t=2$ | 89 |
| Figure 4-23 Moving Target, Changing M_t , $N=8$ | 90 |

CHAPTER 1

INTRODUCTION

The basic functions of radar are detection, parameter estimation and tracking [1], [2]. The most fundamental one among these functions is detection. Detection is the process of determining whether the received signal is an echo returning from a desired target or consists of noise only. The success of the detection process is directly related to SNR at the receiver and the ability of the radar to separate desired target echoes from unwanted reflected signals. So, various techniques are developed to maximize the SNR at the output of the receiver and to increase the ability of the radar to separate targets from unwanted echoes and interference.

After the detection process if it turns out that a target really exists, several parameters of the target like range, velocity and angle of arrival should be estimated from the received signal. The choice of the radar transmit waveform is a major contributor to the resolution of these parameters. Many types of waveforms can be found in the literature ([5], [6]), that improve the resolution of those parameters or other radar system performance metrics.

After localization of a target, radar can provide a target's trajectory and track it by predicting where it will be in the future by observing the target over time and using dedicated filters.

Some types of radar can perform more specialized tasks in addition to these basic functions. One of these tasks performed by more recent radars is imaging. High-resolution two or three dimensional maps of ground can be constructed by using this new technology.

Different types of antennas, transmitter, receiver structures and processing units are employed in radars according to their functions and on which platform the radar is located. The separation of antennas is also determined by radar's function. Conventional radar systems can be classified into three groups based on the number of antennas the system has and the distance between them. These are called monostatic, bistatic and multistatic systems [1]. Majority of radar systems are monostatic. In monostatic systems, transmitter and receiver antennas are co-located and usually there is only one antenna performing both transmitting and receiving tasks in a time multiplexed fashion. In bistatic systems, there are one transmitter and one receiver antenna, but they are significantly separated [2]. Multistatic radar systems have two or more transmitting or receiving antennas with all antennas separated by large distances when compared to the antenna sizes [3].

Recently, a new field of radar research called Multiple Input Multiple Output (MIMO) radar has been developed, which can be thought as a generalization of the multistatic radar concept. MIMO radar has multiple transmit and multiple receive antennas as its name indicates [9]. The transmit and receive antennas may be in the form of an array and the transmit and receive arrays can be co-located or widely separated like phased array systems. Although some types of MIMO radar systems resembles phased array systems, there is a fundamental difference between MIMO radar and phased array radar. The difference is that MIMO radar always transmits multiple probing signals, via its transmit antennas, that may be correlated or uncorrelated with each other, whereas phased array radars transmit scaled versions of a single waveform which are fully correlated. The multiple transmit and receive antennas of a MIMO radar system may also be widely separated as radar networks. The fundamental difference between a multistatic radar network and MIMO radar is that independent radars that form the network perform a significant amount of local processing and there exists a central processing unit that fuses the outcomes of central processing in a reasonable way. For example, every radar makes detection decisions locally then the central processing unit fuses the local detection decisions. Whereas MIMO radar uses all of the available data and jointly processes signals received at multiple receivers to make a single decision about the existence of the target.

The key ideas of MIMO radar concept has been picked up from MIMO communications. MIMO is a technique used in communications to increase data throughput and link range without additional bandwidth or transmit power. This is achieved by higher spectral efficiency and link reliability or diversity [25]. Using MIMO systems in communications made significant improvements when there is serious fading in the communication channel. Radar systems also suffer from fading when there are complex and extended targets. Researchers took the idea of using multiple transmit and receive antennas to overcome the effects of fading from communications and applied it in the field of radar to achieve performance improvements.

In this thesis, the two types of MIMO radar systems, namely coherent MIMO radar and statistical MIMO radar are investigated. The similarities and differences of these radar systems from conventional radar systems are explored. The performance improvements achieved by each type of MIMO radar system are summarized. An overview of a new field of MIMO radar research, namely phased MIMO radar, which is a hybrid of phased array radar and MIMO radar is also covered. The detectors for MIMO radars and phased array radar are provided and their detection performances are compared. New to this study, the detector for Coherent MIMO radar is developed and the detector for STC MIMO is extended to cover moving targets case.

The outline of the thesis is as follows: In Chapter 2, an overview of MIMO radar systems is presented. In Chapter 3, the detection process using space time coded waveforms is explored. In Chapter 4, the simulation results that compare the detection performance of different MIMO radar configurations are examined. Finally, in Chapter 5, conclusions derived from this study is presented along with a short summary.

CHAPTER 2

OVERVIEW OF MIMO RADAR

In this chapter, an overview of MIMO radar is presented. In Section 2. 1, definitions of some basic concepts in radar literature are presented. In Section 2. 2, Multistatic Radar Systems are examined, and in Section 2. 3 Phased Array Radars are covered to give the reader the opportunity to compare those systems with MIMO Radar. In Section 2. 4, the two types of MIMO radar, namely Coherent MIMO Radar and Statistical MIMO radar are investigated and the improvements achieved by those radar systems are presented. In Section 2. 4. 3, a more recent concept in MIMO radar, which is a hybrid of phased array radars and MIMO radar, is also introduced for the sake of completeness.

2. 1 Preliminaries

MISO : This abbreviation stands for Multiple Input Single Output. It describes the systems with multiple transmitters and a single receiver.

SIMO : This abbreviation stands for Single Input Multiple Output. It describes the systems with a single transmitter and multiple receivers.

MIMO: This abbreviation stands for Multiple Input Multiple Output. It describes the systems with multiple transmitters and multiple receivers.

Point Target (Scatterer) : A target whose largest physical dimension is small relative to the size of the radar resolution cell in range, angle or both is called point target [1]. Therefore, the target's individual scattering features are not resolved.

When the sensors of array radars are closely spaced and the range between the target and array is large relative to the extents of the target this target model is used.

Distributed Target (Scatterer): A target whose dimensions are large compared to the resolution cell is called distributed target [1], [2]. Therefore, the target's individual scattering characteristics are resolved. This model accounts for spatial characteristics of the target. When the spacing between the array elements is large, every element sees a different aspect of the target due to its complex shape. This model assumes a target composed of many small and finite number scatterers that are distributed over an area.

Extended Target (Scatterer) : A target that occupies more than one resolution cell is called extended target.

Simple Target : A target that has a simple geometrical shape is called simple target. For example, the sphere, cylinder, rod and cone are simple targets [1]. RCSs of even these simple targets change with aspect angle, polarization and frequency. One exception to this characteristic is sphere whose RCS is independent of aspect angle because of spherical symmetry.

Complex Target : A target that is made up of several scatterers is called complex target. A complex target can be either a point target or a distributed target [1]. In reality, all the targets such as aircraft, missiles, ships, ground vehicles and buildings are complex targets.

In the literature, a target whose RCS does not change with aspect angle is also called point target and complex targets are usually assumed to be composed of this kind of targets.

Frequency, polarization, aspect angle and range to the target determine the amount of energy reflected from the target [2]. Small changes in range or orientation can result in a large increase or decrease in the amount of energy reflected from the target. This change in the energy of the reflected signal is called *target fluctuation*. The term fading is also used in the literature to describe those fluctuations. Because of this complicated behavior, RCS of complex targets are modeled as a random variable with a specified probability density function. In addition to the probability

density function, correlation length in time, frequency and aspect angle of the target should be known. Correlation length determines how much change in time, frequency or angle is required to cause the returned echo amplitudes to decorrelate to a specified degree [2]. If the radar frequency is constant, decorrelation of RCS is induced by changes in range and aspect angle. In conventional radar systems, the range and aspect angle of the target changes in time as a result of the relative motion between the radar and the target. Swerling models are used to model fluctuations and they are a combinations of pdf and decorrelation time without any emphasis or constraint on aspect angle and frequency .

In [2], it is said that the amount of aspect angle rotation required to decorrelate the target echoes when the range to the target is much larger than the target extent can be estimated using the formula in (2-1)

$$\Delta\theta = \frac{\lambda}{2L} \quad (2-1)$$

where L denotes the extent of the target, and λ denotes the wavelength of the transmitted signal.

Uniform Linear Array (ULA): An antenna array is uniform if the separation between the elements is uniform.

Filled array: An array is called filled if the inter element spacing between array elements is half of the wavelength.

Sparse array: An array is called sparse if the inter element spacing between array elements is more than half of the wavelength.

2. 2 Multistatic Radar Systems

Radar systems that have two or more transmitting or receiving antennas with all antennas separated by large distances when compared to the antenna sizes are usually called multistatic radars. But there is no strict and single definition of multistatic radar systems.

Some sources define the radar systems that have only one transmitting and many spatially separated receiving stations as in Figure 2-1 as multistatic radar systems.

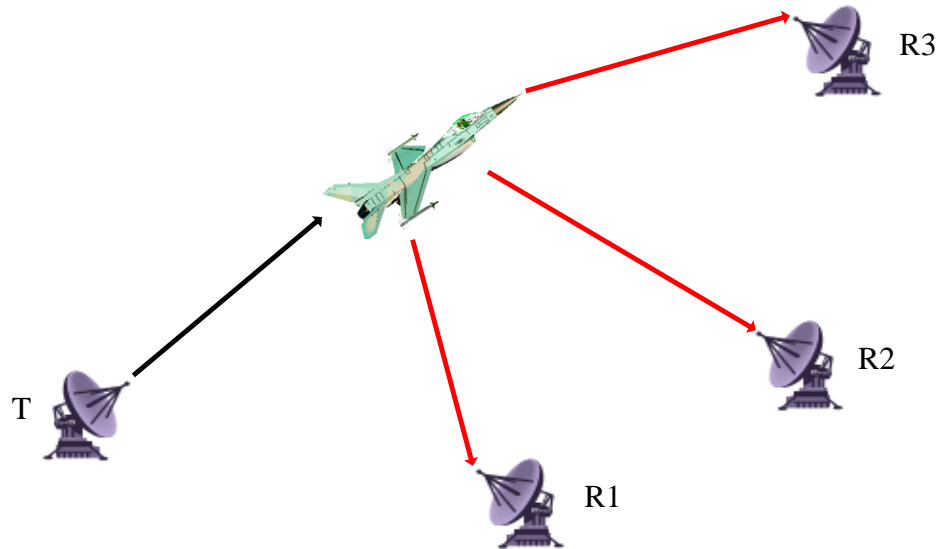


Figure 2-1 Multistatic Radar System Configuration 1 (Multiple Bistatic Case)

Some other sources define radar systems that have arbitrary systems of spatially separated radars where all the received information is fused and jointly processed as multiradar (or Netted Radar) systems [3]. Each of these spatially separated radars may operate in monostatic mode as in Figure 2-2 or in a full multistatic mode as in Figure 2-3. Some other sources define multiside radar systems covering both the multistatic and netted radar systems. A large amount of information about multistatic and multiside radar systems can be found in [3] and [7].

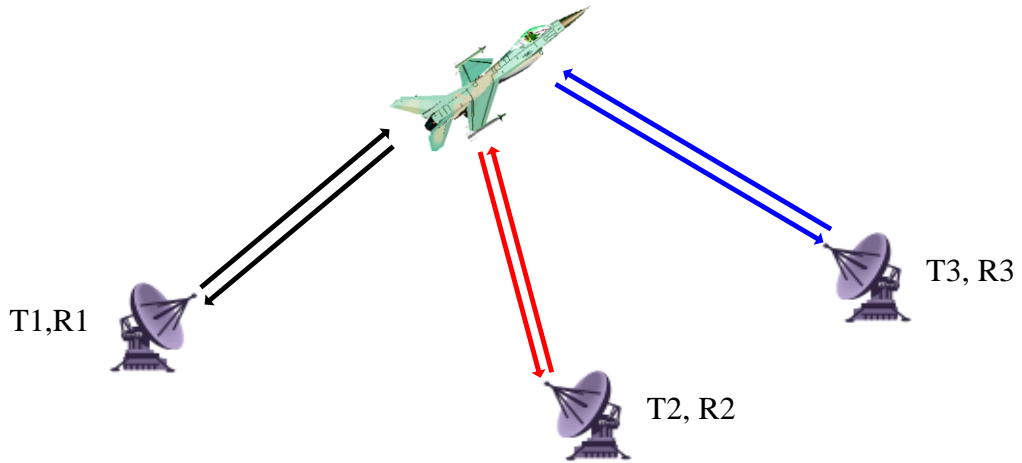


Figure 2-2 Multistatic Radar System Configuration 2 (Multiple Monostatic Case)

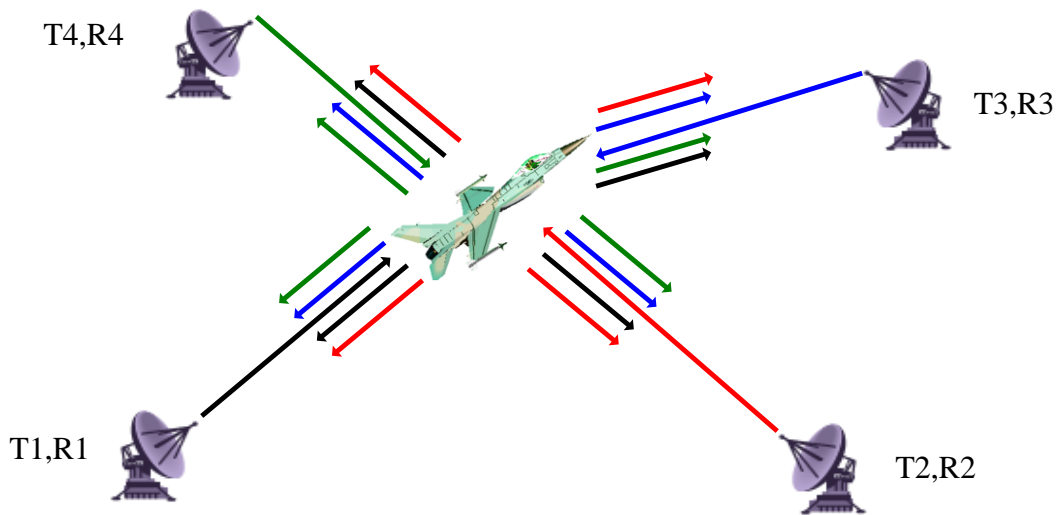


Figure 2-3 Multistatic Radar System Configuration 3 (Fully Multistatic Case)

In multistatic radar systems, all transmit receive pairs may act as independent radars. Each system may process the received signals individually and detection decisions and estimated parameters like range and velocity are fused in a processing center (or fusion center - FC). This is so called decentralized (or distributed) detection. As opposite to this architecture, all the received signals, either RF or video, may be sent to a processing center without any prior processing and the

received signals may be jointly processed there. Data transmission lines like copper cable or fiber cables exist between radar units for this purpose [3].

For joint processing, transferring of received signals is not sufficient. A common time and frequency reference establishing the synchronization between transmit and receive units should exist, and this synchronization should be maintained during the operation. Since the distance between transmitter and receiver units may be huge, it may be difficult to establish and maintain this synchronization. This is the main disadvantage of multistatic radar systems.

There are many advantages of multistatic radar systems [3]. First of all, adding extra transmitter and receiver units to a monostatic system increases the total power and sensitivity of the system and decreases the signal power losses. If the target is illuminated by sufficiently separated transmitting units or the baseline distances are long enough, scattered signal fluctuations are statistically independent at different receiving stations. When the received signals are fused, these fluctuations are smoothed and as a result performance of the detector enhances at high detection probabilities. Simultaneous target observations from different directions make detection probabilities of stealth objects increase. When the angle between directions from a stealth object to a transmitting and receiving unit nears 180 degrees, the scattered signal intensity at the input of the receiver may increase dramatically and this increase cannot be reduced by stealth technologies like body shaping and radar absorbing material coating.

Another advantage of multistatic radar systems is their high accuracy of position estimation of a target. Range measurements of monostatic systems are usually more accurate than angle measurements since angle measurements are related to antenna beamwidth. Accuracy of angle measurements also decreases with increasing range in monostatic systems. On the other hand, multistatic systems can use range measurements of different receivers and special techniques like triangulation and extract angle of arrival information from these range measurements increasing the accuracy of the position estimation.

Increased resolution capability is also an advantage of multistatic radar systems. Resolution capability refers to the detection probability and measurement accuracy

of the radar system in the presence of additional targets and other interference sources. Assume there are two targets at the same range in the resolution cell of a radar receiver. These two targets may be at different ranges to a different radar receiver in the multistatic system so that the targets may be resolved in the range.

When transmitters and receivers of multistatic radar systems are widely separated, intersection of their main beams may be less than a monostatic system resulting reduction in the power returning from the clutter which is another advantage of multistatic radar systems.

The last advantage of multistatic radar systems to be mentioned here is their resistance to jamming and increased survivability. When multistatic radar systems operate in bistatic mode, it is difficult to determine the exact positions of receivers and this makes the receivers less vulnerable to jamming and direct physical attack by anti radiation missiles.

2.3 Phased Array Radar

Phased Array Radar uses antenna arrays for transmitting and receiving signals. These arrays may be linear or planar. In both the linear and planar arrays the separation between the elements is usually uniform. These arrays may be co-located and even transmit and receive functions can be performed by the same array. The two arrays may also be widely separated allowing the radar system to operate in bistatic mode. An example configuration of a phased array radar system is given in Figure 2-4.

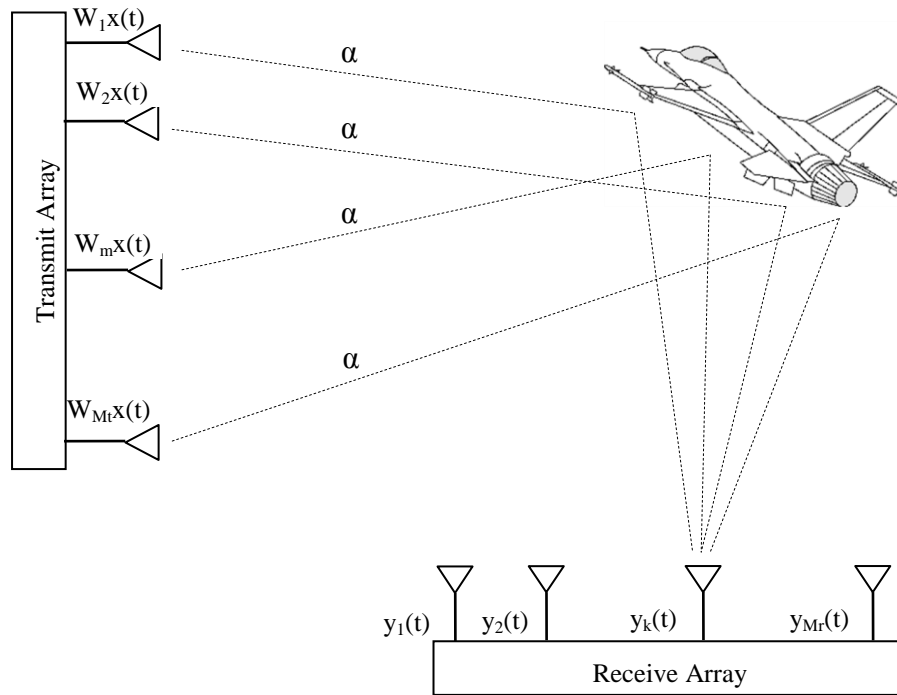


Figure 2-4 Phased Array Radar Configuration

Since the interelement spacing of phased array radar antennas is small, the bistatic RCS seen by every transmit-receive pair in a phased array radar system is assumed to be the same.

In phased array radars, every antenna element of the transmit array sends a scaled version of the same waveform. Although the elements usually being omnidirectional, by properly adjusting these scale factors, a directive antenna with a high gain can be obtained. By changing these scale factors in time, a beam can be steered in space toward any desired direction similar to a conventional radar with a directional antenna. The process of scaling waveforms can be also performed on the signals received by the received elements. This makes the effect of using a directional antenna at the receiver. This process of scaling waveforms at the transmitter and receiver is known as beamforming [1]. That is why phased array radars are also called beamformers. Since this beamforming process is performed electronically, the look direction of the array may change very fast and the region of

interest can be searched very rapidly without any mechanical movement. This is the main advantage of phased array radar systems.

The number of elements in an array may be large enough allowing to steer multiple independent beams at once. These beams may be used to track multiple targets or search different areas of the space simultaneously. Search and track operation may be also performed in a time multiplexed fashion by the same radar system allowing the use of phased array radar system as a multi-function radar [1].

Besides these advantages, its complexity, difficulties in the production stages of phased array antennas and high cost are its main disadvantages.

2.3.1 Signal Model

Consider a phased array radar system that has M_t transmit and M_r receive elements. Assume that transmit and receive arrays are uniform linear arrays with inter element spacing of d_t and d_r respectively.

Let $\sqrt{E_t/M_t}x(t)$ denote the discrete time baseband signal transmitted by the transmit antenna elements where E_t is the total average transmitted energy.

If the transmit array performs transmit beamforming in the direction of $\tilde{\theta}$ the transmitted signal can be written in the vector form as

$$\mathbf{x}(t) = \mathbf{a}(\tilde{\theta}) \sqrt{\frac{E_t}{M_t}} x(t) \quad (2-2)$$

where $\mathbf{a}(\tilde{\theta})$ is the transmitter steering vector. If the transmit array is calibrated $\mathbf{a}(\tilde{\theta})$ is in the form of (2-3)

$$\mathbf{a}(\tilde{\theta}) = \begin{bmatrix} 1 \\ e^{j2\pi f_0 d_t \sin(\tilde{\theta})/c} \\ \vdots \\ e^{j2\pi f_0 (M_t-1) d_t \sin(\tilde{\theta})/c} \end{bmatrix} \quad (2-3)$$

In (2-3), f_0 is the carrier frequency of the radar and c is the speed of light.

Assume there is a stationary target at the far field of the arrays in the direction of θ . Under the assumption of narrowband transmitted signal and the propagation is nondispersive the signal at the target location, $x^t(t)$, can be written as:

$$\begin{aligned} x^t(t) &= \mathbf{a}^H(\theta)\mathbf{x}(t - \tau_t) \\ &= \mathbf{a}^H(\theta)\mathbf{a}(\tilde{\theta})\sqrt{\frac{E_t}{M_t}}x(t - \tau_t) \end{aligned} \quad (2-4)$$

where τ_t is the time delay between the target and the transmit antenna array and $\mathbf{a}(\theta)$ is

$$\mathbf{a}(\theta) = \begin{bmatrix} 1 \\ e^{j2\pi f_0 d_t \sin(\theta)/c} \\ \vdots \\ e^{j2\pi f_0 (M_t - 1) d_t \sin(\theta)/c} \end{bmatrix} \quad (2-5)$$

Since the antenna elements of the phased array radar are closely spaced, all transmit receive pairs see the same bistatic RCS. Assume that α represents this backscattering effect. If the target is at the direction of θ' with respect to the receive array then the signal at the receiver $\mathbf{y}^r(t)$ can be written as

$$\mathbf{y}^r(t) = \alpha \mathbf{b}(\theta') \mathbf{a}^H(\theta) \mathbf{a}(\tilde{\theta}) \sqrt{\frac{E_t}{M_t}} x(t - \tau) + \mathbf{w}(t) \quad (2-6)$$

where τ represents the total time delay between transmitter and receiver ($\tau = \tau_t + \tau_r$) and $\mathbf{b}(\theta')$ is

$$\mathbf{b}(\theta') = \begin{bmatrix} 1 \\ e^{-j2\pi f_0 d_r \sin(\theta')/c} \\ \vdots \\ e^{-j2\pi f_0 (M_r - 1) d_r \sin(\theta')/c} \end{bmatrix} \quad (2-7)$$

$\mathbf{w}(t)$ is a zero mean vector of complex random processes which is in the form of

$$\mathbf{w}(t) = \begin{bmatrix} w_1(t) \\ w_2(t) \\ \vdots \\ w_{M_r}(t) \end{bmatrix} \quad (2-8)$$

These processes may represent receiver noise and other disturbances such as clutter and jamming. Assume that these processes are spatially and temporarily white with a covariance matrix of $\mathbf{C} = \sigma_w^2 \mathbf{I}_{M_r \times M_r}$.

If the receiver also performs beamforming in the direction of $\tilde{\theta}'$ the received signal can be written as

$$\begin{aligned} y(t) &= \alpha \mathbf{b}^H(\tilde{\theta}') \mathbf{b}(\theta') \mathbf{a}^H(\theta) \mathbf{a}(\tilde{\theta}) \sqrt{\frac{E_t}{M_t}} x(t - \tau) + \mathbf{b}^H(\tilde{\theta}') \mathbf{w}(t) \\ &= \alpha \mathbf{b}^H(\tilde{\theta}') \mathbf{b}(\theta') \mathbf{a}^H(\theta) \mathbf{a}(\tilde{\theta}) \sqrt{\frac{E_t}{M_t}} x(t - \tau) + w(t) \end{aligned} \quad (2-9)$$

where $\mathbf{b}(\tilde{\theta}')$ is the receiver steering vector which is defined as

$$\mathbf{b}(\tilde{\theta}') = \begin{bmatrix} 1 \\ e^{-j2\pi f_0 d_r \sin(\tilde{\theta}')/c} \\ \vdots \\ e^{-j2\pi f_0 (M_r - 1) d_r \sin(\tilde{\theta}')/c} \end{bmatrix} \quad (2-10)$$

Since $w(t) = \mathbf{b}^H(\tilde{\theta}') \mathbf{w}(t)$ is a linear transformation in (2-9), $w(t)$ is a zero mean, temporarily white complex normal random process with a variance of $M_r \sigma_w^2$.

If the received signal is fed to a filter matched to $x(t)$, and the output is sampled at time instant τ , the output of the matched filter becomes

$$y = \sqrt{\frac{E_t}{M_t}} \mathbf{b}^H(\tilde{\theta}') \mathbf{b}(\theta') \mathbf{a}^H(\theta) \mathbf{a}(\tilde{\theta}) \alpha + w \quad (2-11)$$

For the case of phased array radar a $M_r \times M_t$ channel matrix \mathbf{H} can be defined as

$$\mathbf{H} = \mathbf{b}(\theta') \mathbf{a}^H(\theta) \alpha \quad (2-12)$$

Although, there is generally no information about the target a priori to any radar signal processing task in reality, for the time being it is assumed that the distribution of α and the direction of the target with respect to the arrays are known. This assumption is made to show the performance bounds of phased array radar system.

If the direction of the target with respect to arrays is known and transmit and receive beams are formed at the direction of the target by making $\theta = \tilde{\theta}$ and $\theta' = \tilde{\theta}'$, then $\mathbf{a}^H(\theta)\mathbf{a}(\tilde{\theta}) = M_t$ and $\mathbf{b}^H(\tilde{\theta}')\mathbf{b}(\theta') = M_r$, resulting a coherent processing gain of $M_t \times M_r$. Then the received signal model becomes [25]

$$y = \sqrt{\frac{E_t}{M_t}} M_r M_t \alpha + w \quad (2-13)$$

Note that if α is small, the amplitude of the received signal will be small despite this processing gain and detection probability will decrease dramatically.

2.3.2 Detection In Phased Array Radar

The detection problem in phased array radar can be formulated as binary hypothesis testing problem:

$$\begin{aligned} H_0: & \quad y = w \\ H_1: & \quad y = \sqrt{\frac{E_t}{M_t}} M_r M_t \alpha + w \end{aligned} \quad (2-14)$$

Assume that α is a zero mean complex normal random variable with a variance of $\sigma_\alpha^2 = 1$.

It is well known that the optimum solution to this hypothesis testing problem under Neyman-Pearson criterion is the Likelihood Ratio Test (LRT) as in (2-15).

$$\frac{p(y|H_1, \sigma_w^2, \sigma_\alpha^2)}{p(y|H_0, \sigma_w^2)} \underset{H_0}{\overset{H_1}{\geq}} T \quad (2-15)$$

Since the distributions of α and w are known, the probability density of y under hypothesis H_1 can be written directly as

$$p(y|H_1, \sigma_w^2, \sigma_\alpha^2) = \frac{1}{\pi(M_r \sigma_w^2 + E_t M_t M_r^2)} \exp\left(-\frac{|y|^2}{M_r \sigma_w^2 + E_t M_t M_r^2}\right) \quad (2-16)$$

Similarly, the probability density of y under hypothesis H_0 can be written as

$$p(y|H_0, \sigma_w^2) = \frac{1}{\pi M_r \sigma_w^2} \exp\left(-\frac{|y|^2}{M_r \sigma_w^2}\right) \quad (2-17)$$

Then the log likelihood ratio can be written as

$$\ln\left(\frac{p(y|H_1, \sigma_w^2, \sigma_\alpha^2)}{p(y|H_0, \sigma_w^2)}\right) = \ln\left(\frac{\sigma_w^2}{\sigma_w^2 + E_t M_t M_r}\right) + \left(\frac{E_t M_t}{\sigma_w^2(\sigma_w^2 + E_t M_t M_r)}\right) |y|^2 \quad (2-18)$$

So the likelihood ratio test [25] can be written as

$$\begin{array}{c} H_1 \\ |y|^2 \geq T' \\ H_0 \end{array} \quad (2-19)$$

where T' is the is the accordingly modified version of T .

When there is no target, the distribution of $|y|^2$ is exponential [4] and can be written as

$$|y|^2 \sim \exp\left(\frac{1}{M_r \sigma_w^2}\right) \quad (2-20)$$

The P_{fa} , namely the probability of false alarm can be calculated as

$$\begin{aligned} P_{fa} &= \text{Prob}\left\{\exp\left(\frac{1}{M_r \sigma_w^2}\right) > T'\right\} \\ &= \exp\left(\frac{-T'}{M_r \sigma_w^2}\right) \end{aligned} \quad (2-21)$$

The corresponding threshold T' can be written as

$$T' = -M_r \sigma_w^2 \ln(P_{fa}) \quad (2-22)$$

When there is target, the distribution of $|y|^2$ is again exponential [4] with rate parameter is equal to $E_t M_t M_r^2 + M_r \sigma_w^2$ and can be written as

$$|y|^2 \sim \exp\left(\frac{1}{E_t M_t M_r^2 + M_r \sigma_w^2}\right) \quad (2-23)$$

The P_d namely the probability of detection can be calculated in terms of threshold as

$$\begin{aligned} P_d &= Prob \left\{ \exp \left(\frac{1}{E_t M_t M_r^2 + M_r \sigma_w^2} \right) > T' \right\} \\ &= \exp \left(\frac{-T'}{E_t M_t M_r^2 + M_r \sigma_w^2} \right) \end{aligned} \quad (2-24)$$

Equivalently P_d can be written in terms of P_{fa} as

$$P_d = \exp \left(\frac{\sigma_w^2 \ln(P_{fa})}{E_t M_t M_r + \sigma_w^2} \right) \quad (2-25)$$

If SNR of the radar system is defined as

$$SNR = \frac{E_t}{\sigma_w^2} \quad (2-26)$$

Then P_d can be written in terms of SNR as

$$P_d = \exp \left(\frac{\ln(P_{fa})}{(SNR) M_t M_r + 1} \right) \quad (2-27)$$

2.4 MIMO Radar

MIMO Radar uses multiple transmit and multiple receive antennas for transmitting and receiving signals. These antennas may be closely spaced being in the form of an array or be widely spaced forming a netted radar like structure.

Every antenna element in a MIMO radar system transmits different waveforms. These may be orthogonal, mutually uncorrelated or simply linearly independent. This is called waveform diversity and it is a distinguishing property of MIMO radar. Correlation of waveforms may also be allowed to some degree for some applications. So designing mutually orthogonal waveforms with desired autocorrelation and crosscorrelation properties is one of the ongoing research areas of MIMO radar [13], [14].

In MIMO radar systems, it is also implicitly assumed that the independency of transmitted signals remains unchanged at the receiver after the signals are reflected from the target.

To benefit from this diversity, in every MIMO radar receiver, there are as many matched filters as the number of transmitted signals. The target returns are passed through these filters matched to every transmitted signal. If the number of transmitter antenna elements is M_t and the number of receiver antenna elements is M_r , there are $M_t M_r$ outputs of these matched filters totally. MIMO radar processes these outputs jointly to decide a target is present or not. An illustration of a MIMO radar receiver is given in Figure 2-5.

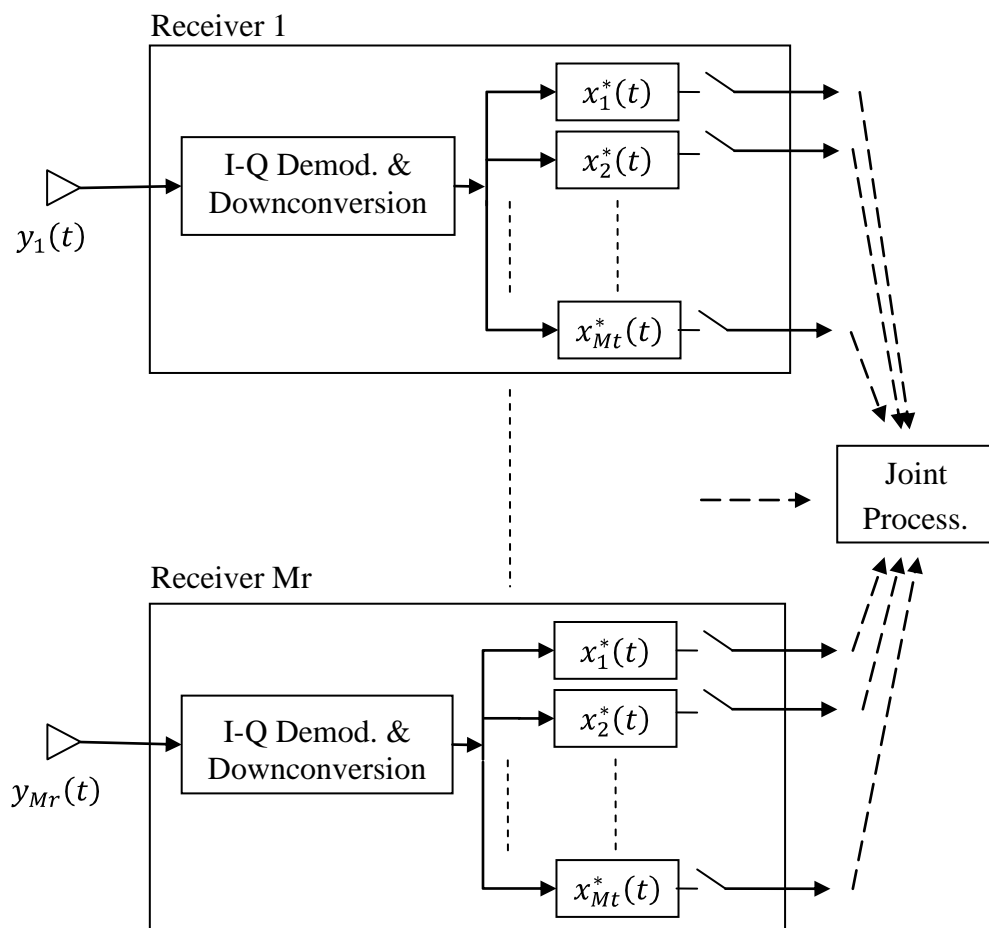


Figure 2-5 Receiver Structure of MIMO Radar

2.4.1 Coherent MIMO Radar (MIMO Radar With Colocated Antennas)

Coherent MIMO radar uses antenna arrays for transmitting and receiving signals. These arrays may be co-located and even transmit and receive functions can be performed by the same array or the arrays may be separated. The separation between the elements may be uniform or non-uniform. The arrays can be filled or sparse depending on the application type. But the separation is always small compared to the range extent of the target. An example deployment of linear arrays of radar antennas of coherent MIMO radar is illustrated in Figure 2-6.

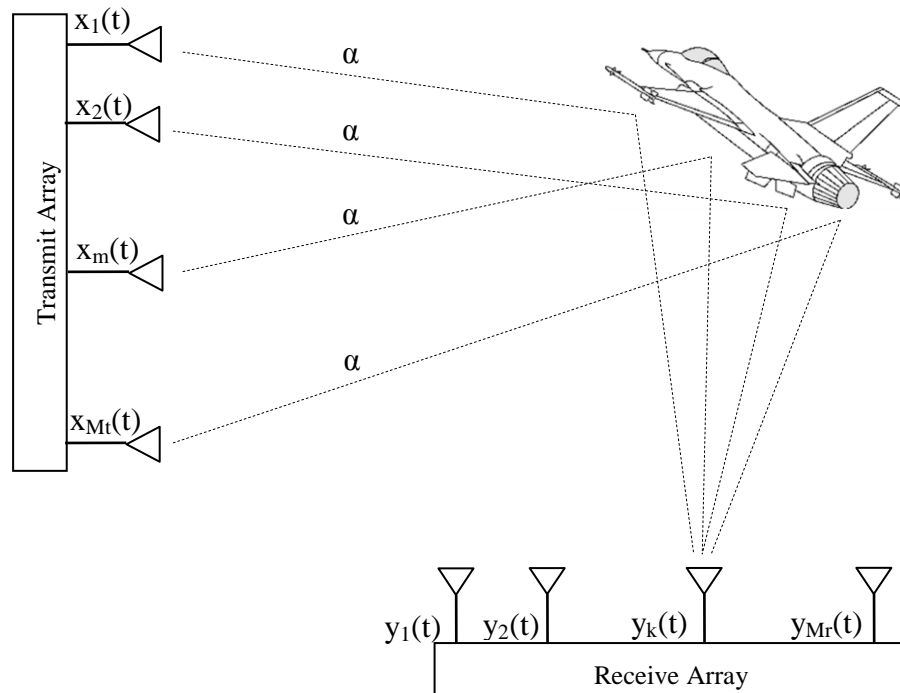


Figure 2-6 Coherent MIMO Radar Configuration

Whatever the separation between the array elements is, the important point in coherent MIMO radar is that the array elements are close enough so that every element sees the same aspect of the target i.e. the same RCS. As a result, point target assumption is generally used in coherent MIMO radar applications.

Coherent MIMO radar resembles the phased array radar because of this deployment scheme of antenna elements. But differently from phased array radar, every antenna element of a Coherent MIMO radar sends different waveforms.

2.4.1.1 Signal Model

Consider a coherent MIMO radar system that has a transmit and a receive array consisting of M_t and M_r elements respectively.

Let $\sqrt{E_t/M_t}x_m(t)$ be the baseband signal transmitted by the m th transmit antenna. and $\|x_m(t)\|^2 = 1$.

Assume that the transmitted signals are mutually orthogonal.

Let a stationary complex target be located at $X_0 = (x_0, y_0)$. Also assume that the direction of the target with respect to transmit and receive arrays are θ and θ' respectively.

Under the assumption that the propagation is nondispersive, the signal at the target location $x_m^t(t)$ can be written as:

$$x_m^t(t) = \sqrt{\frac{E_t}{M_t}} x_m(t - \tau_{tm}(x_0, y_0)), \quad m = 1, \dots, M_t \quad (2-28)$$

where f_0 is the carrier frequency of the radar and $\tau_{tm}(x_0, y_0)$ represents the time delay between target and the m th transmit antenna.

If transmitted signals are narrowband, the sum of all the transmitted signals at the target location can be represented as:

$$\begin{aligned} x^t(t) &= \sqrt{\frac{E_t}{M_t}} \sum_{m=1}^{M_t} x_m^t(t - \tau_{tm}(x_0, y_0)) \\ &= \sqrt{\frac{E_t}{M_t}} \sum_{m=1}^{M_t} e^{-j2\pi f_0 \tau_{tm}(\theta)} x_m(t - \tau_t) \end{aligned} \quad (2-29)$$

where τ_t represents the time delay common to all transmit elements and τ_{tm} represents the time delay between the target and m th transmit antenna.

Define the $M_t \times 1$ transmit steering vector $\mathbf{a}(\theta)$ and transmitted signal vector $\mathbf{x}(t)$ as follows:

$$\mathbf{a}(\theta) = \begin{bmatrix} e^{j2\pi f_0 \tau_{t1}(\theta)} \\ e^{j2\pi f_0 \tau_{t2}(\theta)} \\ \vdots \\ e^{j2\pi f_0 \tau_{tM_t}(\theta)} \end{bmatrix}, \quad \mathbf{x}(t - \tau_t) = \begin{bmatrix} x_1(t - \tau_t) \\ x_2(t - \tau_t) \\ \vdots \\ x_{M_t}(t - \tau_t) \end{bmatrix} \quad (2-30)$$

Then $\mathbf{x}^t(t)$ can be written in the vector form as

$$\mathbf{x}^t(t) = \sqrt{\frac{E_t}{M_t}} \mathbf{a}^H(\theta) \mathbf{x}(t - \tau_t) \quad (2-31)$$

$y_k(t)$ which denotes the baseband signal received by the k th receive antenna can be written as:

$$y_k(t) = \sqrt{\frac{E_t}{M_t}} \alpha_k x^t(t - \tau_{rk}(x_0, y_0)) + w_k(t), \quad m = 1, \dots, M_r \quad (2-32)$$

where $\tau_{rk}(x_0, y_0)$ represents the time delay between target and the k th receive antenna and $w_k(t)$ is a zero mean complex random process which accounts for receiver noise and other disturbances.

In (2-32), α_k is a complex constant that is proportional to the RCS seen by k th receive antenna. Since the antenna elements in the transmit and receive arrays are closely spaced $\alpha_k = \alpha$ and $\tau_{rk}(x_0, y_0) = \tau_r$. So $y_k(t)$ can be rewritten as

$$y_k(t) = \sqrt{\frac{E_t}{M_t}} \alpha e^{-j2\pi f_0 \tau_{r1}(\theta')} \mathbf{a}^H(\theta) \mathbf{x}(t - \tau_t - \tau_r) + w(t) \quad (2-33)$$

Then the transmitted signals can be written in the vector form as

$$\mathbf{y}(t) = \sqrt{\frac{E_t}{M_t}} \alpha \mathbf{b}^*(\theta') \mathbf{a}^H(\theta) \mathbf{x}(t - \tau) + \mathbf{w}(t) \quad (2-34)$$

where $M_r \times 1$ received signal vector $\mathbf{y}(t)$, receive steering vector $\mathbf{b}(\theta')$ and received interference vector $\mathbf{w}(t)$ are defined as

$$\mathbf{b}(\theta') = \begin{bmatrix} e^{j2\pi f_0 \tilde{\tau}_{r1}(\theta')} \\ e^{j2\pi f_0 \tilde{\tau}_{r2}(\theta')} \\ \vdots \\ e^{j2\pi f_0 \tilde{\tau}_{rM_r}(\theta')} \end{bmatrix}, \quad \mathbf{y}(t) = \begin{bmatrix} y_1(t) \\ y_2(t) \\ \vdots \\ y_{M_r}(t) \end{bmatrix}, \quad \mathbf{w}(t) = \begin{bmatrix} w_1(t) \\ w_2(t) \\ \vdots \\ w_{M_r}(t) \end{bmatrix} \quad (2-35)$$

If a $M_r \times M_t$ channel matrix \mathbf{H} is defined as

$$\mathbf{H} = \alpha \mathbf{b}^*(\theta') \mathbf{a}^H(\theta) \quad (2-36)$$

Then the received signal can be written as

$$\mathbf{y}(t) = \sqrt{\frac{E_t}{M_t}} \mathbf{H} \mathbf{x}(t - \tau) + \mathbf{w}(t) \quad (2-37)$$

If this received signal is fed to a bank of matched filters each of which is matched to $x_m(t)$, and the corresponding output is sampled at the time instants τ , then the output of the matched filter bank can be written in the vector form as

$$\bar{\mathbf{y}} = \sqrt{\frac{E_t}{M_t}} \bar{\boldsymbol{\alpha}} + \bar{\mathbf{w}} \quad (2-38)$$

where $\bar{\mathbf{y}}$ is a $M_t M_r \times 1$ complex vector whose entries correspond to the output of the each matched filter at every receiver, $\bar{\mathbf{w}}$ is a $M_t M_r \times 1$ complex noise vector, and $\bar{\boldsymbol{\alpha}}$ is a $M_t M_r \times 1$ complex vector defined as

$$\bar{\boldsymbol{\alpha}} = [\mathbf{b}^*(\theta') \otimes \mathbf{a}^*(\theta)] \alpha \quad (2-39)$$

where \otimes denotes the Kronecker product.

Note that distribution of each entry of $\bar{\boldsymbol{\alpha}}$ is equal to the distribution of α , since elements of $\mathbf{b}^*(\theta')$ and $\mathbf{a}^*(\theta)$ are on the unit circle.

2.4.1.2 Improvements That Coherent MIMO Radar Systems Offer

Waveform diversity makes MIMO radar achieve better performance in several application areas compared to standard phased array radar and is the key of performance improvement for many MIMO radar applications. In the following chapters these improvements offered by Coherent MIMO radar systems will be described.

2.4.1.2.1 Higher Resolution

The equivalent receiver steering vector at the MIMO radar receiver for orthogonal signals is the Kronecker product of transmit and receive steering vectors in Equation (2-39) and is called MIMO steering vector [20]. It can be written as

$$\mathbf{v}_{MIMO} = \mathbf{b}^*(\theta') \otimes \mathbf{a}^*(\theta) \quad (2-40)$$

The MIMO steering vector corresponds to a receiver array which shows the same performance as the MIMO radar system and it includes all possible transmit receive phase difference combinations. To provide a better understanding two examples are provided in subsequent paragraphs.

For a MIMO radar whose transmit (receive) array is a ULA that is a contiguous subset of the receive (transmit) ULA, the MIMO steering vector has $M_t + M_r - 1$ distinct elements. This is the smallest possible number of distinct elements which defines the worst case scenario [9], [15]. In Figure 2-7, an illustration of this worst case scenario is given. In the figure, on the left hand side MIMO radar configuration with four transmit and four receive elements is shown where transmit array is also the receive array. On the right hand side the equivalent virtual receiver array corresponding to MIMO steering vector is given. In the virtual array seven (7) distinct elements exist and the resulting nine elements are repetition of certain array elements.

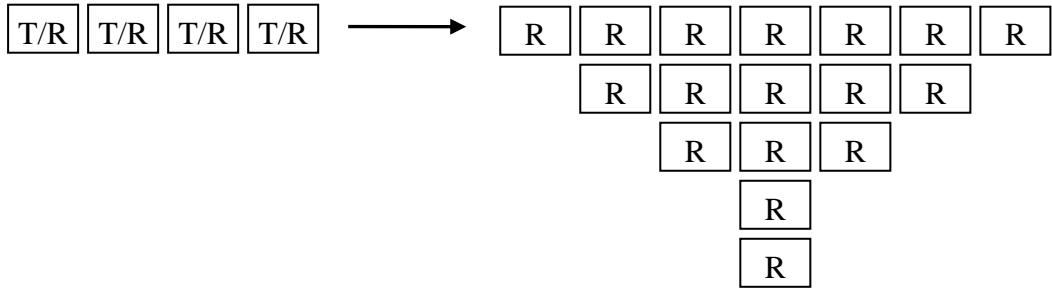


Figure 2-7 Virtual Receiver Array Configuration – The Worst Case [20]

If the transmit steering vector is in the form of

$$\mathbf{a}(\theta) = \begin{bmatrix} 1 \\ e^{j2\pi f_0 M_r \tau(\theta)} \\ \vdots \\ e^{j2\pi f_0 (M_t - 1) M_r \tau(\theta)} \end{bmatrix} \quad (2-41)$$

and the receive steering vector is in the form of

$$\mathbf{b}(\theta) = \begin{bmatrix} 1 \\ e^{j2\pi f_0 \tau(\theta)} \\ \vdots \\ e^{j2\pi f_0 (M_r - 1) \tau(\theta)} \end{bmatrix} \quad (2-42)$$

then MIMO radar steering vector becomes

$$\mathbf{v}_{MIMO} = \begin{bmatrix} 1 \\ e^{j2\pi f_0 \tau(\theta)} \\ \vdots \\ e^{j2\pi f_0 (M_t M_r - 1) \tau(\theta)} \end{bmatrix} \quad (2-43)$$

The equation in (2-43) describes the best case scenario which the MIMO radar steering vector has $M_t M_r$ distinct elements [9], [15]. This corresponds to the case where transmit and receive arrays share few or no antennas.

An illustration of this case is given in Figure 2-8. In the figure a sparse ULA of two elements works as a transmitter array and a filled ULA of four elements works as a receiver array. The resultant virtual array has eight distinct elements and no repetition of array elements exists in the resulting array.

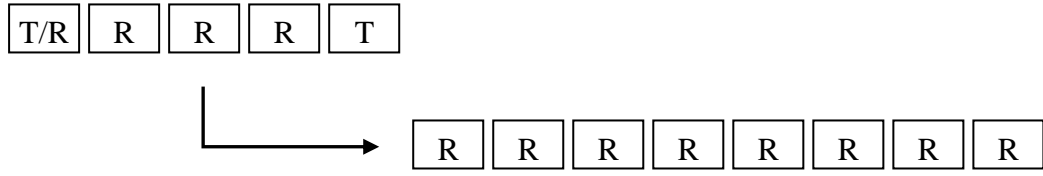


Figure 2-8 Virtual Receiver Array Configuration – The Best Case [20]

As can be seen from the figures, the numbers of distinct elements in virtual arrays are larger than the number of receiver elements in the actual arrays even in the worst case scenario. Consequently, the array aperture is virtually extended. This extension results in higher angular resolution and better detection performance. Higher angular resolution helps to improve the characterization of a target and to improve the rejection capability of the jamming and other interfering sources [20].

Moreover the repetition in virtual array elements also results in sidelobe level reduction in transmit/receive beampatterns [21].

Since the transmitted signals are coherent in a phased array radar system, there is no possibility of formation of an extended virtual array.

2. 4. 1. 2. 2 Parameter Identifiability

One of the other areas that MIMO radar brings performance improvement is the parameter identifiability [12], [15], [16]. Parameter identifiability is defined as the maximum number of targets that can be uniquely identified by the radar. According to [15], the maximum number of targets that can be uniquely identified by the MIMO radar - K_{max} - lies in the interval

$$K_{max} \in \left[\frac{2(M_t + M_r) - 5}{3}, \frac{2M_t M_r}{3} \right) \quad (2-44)$$

where M_t and M_r denotes the number of transmit and receive antennas respectively. The number K_{max} in (2-44) is directly related to the distinct number of elements in MIMO steering vector and changes according to

- the arrays being linear or nonlinear,

- the spacing between the antennas elements being uniform or non-uniform
- the number of elements being shared between the transmit and receive arrays.

The smallest number in (2-44) corresponds to the worst case where the same filled uniform linear array is used for both transmitting and receiving. However, the biggest number in the same equation can be achieved when the receive array is a filled ULA and the transmit array is a sparse ULA with $M_r/2$ inter element spacing [16].

On the other hand, for a phased array radar system, for which all the parameters including the total transmitted power are the same as for the MIMO radar except that $M_t = 1$, K_{max} can be found as

$$K_{max} \in \left\lceil \frac{2M_r - 3}{3} \right\rceil \quad (2-45)$$

where $\lceil \cdot \rceil$ denotes the smallest integer greater than or equal to a given number [15].

When (2-44) and (2-45) are compared, it can be seen that the maximum number of targets that can be uniquely identified by MIMO radar is up to M_t times that of its phased array counterpart and even at the worst case this number is two times that of its phased array counterpart.

2. 4. 1. 2. 3 Transmit Beampattern Synthesis

The beampattern for a single transmit element of a coherent MIMO radar system can be regarded as omnidirectional. Waveform diversity also prevents MIMO radar systems from transmit beamforming and achieving high directivity like phased array systems. Despite this disadvantage, it is still possible approximate a desired beampattern, by using different signals in every transmit element. [16], [17] and [18] investigate this issue.

Recall the equality (2-31) which is given for the signal at the target location. Then the power at the target location is defined as

$$P(\theta) = \frac{E_t}{M_t} \mathbf{a}^H(\theta) \langle \mathbf{x}(t) \mathbf{x}^H(t) \rangle \mathbf{a}(\theta) \quad (2-46)$$

where $\langle \cdot \rangle$ denotes time average [18]. This spatial spectrum is called transmit beampattern.

The covariance matrix of the transmitted signals is defined in [18] by the equality

$$\mathbf{R} = \langle \mathbf{x}(t)\mathbf{x}^H(t) \rangle \quad (2-47)$$

whereas it is defined in [17] as

$$\mathbf{R} = \mathbf{E}\{\mathbf{x}(n)\mathbf{x}^H(n)\} \quad (2-48)$$

Then the transmit beampattern can be rewritten as

$$P(\theta) = \frac{E_t}{M_t} \mathbf{a}^H(\theta) \mathbf{R} \mathbf{a}(\theta) \quad (2-49)$$

Cross-correlation beampattern is also defined similar to transmit beampattern as

$$P_c(\theta) = \frac{E_t}{M_t} \mathbf{a}^H(\theta) \mathbf{R} \mathbf{a}(\bar{\theta}) \quad (2-50)$$

where $\theta \neq \bar{\theta}$. Cross-correlation beampattern can be thought as the covariance or cross-correlation between the transmitted signals at locations θ and $\bar{\theta}$ [17].

By properly designing the covariance matrix of the transmitted signal and transmit beampattern in (2-49), it is possible to [17]

- P1. maximize the total spatial power at a number of known target locations and minimize it anywhere else.
- P2. to approach a desired beampattern
- P3. to achieve a predetermined 3 dB main beamwidth and minimizing the sidelobe levels.

The solution of the problem given in P1 leads to a rank 1 covariance matrix under total power constraint [17]. Unfortunately the form of the covariance matrix and the constraint itself have some disadvantages like:

- The required transmit power for each transmit antenna element may be quite different. This is a problem since it is desirable in a radar system that every transmit element sends the same full power to use all the available power.

- Although the sum of the power at target locations is maximized, it is not guaranteed that this power is evenly distributed to each target. So the power at each target location may be different and may be even less than a desired level at some target locations.
- The cross-correlation beampattern is not controlled. So the signals backscattered to the radar may be fully coherent.

For the solution of P2, [18] offers a gradient search algorithm without any constraint on elemental power whereas [17] uses Semi Definite Quadratic Programming (SQP) techniques to approach a desired beampattern while minimizing the cross-correlation beampattern over the sectors of interest under the uniform elemental transmit power constraint. It is not possible to minimize cross correlations in the phased array radar case since the signals at any two points are fully correlated. Additionally the beampatterns formed by this way by MIMO radar are much better than with its phased array counterpart.

SQP techniques are also used to achieve minimum sidelobe beampattern designs in [17].

For a radar system, it is expected to have no information about the target locations at the beginning of a search process. So initially the radar searches the scene of interest to locate targets. In [17] it is shown that when the target locations are unknown, it is better to transmit constant power at any location θ . This situation enforces to transmit orthogonal signals which are spatially white. After the targets are located, a beampattern can be constructed according to the estimated locations. By this way more power can be transmitted towards the targets of interest and transmission of excess power to unwanted targets, clutter or jammer locations can be avoided.

In [21], a transmit/receive beampattern similar to the cross-correlation beampattern in (2-50) is developed. This beampattern can be simplified as

$$G_{TR}(\theta) = \frac{|\mathbf{a}^H(\theta)\mathbf{R}\mathbf{a}(\bar{\theta})|^2 |\mathbf{b}^H(\theta)\mathbf{b}(\bar{\theta})|^2}{\mathbf{a}^H(\theta)\mathbf{R}\mathbf{a}(\theta)} \quad (2-51)$$

It is shown in [21] that for orthogonal transmitted signals the main beam of this transmit/receive beampattern is narrower and the sidelobe levels are lower than the beampattern of coherent transmitted signals of phased array radar. This improvement can be also interpreted as the contribution of virtual aperture extension.

2. 4. 1. 2. 4 Direct Application Of Adaptive Array Techniques

The use of adaptive localization and detection techniques depends heavily on the returned signals being uncorrelated. Using the ability of transmit beampattern synthesis offered by MIMO radar and minimizing the cross-correlation between the transmitted signals at a number of given target locations; direct application of adaptive array techniques becomes possible. It is known that data dependent adaptive techniques have better resolution, parameter estimation accuracy and interference rejection capability than their data dependent counterparts [9].

In [22], adaptive array algorithms like Capon and APES (Amplitude and Phase Estimation) are applied to MIMO radar. It is found out that Capon gives high resolution and APES gives accurate amplitude estimates. Another robust adaptive technique called robust Capon beamforming is also used achieve accurate estimates of both target locations and target amplitudes in the presence of array calibration errors.

In the phased array radar case the transmitted signals at any two different target locations are fully correlated, and as a result the direct application of standard adaptive array techniques is not possible.

2. 4. 1. 3 Detection In Coherent MIMO Radar

The detection problem here can be formulated as binary hypothesis testing problem as follows

$$\begin{aligned}
 H_0: \quad & \bar{\mathbf{y}} = \bar{\mathbf{w}} \\
 H_1: \quad & \bar{\mathbf{y}} = \sqrt{\frac{E_t}{M_t}} \bar{\boldsymbol{\alpha}} + \bar{\mathbf{w}}
 \end{aligned} \tag{2-52}$$

Assume that the distribution of α is known and equal to

$$\alpha \sim CN(0,1) \quad (2-53)$$

Assume also that the elements of $\bar{\mathbf{w}}$ are spatially and temporarily white Gaussian random variables. So the covariance matrix \mathbf{C} of $\bar{\mathbf{w}}$ can be written as

$$\mathbf{C} = \mathbf{E}\{\bar{\mathbf{w}}\bar{\mathbf{w}}^H\} = \sigma_w^2 \mathbf{I}_{M_r M_t} \quad (2-54)$$

It is well known that the optimum solution to this hypothesis testing problem under Neyman-Pearson criterion is the Likelihood Ratio Test (LRT) [4]. LRT requires the knowledge of probability distribution of $\bar{\alpha}$. Although the distribution of α is known, the angles of direction, θ' and θ , are unknown. As a result the distribution of $\bar{\alpha}$ cannot be known exactly. So in this detection problem, another test namely Generalized Likelihood Ratio Test (GLRT) [4] can be employed by replacing the unknown coefficient vector $\bar{\alpha}$ by its ML estimate

Then the likelihood ratio test can be written as

$$\frac{\max_{\bar{\alpha}} p(\bar{\mathbf{y}}|H_1, \sigma_w^2, \bar{\alpha})}{p(\bar{\mathbf{y}}|H_0, \sigma_w^2)} \underset{H_0}{\overset{H_1}{\geq}} T \quad (2-55)$$

The probability distribution of $\bar{\mathbf{y}}$ under H_1 can be written as

$$p(\bar{\mathbf{y}}|H_1, \sigma_w^2, \bar{\alpha}) = \frac{1}{\pi^{M_t M_r} \sigma_w^{2M_t M_r}} \exp \left(- \frac{\left(\bar{\mathbf{y}} - \sqrt{\frac{E_t}{M_t}} \bar{\alpha} \right)^H \left(\bar{\mathbf{y}} - \sqrt{\frac{E_t}{M_t}} \bar{\alpha} \right)}{\sigma_w^2} \right) \quad (2-56)$$

After differentiating natural logarithm of (2-56) with respect to $\bar{\alpha}$ and equating the result to 0, the ML estimate of $\bar{\alpha}$ can be found as

$$\hat{\bar{\alpha}} = \sqrt{\frac{M_t}{E_t}} \bar{\mathbf{y}} \quad (2-57)$$

If the estimate $\widehat{\bar{\mathbf{a}}}$ is replaced with $\bar{\mathbf{a}}$ in (2-56), the distribution becomes

$$p(\bar{\mathbf{y}}|H_1, \sigma_w^2, \bar{\mathbf{a}}) = \frac{1}{\pi^{M_t M_r} \sigma_w^{2M_t M_r}} \quad (2-58)$$

The probability distribution of $\bar{\mathbf{y}}$ under H_0 is

$$p(\bar{\mathbf{y}}|H_0, \sigma_w^2) = \frac{1}{\pi^{M_t M_r} \sigma_w^{2M_t M_r}} \exp\left(-\frac{\bar{\mathbf{y}}^H \bar{\mathbf{y}}}{\sigma_w^2}\right) \quad (2-59)$$

Then the log likelihood ratio can be written as

$$\ln\left(\frac{p(\bar{\mathbf{y}}|H_1, \sigma_w^2, \bar{\mathbf{a}})}{p(\bar{\mathbf{y}}|H_0, \sigma_w^2)}\right) = -\frac{\bar{\mathbf{y}}^H \bar{\mathbf{y}}}{\sigma_w^2} \quad (2-60)$$

Then the likelihood ratio test becomes

$$\begin{array}{c} H_1 \\ \|\bar{\mathbf{y}}\|^2 \geq T' \\ H_0 \end{array} \quad (2-61)$$

where T' is the accordingly modified version of T and $\|\cdot\|$ represents the Fobenius norm.

Note that the optimal detector in Neyman-Pearson sense in Coherent MIMO radar corresponds to noncoherent summation of matched filter outputs since the direction of arrival of the signal is unknown a priori.

To see the performance limit of coherent MIMO radar, assume that the angle of directions θ' and θ are known. In this case, the effect of the vector $[\mathbf{b}^*(\theta') \otimes \mathbf{a}^H(\theta)]$ in (2-39) can be cancelled by rephrasing all the matched filter outputs properly. Then the elements of the vector $\bar{\mathbf{a}}$ become identical and coherent integration of the received samples becomes possible before detection process. The same effect can be achieved by multiplying the received signal vector by $[\mathbf{b}^*(\theta') \otimes \mathbf{a}^H(\theta)]^H$. After this multiplication the binary hypothesis testing problem turns in the form

$$\begin{aligned}
H_0: \quad y &= w \\
H_1: \quad y &= \sqrt{\frac{E_t}{M_t}} M_t M_r \alpha + w
\end{aligned} \tag{2-62}$$

where w is now a complex number with distribution

$$w \sim CN(0, M_t M_r \sigma_w^2) \tag{2-63}$$

The solution to this hypothesis testing problem under Neyman-Pearson criterion is the Likelihood Ratio Test (LRT) as in (2-64).

$$\frac{p(y|H_1, \sigma_w^2, \sigma_\alpha^2)}{p(y|H_0, \sigma_w^2)} \underset{H_0}{\overset{H_1}{\geq}} T \tag{2-64}$$

Since the distributions of $\bar{\alpha}$ and \bar{w} are known, the probability density of \bar{y} under hypothesis H_1 can be written directly as

$$p(y|H_1, \sigma_w^2, \sigma_\alpha^2) = \frac{1}{\pi(M_t M_r \sigma_w^2 + E_t M_t M_r^2)} \exp\left[-\frac{|y|^2}{M_t M_r \sigma_w^2 + E_t M_t M_r^2}\right] \tag{2-65}$$

and the probability density of y under hypothesis H_0 can be written as

$$p(y|H_0, \sigma_w^2) = \frac{1}{\pi M_t M_r \sigma_w^2} \exp\left[-\frac{|y|^2}{M_t M_r \sigma_w^2}\right] \tag{2-66}$$

Then the log likelihood ratio can be written as

$$\ln\left(\frac{p(y|H_1, \sigma_w^2, \sigma_\alpha^2)}{p(y|H_0, \sigma_w^2)}\right) = \ln\left(\frac{\sigma_w^2}{\sigma_w^2 + E_t M_r}\right) + \left(\frac{E_t}{\sigma_w^2(M_t \sigma_w^2 + E_t M_t M_r)}\right) |y|^2 \tag{2-67}$$

So the likelihood ratio test can be written as

$$|y|^2 \underset{H_0}{\overset{H_1}{\geq}} T' \tag{2-68}$$

where T' is the accordingly modified version of T .

When there is no target, the distribution of $|y|^2$ is exponential and can be written as

$$|y|^2 \sim \exp\left(\frac{1}{M_t M_r \sigma_w^2}\right) \quad (2-69)$$

The P_{fa} , namely the probability of false alarm can be calculated as

$$\begin{aligned} P_{fa} &= \text{Prob}\left\{\exp\left(\frac{1}{M_t M_r \sigma_w^2}\right) > T'\right\} \\ &= \exp\left(\frac{-T'}{M_t M_r \sigma_w^2}\right) \end{aligned} \quad (2-70)$$

The corresponding threshold T' can be written as

$$T' = -M_t M_r \sigma_w^2 \ln(P_{fa}) \quad (2-71)$$

When there is target, the distribution of $|y|^2$ is again exponential [4] with rate parameter is equal to $E_t M_t M_r^2 + M_t M_r \sigma_w^2$ and can be written as

$$|y|^2 \sim \exp\left(\frac{1}{E_t M_t M_r^2 + M_t M_r \sigma_w^2}\right) \quad (2-72)$$

The P_d namely the probability of false alarm can be calculated in terms of threshold as

$$\begin{aligned} P_d &= \text{Prob}\left\{\exp\left(\frac{1}{E_t M_t M_r^2 + M_t M_r \sigma_w^2}\right) > T'\right\} \\ &= \exp\left(\frac{-T'}{E_t M_t M_r^2 + M_t M_r \sigma_w^2}\right) \end{aligned} \quad (2-73)$$

Equivalently P_d can be written in terms of P_{fa} as

$$P_d = \exp\left(\frac{\sigma_w^2 \ln(P_{fa})}{E_t M_r + \sigma_w^2}\right) \quad (2-74)$$

If SNR of the radar system is defined as

$$SNR = \frac{E_t}{\sigma_w^2} \quad (2-75)$$

Then P_d can be written in terms of SNR as

$$P_d = \exp\left(\frac{\ln(P_{fa})}{(SNR)M_r + 1}\right) \quad (2-76)$$

Note that the probability of detection does not depend on the number of transmit antennas but depends only on number of receive antennas and SNR.

2.4.2 Statistical MIMO Radar (MIMO Radar with Widely Separated Antennas)

Statistical MIMO radar employs antenna arrays which are widely separated. The inter element spacing in an array is also so large that each transmit-receive pair sees a different aspect of the target and thus sees different RCS due to target's complex shape. An illustration of this situation is given in Figure 2-9.

If the spacing between the antenna elements is wide enough, received signals from each transmit receive pair become independent. This is called Spatial or Angular Diversity [25]. Statistical MIMO radar focuses on this property.

MIMO communication systems use the same principle to overcome fading in the communication channel and to improve the system performance. The concept of MIMO radar with widely separated antennas is inspired by this property of MIMO communications and exploits the statistical properties of target RCS. This is why it is referred as Statistical MIMO radar by the authors who introduced this concept [25].

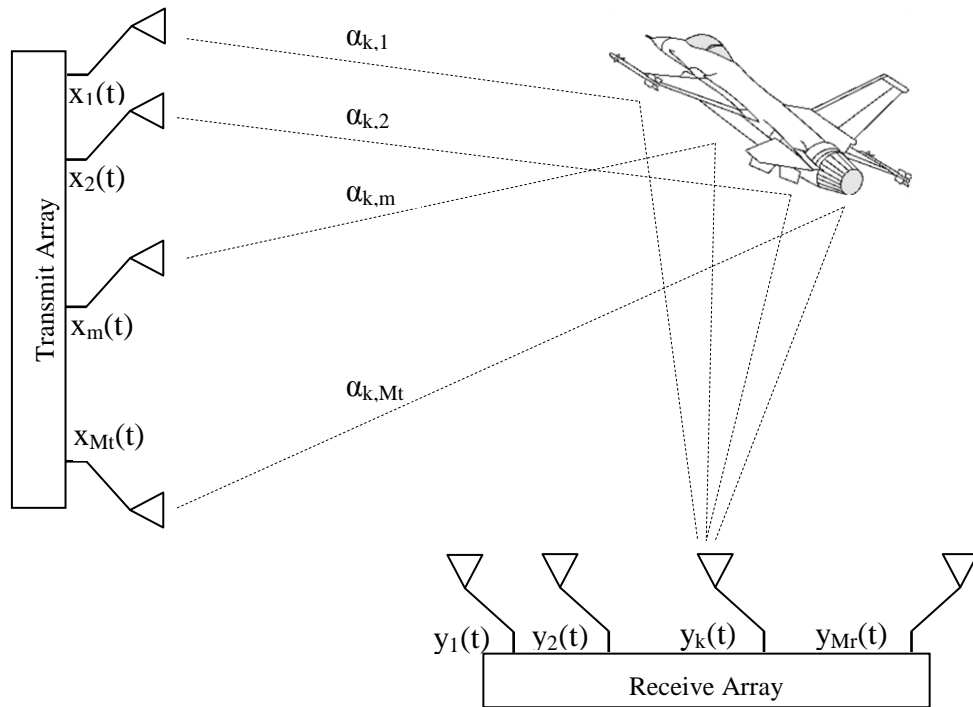


Figure 2-9 Statistical MIMO Radar Configuration 1

Statistical MIMO radar is not the only system that uses the idea of angular diversity and multiple transmit and receive antennas. Multistatic radar systems also benefit from angular spread if time and phase synchronization is maintained among them during operation and if the received signals are processed jointly in a processing center [3]. So Statistical MIMO Radar concept can be thought as a particular form of multistatic radar [29].

Generally classical approach is used in detection process of multistatic radar systems. The target RCS and clutter are assumed to be deterministic unknowns and tried to be estimated first as a part of the detection process [25]. But in [25] a probabilistic model is used for the unknown parameters and the Bayesian approach is used to find the optimal detectors.

Since the target is seen from spatially different aspects in statistical MIMO radar system, the classical point target model is not adequate to model the RCS variation

of the target with aspect angle. So a complex target model is derived in [25] by extending classical Swerling models in the following way:

Assume that there is a rectangular target composed of an infinite number of random, isotropic and independent scatterers, uniformly distributed over $[x_0 - (\Delta x/2), x_0 + (\Delta x/2)] \times [y_0 - (\Delta y/2), y_0 + (\Delta y/2)]$ as in Figure 2-10. Denote the complex gain of the scatterer located at $(x_0 + x, y_0 + y)$ by $\Sigma(x, y)$ where $(x, y) \in [-(\Delta x/2), +(\Delta x/2)] \times [-(\Delta y/2), +(\Delta y/2)]$. $\Sigma(x, y)$ is modeled as a zero mean, white, complex random variable and $E\{|\Sigma(x, y)|^2\} = 1/(\Delta x \Delta y)$. Let the RCS of this complex target seen between the m th transmitter and k th receiver be denoted by α_{km} . Although the exact distribution of α_{km} depends on the exact distribution of $\Sigma(x, y)$, due to the central limit theorem α_{km} is approximately a complex normal random variable and the distribution of α_{km} can be written as

$$\alpha_{km} \sim CN(0, 1) \quad (2-77)$$

2.4.2.1 Signal Model

Consider a Statistical MIMO radar system that has M_t transmitters and M_r receivers. Let the transmitters and receivers be widely separated as in Figure 2-10 and let (x_{tm}, y_{tm}) and (x_{rk}, y_{rk}) denote the location parameters of m th transmitter and k th receiver respectively.

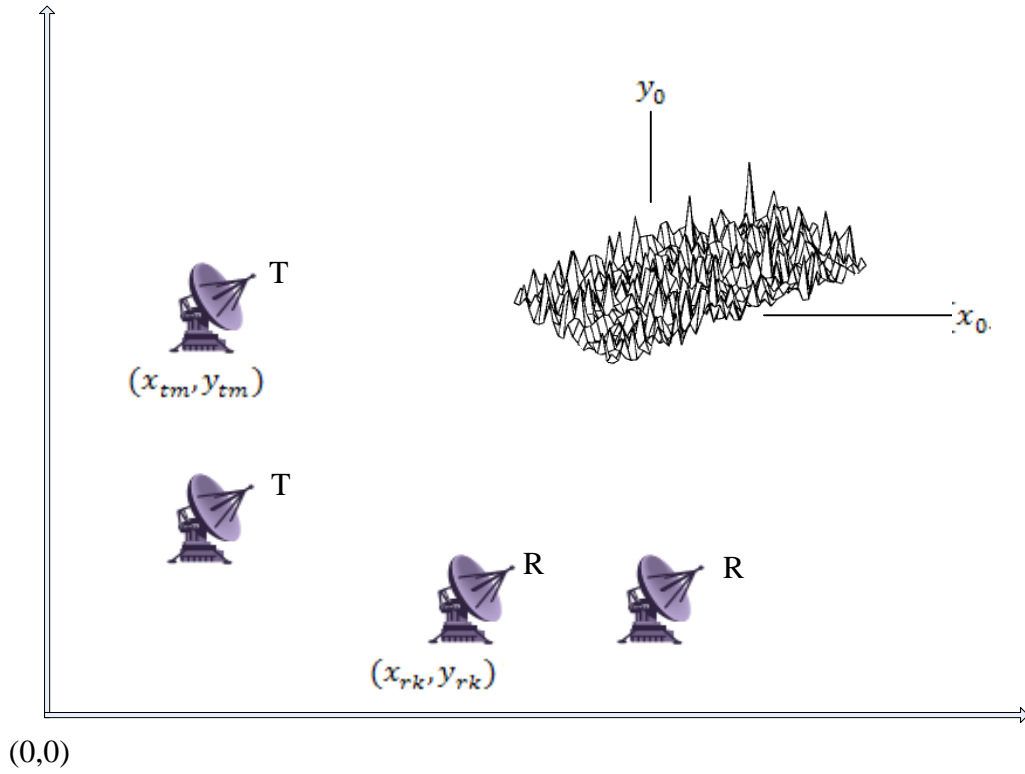


Figure 2-10 Statistical MIMO Radar Configuration 2

Assume there is a stationary complex target, whose distribution of RCS is given in (2-77), is located at $X_0 = (x_0, y_0)$

Assume also that a narrow band signal $\sqrt{E_t/M_t}x_m(t)$ is transmitted from the m th transmitter where $\|x_m(t)\|^2 = 1$.

Under the assumption that the propagation is non-dispersive, the signal at the target location $x_m^t(t)$ can be written as:

$$x_m^t(t) = \sqrt{\frac{E_t}{M_t}} x_m(t - \tau_{tm}(x_0, y_0)), \quad m = 1, \dots, M_t \quad (2-78)$$

where $\tau_{tm}(x_0, y_0)$ represents the time delay between target and the m th transmit antenna.

The baseband equivalent of the signal received by the k th receive antenna can be written as:

$$y_k(t) = \sqrt{\frac{E_t}{M_t}} \sum_{m=1}^{M_t} \alpha_{km} x_m^t(t - \tau_{rk}(x_0, y_0)), \quad k = 1, \dots, M_r \quad (2-79)$$

$$y_k(t) = \sqrt{\frac{E_t}{M_t}} \sum_{m=1}^{M_t} \alpha_{km} x_m(t - \tau_{tm}(x_0, y_0) - \tau_{rk}(x_0, y_0)) \quad (2-80)$$

where $\tau_{rk}(x_0, y_0)$ represents the time delay between target and the k th receive antenna and α_{km} represents the bistatic RCS seen between m th transmit and k th receive antenna.

Since the transmitted signal is narrow band, the received signal can be written as [25]

$$y_k(t) = \sqrt{\frac{E_t}{M_t}} \sum_{m=1}^{M_t} \alpha_{km} e^{-j\tau_{tm}(\theta)} e^{-j\tau_{rk}(\theta')} x_m(t - \tau) \quad (2-81)$$

where $\tau = \tau_{tm}(x_0, y_0) + \tau_{rk}(x_0, y_0)$, $\tau_{tm}(\theta) = 2\pi f_0(\tau_{tm}(x_0, y_0) + \tau_{t1}(x_0, y_0))$ and $\tau_{rk}(\theta') = 2\pi f_0(\tau_{rk}(x_0, y_0) + \tau_{r1}(x_0, y_0))$.

Define the $M_t \times 1$ transmit array steering vector $\mathbf{a}(\theta)$ $M_t \times 1$ transmit signal vector $\mathbf{x}(t)$ as follows:

$$\mathbf{a}(\theta) = \begin{bmatrix} e^{-j\tau_{t1}(\theta)} \\ e^{-j\tau_{t2}(\theta)} \\ \vdots \\ e^{-j\tau_{tM_t}(\theta)} \end{bmatrix}, \quad \mathbf{x}(t - \tau) = \begin{bmatrix} x_1(t - \tau) \\ x_2(t - \tau) \\ \vdots \\ x_{M_t}(t - \tau) \end{bmatrix} \quad (2-82)$$

Define the $M_r \times 1$ receive array steering vector as $\mathbf{b}(\theta')$ and $M_r \times 1$ received signal vector $\mathbf{y}(t)$ as follows:

$$\mathbf{b}(\theta') = \begin{bmatrix} e^{-j\tau_{r1}(\theta')} \\ e^{-j\tau_{r2}(\theta')} \\ \vdots \\ e^{-j\tau_{rM_r}(\theta')} \end{bmatrix}, \quad \mathbf{y}(t) = \begin{bmatrix} y_1(t) \\ y_2(t) \\ \vdots \\ y_{M_r}(t) \end{bmatrix} \quad (2-83)$$

Then the received signal vector can be represented as [25]:

$$\mathbf{y}(t) = \sqrt{\frac{E_t}{M_t}} \text{diag}(\mathbf{b}(\theta')) \boldsymbol{\alpha} \text{diag}(\mathbf{a}(\theta)) \mathbf{x}(t - \tau) + \mathbf{w}(t) \quad (2-84)$$

where $\mathbf{w}(t)$ represents zero mean complex Gaussian interferences which accounts for receiver noise, clutter and jamming.

In (2-84) $\boldsymbol{\alpha}$ is the $M_r \times M_t$ matrix whose km th entry corresponds to the bistatic RCS between m th transmitter and k th receiver as in (2-85).

$$\boldsymbol{\alpha} = \begin{bmatrix} \alpha_{11} & \alpha_{12} & \dots & \alpha_{1M_t} \\ \alpha_{21} & \alpha_{22} & \dots & \alpha_{2M_t} \\ \vdots & \vdots & \ddots & \vdots \\ \alpha_{M_r 1} & \alpha_{M_r 2} & \dots & \alpha_{M_r M_t} \end{bmatrix} \quad (2-85)$$

An important point here is that how much separation between the transmit and receive antennas of the radar system is required for the elements of the matrix $\boldsymbol{\alpha}$ to be uncorrelated.

In [25] and [26] it is stated that if at least one of the four conditions in (2-86) is satisfied the km th and li th elements of $\boldsymbol{\alpha}$ become uncorrelated.

$$\begin{aligned} (1) \quad x_{rk} - x_{rl} &> \frac{\lambda}{\Delta x} d(R_k, X_0) \\ (2) \quad y_{rk} - y_{rl} &> \frac{\lambda}{\Delta y} d(R_k, X_0) \\ (3) \quad x_{tm} - x_{ti} &> \frac{\lambda}{\Delta x} d(T_m, X_0) \\ (4) \quad y_{tm} - y_{ti} &> \frac{\lambda}{\Delta y} d(T_m, X_0) \end{aligned} \quad (2-86)$$

In contrast to the above condition, if the conditions in (2-87) hold jointly, the km th and li th elements of α become fully correlated [25]

$$\begin{aligned}
(1) \quad x_{rk} - x_{rl} &\ll \frac{\lambda}{\Delta x} d(R_k, X_0) \\
(2) \quad y_{rk} - y_{rl} &\ll \frac{\lambda}{\Delta y} d(R_k, X_0) \\
(3) \quad x_{tm} - x_{ti} &\ll \frac{\lambda}{\Delta x} d(T_m, X_0) \\
(4) \quad y_{tm} - y_{ti} &\ll \frac{\lambda}{\Delta y} d(T_m, X_0)
\end{aligned} \tag{2-87}$$

In (2-86), $d(T_m, X_0)$ denotes the distance between k th transmitter and the target, $d(R_k, X_0)$ denotes the distance between m th receiver and the target and λ denotes the wavelength of the carrier signal.

In (2-86) and (2-87) the expression $\lambda/\Delta x$ reminds the antenna beamwidth expression and $(\lambda/\Delta x) d(R_k, X_0)$ resembles the formula which gives the arc length of the radar resolution cell in the cross-range dimension. So if the target is regarded as an antenna with aperture sizes Δx and Δy , conditions above tell us that α_{km} and α_{li} are uncorrelated when both the k th and l th receivers or m th and i th transmitters are not within the beamwidth of the target.

Here further discussion is required for the special cases of α matrix. There are 3 special cases:

1. Transmit antennas are closely spaced ensuring the condition in (2-87) and receive antennas are widely spaced ensuring the condition in (2-86)

In this case, there are M_r different RCS values and the columns of α matrix are identical. A coherent process gain that is equal to M_t can be achieved.

2. Transmit antennas are widely spaced ensuring the condition in (2-86) and receive antennas are closely spaced ensuring the condition in (2-87)

In this case, there are M_t different RCS values and the rows of α matrix are identical. A coherent process gain that is equal to M_r can be achieved.

The received signal vector can be written as

$$\mathbf{y}(n) = \sqrt{\frac{E_t}{M_t}} \mathbf{b}(\theta') \boldsymbol{\alpha}^H \mathbf{a}(\theta) x(n) + \mathbf{w}(n) \quad (2-88)$$

where $\boldsymbol{\alpha}$ is $M_t \times 1$ vector representing RCS values.

3. Transmit and receive antennas are closely spaced ensuring the condition in (2-87).

When this condition occurs, the RCS seen between each transmit receive pair becomes identical, the matrix $\boldsymbol{\alpha}$ reduces to a single coefficient α . The target model of statistical MIMO radar becomes equivalent to the target model of conventional radar or phased array radar systems. And the received signal model becomes equivalent to the model of the Coherent MIMO radar.

If a channel matrix \mathbf{H} is defined as

$$\mathbf{H} = \text{diag}(\mathbf{b}(\theta')) \boldsymbol{\alpha} \text{diag}(\mathbf{a}(\theta)) \quad (2-89)$$

Then the received signal can be written as

$$\mathbf{y}(t) = \sqrt{\frac{E_t}{M_t}} \mathbf{H} \mathbf{x}(t - \tau) + \mathbf{w}(t) \quad (2-90)$$

Note that distribution of \mathbf{H} is equal to the distribution of $\boldsymbol{\alpha}$, since $\text{diag}(\mathbf{b}^*(\theta'))$ and $\text{diag}(\mathbf{a}^*(\theta))$ are diagonal matrices with elements on the unit circle.

If this received signal is fed to a bank of matched filters each of which is matched to $x_m(t)$, and the corresponding output is sampled at the time instant τ , then the output of the matched filter bank can be written in the vector form as

$$\bar{\mathbf{y}} = \sqrt{\frac{E_t}{M_t}} \bar{\boldsymbol{\alpha}} + \bar{\mathbf{w}} \quad (2-91)$$

where $\bar{\mathbf{y}}$ is a $M_t M_r \times 1$ complex vector whose entries correspond to the output of the each matched filter at every receiver, $\bar{\boldsymbol{\alpha}}$ is a $M_t M_r \times 1$ complex vector that contains all the elements of channel matrix \mathbf{H} and $\bar{\mathbf{w}}$ is a $M_t M_r \times 1$ complex noise vector.

(2-91) can be rewritten in the explicit form as

$$\begin{bmatrix} y_{11} \\ y_{12} \\ \vdots \\ y_{1M_t} \\ y_{21} \\ \vdots \\ y_{M_r M_t} \end{bmatrix} = \sqrt{\frac{E_t}{M_t}} \begin{bmatrix} \alpha_{11} \\ \alpha_{12} \\ \vdots \\ \alpha_{1M_t} \\ \alpha_{21} \\ \vdots \\ \alpha_{M_r M_t} \end{bmatrix} + \begin{bmatrix} w_{11} \\ w_{12} \\ \vdots \\ w_{1M_t} \\ w_{21} \\ \vdots \\ w_{M_r M_t} \end{bmatrix} \quad (2-92)$$

2. 4. 2. 2 Improvements That Statistical MIMO Radar Systems Offer

2. 4. 2. 2. 1 Direction of Arrival Estimation

Employment of angular diversity is again the key of performance improvement in direction of arrival estimation. For direction finding applications using MIMO radar, widely separated antennas are used at the transmitter site to benefit from angular diversity. On the other hand, array of closely spaced antennas are used at the receiver site to prevent ambiguity in direction of arrival estimation. It is shown in [23] that the use of MIMO radar enhances direction finding performance even if the signals returned from the target are correlated.

2. 4. 2. 2. 2 Detection Performance

If the aspect angle of the target relative to the antennas changes in a radar system there will be change in the phase and amplitude of the received signal. This change results in target RCS fluctuations or in other words RCS fading [1]. The reduction in the received energy because of these RCS fluctuations may be so high that, the reliable detection of the target may not be possible. Different diversity mechanisms like frequency diversity, polarization diversity are used to decrease the effects of RCS fluctuations and increase the probability of detection. Angular diversity is also one of these methods [26].

Radar systems that are widely separated see different aspects of the target. If a signal return from one side of the target vanishes, there is still a chance to receive a

powerful return from the other side. And since the returned signals are mutually uncorrelated, they can be processed incoherently to smooth signal fluctuations and reduce energy loss. By this way detection probabilities of targets can be improved. This is called diversity gain [24].

The same principle is used in multistatic radars to improve detection probabilities of stealth aircraft [3].

2. 4. 2. 2. 3 Detection Performance in Clutter

The detection performance of statistical MIMO radar under different clutter conditions is also an ongoing research topic in the literature. MIMO radar detectors which show greater detection performance under compound-Gaussian [33], heterogeneous and non-Gaussian [32] clutter conditions have been developed. It has also been shown that the detection performance of MIMO radar is superior compared to single radar in K-distributed sea clutter and this enhancement increases as the number of MIMO radar nodes increases [31].

2. 4. 2. 2. 4 Moving Target Detection Performance

The performance enhancement in moving target detection and its velocity estimation is another result of angular spread of transmit and receive antennas of the MIMO radar system. Like the performance enhancement in detection by the help of experiencing different RCS values, the radar receivers of a MIMO radar system may experience different radial velocities. By this way, some of the receivers may experience high radial speeds, while some of them experience very small radial speeds. Using this fact MIMO radar improves performance for Doppler processing and moving target detection [26].

2. 4. 2. 3 Detection In Statistical MIMO Radar

The detection problem in Statistical MIMO Radar can be formulated as binary hypothesis testing problem:

$$\begin{aligned} H_0: \quad & \bar{\mathbf{y}} = \bar{\mathbf{w}} \\ H_1: \quad & \bar{\mathbf{y}} = \sqrt{\frac{E_t}{M_t}} \bar{\boldsymbol{\alpha}} + \bar{\mathbf{w}} \end{aligned} \quad (2-93)$$

Assume that the covariance matrix \mathbf{C} of the zero mean Gaussian distributed complex noise is:

$$\mathbf{C} = \mathbf{E}\{\bar{\mathbf{w}}\bar{\mathbf{w}}^H\} = \sigma_w^2 \mathbf{I}_{M_r M_t} \quad (2-94)$$

When the separation between the transmit and receive antennas are wide enough ensuring the condition in (2-93), the covariance matrix of the random vector $\bar{\boldsymbol{\alpha}}$ can be written as

$$\mathbf{A} = \mathbf{E}\{\bar{\boldsymbol{\alpha}}\bar{\boldsymbol{\alpha}}^H\} = \mathbf{I}_{M_r M_t} \quad (2-95)$$

It is well known that the optimum solution to this hypothesis testing problem under Neyman-Pearson criterion is the Likelihood Ratio Test (LRT) as in (2-96).

$$\frac{p(\bar{\mathbf{y}}|H_1, \mathbf{C}, \mathbf{A})}{p(\bar{\mathbf{y}}|H_0, \mathbf{C})} \underset{H_0}{\overset{H_1}{\geq}} T \quad (2-96)$$

Since the distributions of $\bar{\boldsymbol{\alpha}}$ and $\bar{\mathbf{w}}$ are known, the probability density of $\bar{\mathbf{y}}$ under hypothesis H_1 can be written directly as

$$\begin{aligned} p(\bar{\mathbf{y}}|H_1, \mathbf{C}, \mathbf{A}) &= \frac{1}{\pi^{M_r M_t} \det\left(\mathbf{C} + \frac{E_t}{M_t} \mathbf{A}\right)} \exp\left[-\bar{\mathbf{y}}^H \left(\mathbf{C} + \frac{E_t}{M_t} \mathbf{A}\right)^{-1} \bar{\mathbf{y}}\right] \\ &= \frac{1}{\pi^{M_r M_t} \left(\sigma_w^2 + \frac{E_t}{M_t}\right)^{M_r M_t}} \exp\left[-\bar{\mathbf{y}}^H \left(\left(\sigma_w^2 + \frac{E_t}{M_t}\right) \mathbf{I}\right)^{-1} \bar{\mathbf{y}}\right] \end{aligned} \quad (2-97)$$

and the probability density of $\bar{\mathbf{y}}$ under hypothesis H_0 can be written as

$$\begin{aligned} p(\bar{\mathbf{y}}|H_0, \mathbf{C}) &= \frac{1}{\pi^{M_r M_t} \det(\mathbf{C})} \exp[-\bar{\mathbf{y}}^H \mathbf{C}^{-1} \bar{\mathbf{y}}] \\ &= \frac{1}{\pi^{M_r M_t} (\sigma_w^2)^{M_r M_t}} \exp[-\bar{\mathbf{y}}^H (\sigma_w^2 \mathbf{I})^{-1} \bar{\mathbf{y}}] \end{aligned} \quad (2-98)$$

The natural logarithm of the likelihood ratio can be taken as

$$\ln \left(\frac{p(\bar{\mathbf{y}}|H_1, \mathbf{C}, \mathbf{A})}{p(\bar{\mathbf{y}}|H_0, \mathbf{C})} \right) = M_r M_t \ln \left(\frac{\sigma_w^2}{\sigma_w^2 + \frac{E_t}{M_t}} \right) + \left(\frac{\frac{E_t}{M_t}}{\sigma_w^2 \left(\sigma_w^2 + \frac{E_t}{M_t} \right)} \right) \bar{\mathbf{y}}^H \bar{\mathbf{y}} \quad (2-99)$$

So the likelihood ratio test can be written as

$$\begin{array}{c} H_1 \\ \bar{\mathbf{y}}^H \bar{\mathbf{y}} \geq T' \\ H_0 \end{array} \quad (2-100)$$

where T' is the accordingly modified version of T .

Equivalently the equation in (2-100) can be written as [25]

$$\begin{array}{c} H_1 \\ \|\bar{\mathbf{y}}\|^2 \geq T' \\ H_0 \end{array} \quad (2-101)$$

where $\|\bar{\mathbf{y}}\|$ represents the Frobenious norm of $\bar{\mathbf{y}}$.

This is an expected result because when RCS fluctuations occur, it is reasonable to sum the matched filter outputs noncoherently to increase the probability of detection.

When there is no target the distribution of $\bar{\mathbf{y}}^H \bar{\mathbf{y}}$ is central Chi-squared with $2M_t M_r$ degrees of freedom [25] and can be written as

$$\bar{\mathbf{y}}^H \bar{\mathbf{y}} \sim \frac{\sigma_w^2}{2} \chi_{2M_t M_r}^2 \quad (2-102)$$

The P_{fa} , namely the probability of false alarm, can be calculated as

$$\begin{aligned}
P_{fa} &= Prob \left\{ \frac{\sigma_w^2}{2} \chi_{2M_t M_r}^2 > T' \right\} \\
&= Prob \left\{ \chi_{2M_t M_r}^2 > \frac{2}{\sigma_w^2} T' \right\} \\
&= 1 - Q_{\chi_{2M_t M_r}^2} \exp \left(\frac{2}{\sigma_w^2} T' \right)
\end{aligned} \tag{2-103}$$

where $Q_{\chi_{2M_t M_r}^2}$ represents the cumulative distribution function of a Chi-squared random variable with $2M_t M_r$ degrees of freedom.

The corresponding threshold T' can be written as

$$T' = \frac{\sigma_w^2}{2} Q_{\chi_{2M_t M_r}^2}^{-1} (1 - P_{fa}) \tag{2-104}$$

where $Q_{\chi_{2M_t M_r}^2}^{-1}$ represents inverse cumulative distribution function of a Chi-squared random variable with $2M_t M_r$ degrees of freedom.

When there is a target, the distribution of $\bar{\mathbf{y}}^H \bar{\mathbf{y}}$ is again central Chi-squared with $2M_t M_r$ degrees of freedom [25] and can be written as

$$\bar{\mathbf{y}}^H \bar{\mathbf{y}} \sim \left(\frac{E_t}{2M_t} + \frac{\sigma_w^2}{2} \right) \chi_{2M_t M_r}^2 \tag{2-105}$$

The P_d , namely the probability of detection, can be calculated in terms of P_{fa} as

$$\begin{aligned}
P_d &= Prob \left\{ \left(\frac{E_t}{2M_t} + \frac{\sigma_w^2}{2} \right) \chi_{2M_t M_r}^2 > T' \right\} \\
&= Prob \left\{ \left(\frac{E_t}{2M_t} + \frac{\sigma_w^2}{2} \right) \chi_{2M_t M_r}^2 > \frac{\sigma_w^2}{2} Q_{\chi_{2M_t M_r}^2}^{-1} (1 - P_{fa}) \right\} \\
&= Prob \left\{ \chi_{2M_t M_r}^2 > \frac{\sigma_w^2}{\left(\frac{E_t}{M_t} + \sigma_w^2 \right)} Q_{\chi_{2M_t M_r}^2}^{-1} (1 - P_{fa}) \right\}
\end{aligned}$$

$$= 1 - Q_{\chi^2_{2M_t M_r}} \left(\frac{\sigma_w^2}{\left(\frac{E_t}{M_t} + \sigma_w^2\right)} Q_{\chi^2_{2M_t M_r}}^{-1} (1 - P_{fa}) \right) \quad (2-106)$$

Or equivalently P_d can be written in terms of SNR as

$$P_d = 1 - Q_{\chi^2_{2M_t M_r}} \left(\frac{1}{\left(\frac{SNR}{M_t} + 1\right)} Q_{\chi^2_{2M_t M_r}}^{-1} (1 - P_{fa}) \right) \quad (2-107)$$

2. 4. 3 Phased-MIMO Radar [27]

Phased MIMO radar is a new concept which tries to bring superior aspects of both phased array and MIMO radar together in a single radar system. This radar system employs transmit and receive arrays which has closely spaced antenna elements like Coherent MIMO radar. Transmit array is partitioned into a number of subarrays that are allowed to overlap. Each subarray coherently transmits waveforms and performs beamforming towards a certain direction in space. By this way a coherent processing gain can be achieved like a phased array radar system. Waveforms transmitted by every transmit subarray are orthogonal to each other to achieve advantages of waveform diversity like a MIMO radar system.

The advantages of phased-MIMO radar system can be summarized as:

- It benefits from all advantages of the MIMO radar, i.e. improved angular resolution and parameter identifiability, detecting a higher number of targets.
- It enables the application of conventional beamforming techniques at both transmitter and receiver
- It offers improved robustness against strong interference

The transmitted signal vector $\boldsymbol{\varphi}(t)$ can be written as

$$\boldsymbol{\varphi}(t) = \sqrt{\frac{M_t}{K}} \mathbf{W}^* \mathbf{x}(t)$$

$$\begin{bmatrix} \varphi_1(t) \\ \varphi_2(t) \\ \vdots \\ \varphi_{M_t}(t) \end{bmatrix} = \begin{bmatrix} w_{1,1} & w_{1,2} & \cdots & w_{1,K} \\ w_{2,1} & w_{2,2} & \ddots & w_{2,K} \\ \vdots & \vdots & \ddots & \vdots \\ w_{M_t,1} & w_{M_t,2} & \cdots & w_{M_t,K} \end{bmatrix} \begin{bmatrix} x_1(t) \\ x_2(t) \\ \vdots \\ x_K(t) \end{bmatrix} \quad (2-108)$$

Note that, as can be seen from (2-108), different antenna elements transmit linear combinations of the K orthogonal waveforms. And although the signals $x_i(t)$, $i = 1, \dots, K$ are orthogonal to each other, the signals $\varphi_j(t)$, $j = 1, \dots, M_t$ are not orthogonal.

The cross correlation matrix for phased-MIMO radar can be defined as

$$\mathbf{R}_\varphi = \mathbf{E}\{\boldsymbol{\varphi}(t)\boldsymbol{\varphi}^H(t)\} = \mathbf{W}^* \mathbf{W}^T \quad (2-109)$$

And the transmit power distribution at a point at the direction θ can be written similar to (2-48) and (2-49) of coherent MIMO radar as

$$P(\theta) = \frac{M_t}{K} \mathbf{a}^H(\theta) \mathbf{R}_\varphi \mathbf{a}(\theta) \quad (2-110)$$

where $\mathbf{a}(\theta)$ is the transmit steering vector.

It is seen from (2-110) that in phased-MIMO radar, it is enough to design the weight matrix \mathbf{W} to obtain desired cross-correlation matrix and transmit beam pattern. After \mathbf{W} is found, the problem of designing $x_i(t)$ can be solved such that $\varphi_j(t)$ satisfies desired properties such as power transmitted by every element being uniform. Similar to transmit beamforming, weight coefficient may also be used at the receiver to enable the system do beamforming at the receiver since coherent processing becomes possible for a phased-MIMO radar.

In [27], analysis and simulations of a phased-MIMO radar system are performed for ULA transmit and receive arrays with fully overlapped subarrays. Fully overlapped subarrays correspond to the case where k th subarray is composed of the antennas located at the k th up to the $(M_t - K + k)$ th positions and each subarray consists of

$(M_t - K + 1)$ elements. It is also assumed in simulations that beamforming is performed at both transmitter and receiver sides.

Analysis results show that when there are no or a few number of weak interfering targets and the receiver noise power dominates these interferers, the phased array radar performs better than the phased-MIMO system in terms of SINR (Signal-to-Interference and Noise Ratio) and phased MIMO radar system performs better than coherent MIMO radar system. Whereas, when there are strong interfering targets whose powers are very high compared to the receiver noise, the SINR performance of the phased array radar system and coherent MIMO radar system are comparable and phased-MIMO radar provides better SINR performance than them.

It is also shown in [27] that the sidelobe levels of transmit/receive beampattern of the phased-MIMO radar with K subarrays are lower than its phased array counterpart.

CHAPTER 3

DETECTION IN MIMO RADAR USING SPACE TIME CODED WAVEFORMS

In the detection problems studied so far, the transmitted signals by MIMO radar are assumed to be orthogonal and the detectors are developed without including these space time coded (STC) signals explicitly. The effects of clutter or other interfering sources on the detection process are also ignored.

In [28] the transmitted signals are modeled as a train of rectangular pulses whose amplitudes are modulated by space time codes and the corresponding detectors are developed. With this approach, the transmitted signals can be further optimized to better a given performance metric. Another difference between the approach to the detection problem presented in this chapter and the one in Chapter 2. 4. 2. 3 is that, the target RCS values are assumed to be unknown constants instead of random variables.

For the development of the signal model the approach in statistical MIMO radar is used, in other words, the spacing between transmit and receive elements are assumed to be wide enough that the signals at the output of the every matched filter in the receivers are uncorrelated.

An illustration of the space time coded MIMO radar system describing configuration of the system and the form of the transmitted signals is given in Figure 3-1.

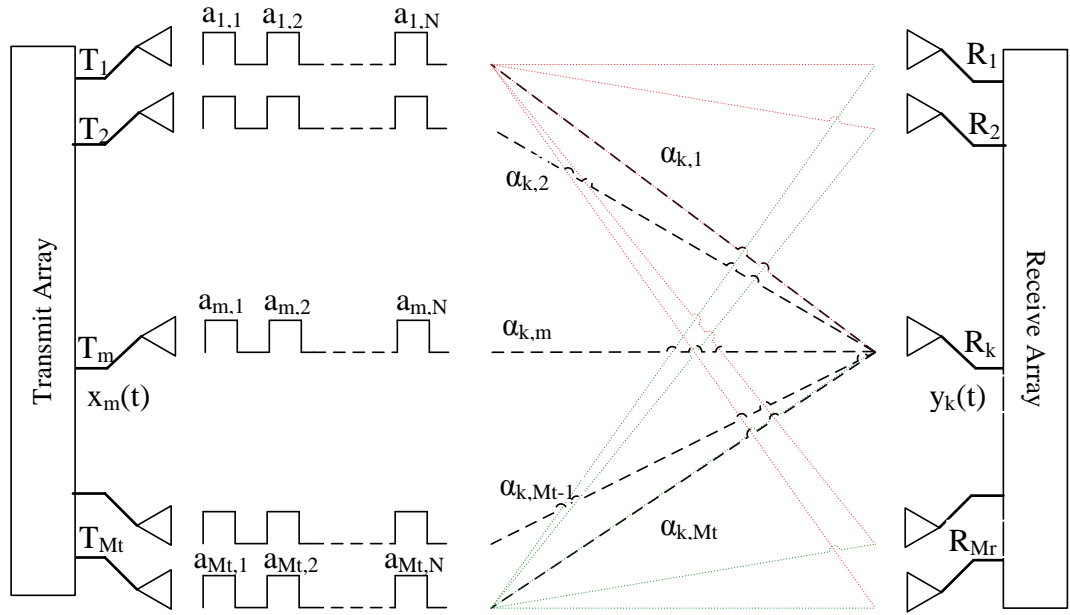


Figure 3-1 STC MIMO Radar Configuration [28]

3. 1 Signal Model [28]

Consider a MIMO radar that has transmit array of M_t elements and a receive array of M_r elements.

Assume each transmit antenna sends a coded pulse train of N pulses. The baseband equivalent of the transmitted signal by the m th transmit antenna can be written as

$$x_m(n) = \sum_{j=1}^N a_{m,j} p(t - (j-1)T_p) \quad m = 1, \dots, M_t \quad (3-1)$$

In Equation (3-1), $p(t)$ represents the transmitted pulse with unit energy and duration τ_p , T_p represents pulse repetition period (PRI) and $a_{m,j}$ is a complex number which represents the code that modulates the j th pulse of the m th transmitting element in both amplitude and phase.

Assume that there is a stationary target at the far field region of the arrays.

By assuming transmit and receive antenna elements are widely spaced ensuring that each transmit receive pair of antenna elements sees a different aspect of the target, the baseband equivalent of the received signal by the k th receive antenna can be written as

$$y_k(t) = \sum_{m=1}^{M_t} \alpha_{k,m} x_m(t - \tau_{k,m}) + w_k(t) \quad k = 1, \dots, M_r \quad (3-2)$$

In Equation (3-2), $\alpha_{k,m}$ is a complex coefficient which accounts for the target backscattering and channel propagation effects. $\tau_{k,m}$ represents the two way time delay between m th transmitter and the k th receiver. Since the target is in the far field region and stationary the time delay may be assumed to be equal for all transmit receive pairs, $\tau_{k,m} = \tau$. And $w_k(t)$ represents zero mean spatially uncorrelated complex Gaussian interferences which accounts for receiver noise, clutter and jamming

If Equation (3-1) and Equation (3-2) are merged, the following equation is obtained.

$$y_k(t) = \sum_{m=1}^{M_t} \alpha_{k,m} \sum_{j=1}^N a_{m,j} p(t - \tau - (j-1)T_p) + w_k(t) \quad k = 1, \dots, M_r \quad (3-3)$$

If $y_k(n)$ is fed to a filter matched to $p(t)$ and the output of the matched filter is sampled at time instants $\tau + (j-1)T_p$, $j = 1, \dots, N$, the received signal at the j th interval becomes

$$y_k(j) = \sum_{m=1}^{M_t} \alpha_{k,m} a_{m,j} + w_k(j) \quad j = 1, \dots, N \quad (3-4)$$

where $w_k(j)$ is the filtered interference sample.

Define the $M_t \times 1$ dimensional complex coefficient vector $\mathbf{\alpha}_k$ and $N \times 1$ dimensional code vector \mathbf{a}_m of m th transmit antenna as follows:

$$\mathbf{a}_k = \begin{bmatrix} \alpha_{k,1} \\ \vdots \\ \alpha_{k,M_t} \end{bmatrix}, \quad \mathbf{a}_m = \begin{bmatrix} a_{m,1} \\ \vdots \\ a_{m,N} \end{bmatrix} \quad (3-5)$$

\mathbf{a}_k will be called code word of kth transmit antenna after this point.

The $N \times M_t$ dimensional code matrix \mathbf{A} of the system can be defined as:

$$\mathbf{A} = [\mathbf{a}_1 \quad \dots \quad \mathbf{a}_{M_t}] \quad (3-6)$$

Then an equation for the received signal can be written as:

$$\mathbf{y}_k = \mathbf{A}\mathbf{a}_k + \mathbf{w}_k \quad k = 1, \dots, M_r \quad (3-7)$$

where $N \times 1$ dimensional received signal vector \mathbf{y}_k and $N \times 1$ dimensional interference vector \mathbf{w}_k are defined as follows:

$$\mathbf{y}_k = \begin{bmatrix} y_k(1) \\ \vdots \\ y_k(N) \end{bmatrix} \quad \mathbf{w}_k = \begin{bmatrix} w_k(1) \\ \vdots \\ w_k(N) \end{bmatrix} \quad (3-8)$$

In order to make visualization of the Equation (3-7) easier, the representation in Figure 3-2 can be examined.

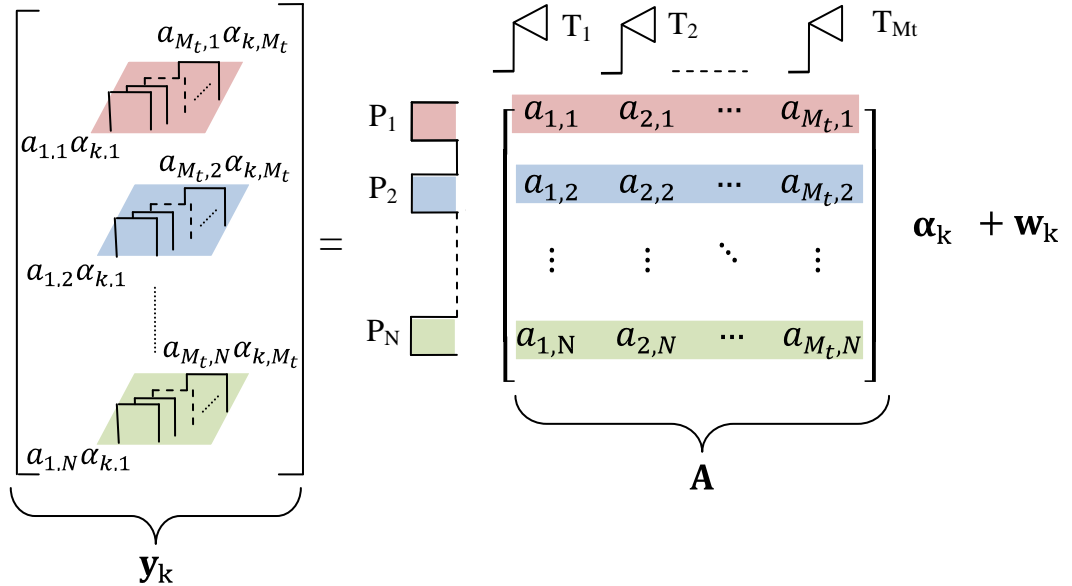


Figure 3-2 The visualization of Equation (3-7)

3. 2 Detection in MIMO Radar Using STC Waveforms

The detection problem can be formulated as a binary hypothesis testing problem as:

$$\begin{aligned} H_0: \mathbf{y}_k &= \mathbf{w}_k & k = 1, \dots, M_r \\ H_1: \mathbf{y}_k &= \mathbf{A}\boldsymbol{\alpha}_k + \mathbf{w}_k & k = 1, \dots, M_r \end{aligned} \quad (3-9)$$

Define the covariance matrix \mathbf{C} of the interference vector as:

$$\mathbf{C} = \mathbf{E}\{\mathbf{w}_k\mathbf{w}_k^H\} \quad (3-10)$$

Assume that \mathbf{C} is positive definite and known.

It is well known that the optimum solution to this hypothesis testing problem under Neyman-Pearson criterion is the Likelihood Ratio Test (LRT) [4]. LRT requires the knowledge of probability distribution of \mathbf{y}_k under each hypothesis. These distributions cannot be known without knowledge of the exact value or pdf of complex coefficient vector $\boldsymbol{\alpha}_k$. So in this detection problem, another test namely Generalized Likelihood Ratio Test (GLRT) can be employed by replacing the unknown coefficient vector $\boldsymbol{\alpha}_k$ by its ML estimate [4].

The conditional probability distribution of \mathbf{y}_k under H_1 can be written as:

$$\begin{aligned} p(\mathbf{y}_k|H_1, \mathbf{C}, \boldsymbol{\alpha}_k) \\ = \frac{1}{\pi^N \det(\mathbf{C})} \exp[(\mathbf{y}_k - \mathbf{A}\boldsymbol{\alpha}_k)^H \mathbf{C}^{-1} (\mathbf{y}_k - \mathbf{A}\boldsymbol{\alpha}_k)] \end{aligned} \quad (3-11)$$

If all the received signals from all of the receivers are combined to form a larger vector as

$$\mathbf{y} = \begin{bmatrix} \mathbf{y}_1 \\ \vdots \\ \mathbf{y}_{M_r} \end{bmatrix} \quad (3-12)$$

then the joint distribution of \mathbf{y} under H_1 can be written as the product of the individual pdfs of \mathbf{y}_k as in Equation (3-13) [28], since the disturbance vectors \mathbf{w}_k are spatially uncorrelated.

$$\begin{aligned}
& p(\mathbf{y}_1, \dots, \mathbf{y}_{M_r} | H_1, \mathbf{C}, \boldsymbol{\alpha}_1, \dots, \boldsymbol{\alpha}_{M_r}) \\
&= \frac{1}{\pi^{NM_r} \det^{M_r}(\mathbf{C})} \exp \left[- \sum_{k=1}^{M_r} (\mathbf{y}_k - \mathbf{A}\boldsymbol{\alpha}_k)^H \mathbf{C}^{-1} (\mathbf{y}_k - \mathbf{A}\boldsymbol{\alpha}_k) \right] \quad (3-13)
\end{aligned}$$

The joint distribution of \mathbf{y} under H_0 can be written as [28]:

$$p(\mathbf{y}_1, \dots, \mathbf{y}_{M_r} | H_0, \mathbf{C}) = \frac{1}{\pi^{NM_r} \det^{M_r}(\mathbf{C})} \exp \left[- \sum_{k=1}^{M_r} \mathbf{y}_k^H \mathbf{C}^{-1} \mathbf{y}_k \right] \quad (3-14)$$

The GLRT for the detection problem formulated in (3-9) can be written as [28]

$$\frac{\max_{\boldsymbol{\alpha}_1, \dots, \boldsymbol{\alpha}_{M_r}} p(\mathbf{y}_1, \dots, \mathbf{y}_{M_r} | H_1, \mathbf{C}, \boldsymbol{\alpha}_1, \dots, \boldsymbol{\alpha}_{M_r})}{p(\mathbf{y}_1, \dots, \mathbf{y}_{M_r} | H_0, \mathbf{C})} \underset{H_0}{\overset{H_1}{\geq}} T \quad (3-15)$$

The values of $\boldsymbol{\alpha}_k$ that maximize the probability distribution in numerator can be found by taking derivative of the distribution with respect to $\boldsymbol{\alpha}_k$. Since natural logarithm is a non-decreasing function taking the natural logarithm of the distributions first and taking derivative afterwards gives the same result as taking derivative directly.

The natural logarithm of the distribution under H_1 can be written as

$$\begin{aligned}
& \ln[p(\mathbf{y}_1, \dots, \mathbf{y}_{M_r} | H_1, \mathbf{C}, \boldsymbol{\alpha}_1, \dots, \boldsymbol{\alpha}_{M_r})] \\
&= \ln \left[\frac{1}{\pi^{NM_r} \det^{M_r}(\mathbf{C})} \right] - \left[\sum_{k=1}^{M_r} (\mathbf{y}_k - \mathbf{A}\boldsymbol{\alpha}_k)^H \mathbf{C}^{-1} (\mathbf{y}_k - \mathbf{A}\boldsymbol{\alpha}_k) \right] \\
&= \ln \left[\frac{1}{\pi^{NM_r} \det^{M_r}(\mathbf{C})} \right] \\
&\quad - \left[\sum_{k=1}^{M_r} \mathbf{y}_k^H \mathbf{C}^{-1} \mathbf{y}_k - 2\mathbf{y}_k^H \mathbf{C}^{-1} \mathbf{A}\boldsymbol{\alpha}_k + \boldsymbol{\alpha}_k^H \mathbf{A}^H \mathbf{C}^{-1} \mathbf{A}\boldsymbol{\alpha}_k \right] \quad (3-16)
\end{aligned}$$

If the derivative of (3-16) is taken, then (3-17) is obtained.

$$\frac{\partial \ln[p(\mathbf{y}_1, \dots, \mathbf{y}_{M_r} | H_1, \mathbf{C}, \boldsymbol{\alpha}_1, \dots, \boldsymbol{\alpha}_{M_r})]}{\partial \boldsymbol{\alpha}_k} = 2\mathbf{A}^H \mathbf{C}^{-1} \mathbf{y}_k - 2\mathbf{A}^H \mathbf{C}^{-1} \mathbf{A}\boldsymbol{\alpha}_k \quad (3-17)$$

Then, the values of α_k can be found by equating (3-17) to 0.

$$\mathbf{A}^H \mathbf{C}^{-1} \mathbf{y}_k = \mathbf{A}^H \mathbf{C}^{-1} \mathbf{A} \alpha_k \quad (3-18)$$

To find the ML estimates of α_k , inverse of $M_t \times M_t$ matrix $\mathbf{A}^H \mathbf{C}^{-1} \mathbf{A}$ should be calculated.

3. 2. 1 Full Rank Code Matrix

Assume that A has full rank [28]. This corresponds to the case where all the transmitters send linearly independent waveforms. Under this assumption two different cases arise for the solution of (3-18).

3. 2. 1. 1 Case 1: $N \geq M_t$:

This case means that all the transmitted signals are linearly independent.

In this case, $\mathbf{A}^H \mathbf{C}^{-1} \mathbf{A}$ has M_t linearly independent columns resulting in a unique solution for α_k estimate as in Equation (3-19) [28].

$$\hat{\alpha}_k = (\mathbf{A}^H \mathbf{C}^{-1} \mathbf{A})^{-1} \mathbf{A}^H \mathbf{C}^{-1} \mathbf{y}_k \quad k = 1, \dots, M_r \quad (3-19)$$

The numerator of GLRT becomes

$$p(\mathbf{y}_1, \dots, \mathbf{y}_{M_r} | H_1, \mathbf{C}, \alpha_1, \dots, \alpha_{M_r}) = \frac{1}{\pi^{NM_r} \det^{M_r}(\mathbf{C})} \exp \left[- \sum_{k=1}^{M_r} (\mathbf{y}_k^H \mathbf{C}^{-1} \mathbf{y}_k - \mathbf{y}_k^H \mathbf{C}^{-1} \mathbf{A} (\mathbf{A}^H \mathbf{C}^{-1} \mathbf{A})^{-1} \mathbf{A}^H \mathbf{C}^{-1} \mathbf{y}_k) \right] \quad (3-20)$$

when α_k in Equation (3-16) is replaced by its estimate $\hat{\alpha}_k$.

Then the GLRT turns into the form [28]

$$\sum_{k=1}^{M_r} \mathbf{y}_k^H \mathbf{C}^{-1} \mathbf{A} (\mathbf{A}^H \mathbf{C}^{-1} \mathbf{A})^{-1} \mathbf{A}^H \mathbf{C}^{-1} \mathbf{y}_k \underset{H_0}{\overset{H_1}{\geq}} T' \quad (3-21)$$

where T' is the accordingly modified version of T .

Let's define $N \times N$ \mathbf{P} matrix as:

$$\mathbf{P} = \mathbf{C}^{-1} \mathbf{A} (\mathbf{A}^H \mathbf{C}^{-1} \mathbf{A})^{-1} \mathbf{A}^H \mathbf{C}^{-1} \quad (3-22)$$

Here some conclusions about the structure of \mathbf{P} are worth to made.

1. \mathbf{P} is Hermitian symmetric. $\mathbf{P} = \mathbf{P}^H$
2. If \mathbf{C} is identity matrix, $\mathbf{P} = \mathbf{P} \mathbf{P}^H = \mathbf{P} \mathbf{P} = \mathbf{P}^2$.
3. If \mathbf{C} is identity matrix and $N = M_t$, $\mathbf{P} = \mathbf{I}$

If the condition in 3 is satisfied, then the detector in (3-21) becomes

$$\sum_{k=1}^{M_r} \mathbf{y}_k^H \mathbf{y}_k \underset{H_0}{\overset{H_1}{\geq}} T' \quad (3-23)$$

Or, equivalently it can be written as

$$\sum_{k=1}^{M_r} \|\mathbf{y}_k\|^2 \underset{H_0}{\overset{H_1}{\geq}} T' \quad (3-24)$$

where $\|\mathbf{y}_k\|$ represents the Frobenious norm of \mathbf{y}_k . One important comment here is that the detector in Equation (3-24) has the same form as in Equation (2-100).

Note that the expression on the LHS of is quadratic in \mathbf{y}_k and \mathbf{y}_k s are functions of \mathbf{w}_k s which are spatially independent and identically distributed Gaussian random variables.

When there is no target, the mean vector and covariance matrix \mathbf{Y} of the vector \mathbf{y}_k can be found as

$$\mathbf{E}\{\mathbf{y}_k\} = \mathbf{E}\{\mathbf{w}_k\} = \mathbf{0} \quad (3-25)$$

$$\mathbf{Y} = \mathbf{E}\{\mathbf{y}_k \mathbf{y}_k^H\} = \mathbf{E}\{\mathbf{w}_k \mathbf{w}_k^H\} = \mathbf{C} \quad (3-26)$$

When a target is present, the mean vector and covariance matrix \mathbf{Y} of the vector \mathbf{y}_k can be found as in (3-27) and (3-28) under the assumption that $\boldsymbol{\alpha}_k$ s are known.

$$\mathbf{E}\{\mathbf{y}_k\} = \mathbf{E}\{\mathbf{A} \boldsymbol{\alpha}_k + \mathbf{w}_k\} = \mathbf{A} \boldsymbol{\alpha}_k \quad (3-27)$$

$$\mathbf{Y} = \mathbf{E}\{(\mathbf{y}_k - \mathbf{A}\boldsymbol{\alpha}_k)(\mathbf{y}_k - \mathbf{A}\boldsymbol{\alpha}_k)^H\} = \mathbf{E}\{\mathbf{w}_k\mathbf{w}_k^H\} = \mathbf{C} \quad (3-28)$$

If \mathbf{C} is identity matrix, namely the disturbance vectors \mathbf{w}_k are also temporarily uncorrelated besides being spatially uncorrelated, and there is no target it is known that the distribution of $\mathbf{y}_k^H \mathbf{P} \mathbf{y}_k$ is central Chi-squared with $2M_t$ degrees of freedom. As a result, the distribution of decision statistics $\sum_{k=1}^{M_r} \mathbf{y}_k^H \mathbf{P} \mathbf{y}_k$ is central Ci-squared with $2M_r M_t$ degrees of freedom.

When there is target, the distribution of $\mathbf{y}_k^H \mathbf{P} \mathbf{y}_k$ becomes non-central Chi-squared with $2M_t$ degrees of freedom and the distribution of $\sum_{k=1}^{M_r} \mathbf{y}_k^H \mathbf{P} \mathbf{y}_k$ becomes non-central Chi-squared with $2M_t M_r$ degrees of freedom.

If \mathbf{C} is not identity matrix, the positive semi-definite matrix $\mathbf{C}^{-1/2}$ can be defined as in Equation (3-29) which is the square root of matrix \mathbf{C}^{-1}

$$\mathbf{C}^{-1} = \mathbf{C}^{-1/2} \mathbf{C}^{-1/2} \quad (3-29)$$

Then the vector \mathbf{r}_k can be defined as

$$\mathbf{r}_k = \mathbf{C}^{-1/2} \mathbf{y}_k \quad (3-30)$$

The mean vector and the auto covariance matrix of \mathbf{r}_k becomes

$$\mathbf{E}\{\mathbf{r}_k\} = \mathbf{E}\{\mathbf{C}^{-1/2} \mathbf{A} \boldsymbol{\alpha}_k + \mathbf{C}^{-1/2} \mathbf{w}_k\} = \mathbf{C}^{-1/2} \mathbf{A} \boldsymbol{\alpha}_k \quad (3-31)$$

$$\begin{aligned} \mathbf{R} &= \mathbf{E}\left\{(\mathbf{C}^{-1/2} \mathbf{y}_k - \mathbf{C}^{-1/2} \mathbf{A} \boldsymbol{\alpha}_k)(\mathbf{C}^{-1/2} \mathbf{y}_k - \mathbf{C}^{-1/2} \mathbf{A} \boldsymbol{\alpha}_k)^H\right\} \\ &= \mathbf{C}^{-1/2} \mathbf{E}\{\mathbf{w}_k \mathbf{w}_k^H\} \mathbf{C}^{-1/2} = \mathbf{I} \end{aligned} \quad (3-32)$$

This means that the detector whitens the received signal before the detection process.

Then the GLRT in Equation (3-21) can be redefined as [28]:

$$\sum_{k=1}^{M_r} \mathbf{r}_k^H \mathbf{C}^{-1/2} \mathbf{A} (\mathbf{A}^H \mathbf{C}^{-1} \mathbf{A})^{-1} \mathbf{A}^H \mathbf{C}^{-1/2} \mathbf{r}_k \underset{H_0}{\overset{H_1}{\geq}} T' \quad (3-33)$$

Let's define $N \times N$ $\mathbf{P}_{\mathbf{C}^{-1/2}\mathbf{A}}$ matrix as:

$$\mathbf{P}_{\mathbf{C}^{-1/2}\mathbf{A}} = \mathbf{C}^{-1/2}\mathbf{A}(\mathbf{A}^H\mathbf{C}^{-1}\mathbf{A})^{-1}\mathbf{A}^H\mathbf{C}^{-1/2} \quad (3-34)$$

Conclusions about the structure of $\mathbf{P}_{\mathbf{C}^{-1/2}\mathbf{A}}$ can be made similar to the conclusions about \mathbf{P}

1. $\mathbf{P}_{\mathbf{C}^{-1/2}\mathbf{A}}$ is Hermitian symmetric.
2. $\mathbf{P}_{\mathbf{C}^{-1/2}\mathbf{A}} = \mathbf{P}_{\mathbf{C}^{-1/2}\mathbf{A}}\mathbf{P}_{\mathbf{C}^{-1/2}\mathbf{A}}^H = \mathbf{P}_{\mathbf{C}^{-1/2}\mathbf{A}}\mathbf{P}_{\mathbf{C}^{-1/2}\mathbf{A}}$.

When there is no target it can be seen that the distribution of $\mathbf{r}_k^H\mathbf{P}_{\mathbf{C}^{-1/2}\mathbf{A}}\mathbf{r}_k$ is still central Chi-squared with $2M_t$ degrees of freedom. So the distribution of decision statistics $\sum_{k=1}^{M_r}\mathbf{r}_k^H\mathbf{P}_{\mathbf{C}^{-1/2}\mathbf{A}}\mathbf{r}_k$ is central Chi-squared with $2M_rM_t$ degrees of freedom [9].

When there is target, the distribution of $\mathbf{r}_k^H\mathbf{P}_{\mathbf{C}^{-1/2}\mathbf{A}}\mathbf{r}_k$ becomes non-central Chi-squared with $2M_t$ degrees of freedom. As a result, the distribution of $\sum_{k=1}^{M_r}\mathbf{r}_k^H\mathbf{P}_{\mathbf{C}^{-1/2}\mathbf{A}}\mathbf{r}_k$ becomes non-central Chi-squared with $2M_tM_r$ degrees of freedom and with noncentrality parameter $\sum_{k=1}^{M_r}(\mathbf{A}\boldsymbol{\alpha}_k)^H\mathbf{C}^{-1}\mathbf{A}\boldsymbol{\alpha}_k$ [9].

If the radar system is MISO (Multiple Input Single Output) the detection statistics in (3-21) becomes

$$\mathbf{y}^H\mathbf{C}^{-1}\mathbf{A}(\mathbf{A}^H\mathbf{C}^{-1}\mathbf{A})^{-1}\mathbf{A}^H\mathbf{C}^{-1}\mathbf{y} \underset{H_0}{\overset{H_1}{\geq}} T' \quad (3-35)$$

If the radar system is SIMO (Single Input Multiple Output), the code matrix \mathbf{A} turns into a code vector \mathbf{a} . By using this code vector, the diagonal code matrix $\mathbf{A}_{diag} = \text{diag}(\mathbf{A})$ can be constructed. Then the detection statistic in (3-21) becomes

$$\sum_{k=1}^{M_r}\mathbf{y}_k^H\mathbf{C}^{-1}\mathbf{A}_{diag}(\mathbf{A}_{diag}^H\mathbf{C}^{-1}\mathbf{A}_{diag})^{-1}\mathbf{A}_{diag}^H\mathbf{C}^{-1}\mathbf{y}_k \underset{H_0}{\overset{H_1}{\geq}} T' \quad (3-36)$$

where in this case

$$\mathbf{y}_k = \mathbf{a}\alpha_k + \mathbf{w}_k \quad (3-37)$$

And α_k is a scalar representing the channel coefficient between the transmitter and kth receiver.

3. 2. 1. 2 Case 2: $N \leq M_t$.

This case means that not all the signals transmitted by the MIMO radar signal are linearly independent. Some of the signals are the same or multiples of each other.

When $N \leq M_t$, $M_t \times M_t$ matrix $\mathbf{A}^H \mathbf{C}^{-1} \mathbf{A}$ has N linearly independent rows, so it is not invertible. But the Equation (3-18) can be converted in a form that allows to find solutions. To do this, first multiply both sides of the operation by \mathbf{A} on the left.

$$\mathbf{A}\mathbf{A}^H \mathbf{C}^{-1} \mathbf{y}_k = \mathbf{A}\mathbf{A}^H \mathbf{C}^{-1} \mathbf{A}\alpha_k \quad (3-38)$$

In Equation (3-38) $N \times N$ matrix $\mathbf{A}\mathbf{A}^H$ is invertible since it has N linearly independent columns. After multiplying both sides of Equation (3-38) $(\mathbf{A}\mathbf{A}^H)^{-1}$ on the left, the Equation (3-39) is obtained.

$$\mathbf{C}^{-1} \mathbf{y}_k = \mathbf{C}^{-1} \mathbf{A}\alpha_k \quad (3-39)$$

Equation (3-39) has M_t unknowns but N equations. So this system is underdetermined. The minimum norm solution of the system can be found as:

$$\hat{\alpha}_k = (\mathbf{C}^{-1} \mathbf{A})^H (\mathbf{C}^{-1} \mathbf{A}\mathbf{A}^H \mathbf{C}^{-1})^{-1} \mathbf{C}^{-1} \mathbf{y}_k \quad (3-40)$$

If we rearrange Equation (3-40), $\hat{\alpha}_k$ is obtained as

$$\hat{\alpha}_k = \mathbf{A}^H (\mathbf{A}\mathbf{A}^H)^{-1} \mathbf{y}_k \quad (3-41)$$

In this case

$$\mathbf{y}_k - \mathbf{A}\hat{\alpha}_k = \mathbf{y}_k - (\mathbf{A}\mathbf{A}^H)(\mathbf{A}\mathbf{A}^H)^{-1} \mathbf{y}_k = 0 \quad (3-42)$$

So the GLRT turns into the form given in inequality in (3-43) [28]

$$\sum_{k=1}^{M_r} \mathbf{y}_k^H \mathbf{C}^{-1} \mathbf{y}_k \underset{H_0}{\overset{H_1}{\geq}} T' \quad (3-43)$$

Note that although some of the transmitted signals are not orthogonal in this case, the detector still performs noncoherent summation of the received signals because of angular diversity.

In fact there is no need to calculate $\hat{\boldsymbol{\alpha}}_k$ here. Because when $N \leq M_t$, the equation

$$\mathbf{y}_k = \mathbf{A}\boldsymbol{\alpha}_k \quad (3-44)$$

is solvable and so we can directly write $\mathbf{y}_k - \mathbf{A}\boldsymbol{\alpha}_k = \mathbf{0}$

We also know that $(\mathbf{y}_k - \mathbf{A}\boldsymbol{\alpha}_k)^H \mathbf{C}^{-1} (\mathbf{y}_k - \mathbf{A}\boldsymbol{\alpha}_k)$ is greater than or equal to zero since \mathbf{C}^{-1} is positive semi-definite and attains its minimum value 0 when

$$\mathbf{y}_k = \mathbf{A}\boldsymbol{\alpha}_k \quad (3-45)$$

So GLRT for this case can be directly written as in (3-43).

(3-43) can also be rewritten as

$$\sum_{k=1}^{M_r} \mathbf{r}_k^H \mathbf{r}_k \underset{H_0}{\overset{H_1}{\geq}} T' \quad (3-46)$$

If \mathbf{r}_k is defined as the same way as in (3-30).

When there is no target, it is known that the distribution of $\mathbf{y}_k^H \mathbf{C}^{-1} \mathbf{y}_k$ is central Chi-squared with N degrees of freedom. As a result the distribution of decision statistics $\sum_{k=1}^{M_r} \mathbf{y}_k^H \mathbf{C}^{-1} \mathbf{y}_k$ is central Ci-squared with $M_r N$ degrees of freedom.

When there is target, the distribution of $\mathbf{y}_k^H \mathbf{C}^{-1} \mathbf{y}_k$ is noncentral Chi-squared with N degrees of freedom and the distribution of decision statistics $\sum_{k=1}^{M_r} \mathbf{y}_k^H \mathbf{C}^{-1} \mathbf{y}_k$ is noncentral Ci-squared with $M_r N$ degrees of freedom and with noncentrality parameter $\sum_{k=1}^{M_r} (\mathbf{A}\boldsymbol{\alpha}_k)^H \mathbf{C}^{-1} \mathbf{A}\boldsymbol{\alpha}_k$ [9].

If the radar system is MISO, the detection statistics in (3-43) becomes

$$\mathbf{y}^H \mathbf{C}^{-1} \mathbf{y} \underset{H_0}{\overset{H_1}{\geq}} T' \quad (3-47)$$

whereas if the radar system is SIMO the detection statistics becomes

$$\sum_{k=1}^{M_r} \mathbf{y}_k^H \mathbf{C}^{-1} \mathbf{y}_k \underset{H_0}{\overset{H_1}{\geq}} T' \quad (3-48)$$

where \mathbf{y}_k is in the form as in Equation (3-37).

When $N = M_t$, \mathbf{A} matrix becomes invertible. So GLRT test in (3-21) reduces to test in (3-43).

3. 2. 2 Rank 1 Code Matrix

Now let's look at a special case where the code matrix \mathbf{A} does not have full rank but has rank 1. This situation occurs when every transmit antenna sends a multiple of the same coded pulse sequence in other words the transmitted signals are not linearly independent any more. In this case the code matrix can be written as the product of a N dimensional column and a M_t dimensional row vector as in Equation (3-49).

$$\mathbf{A} = \mathbf{u}\mathbf{v}^H \quad (3-49)$$

Then

$$\mathbf{y}_k - \mathbf{A}\boldsymbol{\alpha}_k = \mathbf{y}_k - \mathbf{u}\mathbf{v}^H\boldsymbol{\alpha}_k \quad (3-50)$$

Then the Equation (3-18) turns into the form

$$\mathbf{v}\mathbf{u}^H \mathbf{C}^{-1} \mathbf{y}_k = \mathbf{v}\mathbf{u}^H \mathbf{C}^{-1} \mathbf{u}\mathbf{v}^H \boldsymbol{\alpha}_k \quad (3-51)$$

Note that $\mathbf{u}\mathbf{C}^{-1}\mathbf{u}$ is a real constant, so inverse of it exists, leading to the form

$$\mathbf{v}(\mathbf{u}^H \mathbf{C}^{-1} \mathbf{u})^{-1} \mathbf{u}^H \mathbf{C}^{-1} \mathbf{y}_k = \mathbf{v}\mathbf{v}^H \boldsymbol{\alpha}_k \quad (3-52)$$

If we multiply Equation (3-52) by \mathbf{v}^H on the left, and simplifying the constant $\mathbf{v}^H \mathbf{v}$ terms on both sides, Equation (3-53) is obtained [28]:

$$\mathbf{v}^H \hat{\boldsymbol{\alpha}}_k = (\mathbf{u}^H \mathbf{C}^{-1} \mathbf{u})^{-1} \mathbf{u}^H \mathbf{C}^{-1} \mathbf{y}_k \quad (3-53)$$

Replacing $\mathbf{v}^H \boldsymbol{\alpha}_k$ in eq aa with $\mathbf{v}^H \hat{\boldsymbol{\alpha}}_k$ and making the necessary simplifications, the GLRT becomes

$$\sum_{k=1}^{M_r} \frac{\mathbf{y}_k^H \mathbf{C}^{-1} \mathbf{u} \mathbf{u}^H \mathbf{C}^{-1} \mathbf{y}_k}{\mathbf{u}^H \mathbf{C}^{-1} \mathbf{u}} \underset{H_0}{\overset{H_1}{\geq}} T' \quad (3-54)$$

Or equivalently [28],

$$\sum_{k=1}^{M_r} \frac{|\mathbf{u}^H \mathbf{C}^{-1} \mathbf{y}_k|^2}{\mathbf{u}^H \mathbf{C}^{-1} \mathbf{u}} \underset{H_0}{\overset{H_1}{\geq}} T' \quad (3-55)$$

When there is no target, the distribution of detection statistics is a central Chi-squared with $2M_r$ degrees of freedom. And when there is a target, the distribution becomes a noncentral Chi-squared with noncentrality parameter of $\sum_{k=1}^{M_r} (\mathbf{A} \boldsymbol{\alpha}_k)^H \mathbf{C}^{-1} \mathbf{A} \boldsymbol{\alpha}_k = \mathbf{u}^H \mathbf{C}^{-1} \mathbf{u} \sum_{k=1}^{M_r} |\mathbf{v}^H \boldsymbol{\alpha}_k|^2$ and $2M_r$ degrees of freedom.

3. 2. 3 Detection of Moving Targets

In this section, the problem of moving target detection is investigated.

Assume that the target is moving with a velocity of \mathbf{v}_t , and assume also that all transmit receive pairs experience the same Doppler shift during the coherent processing interval of N pulses due to this velocity.

The phase shift between every pulse in the received pulse sequence can be written as [2]

$$\phi = f_d T_p \quad (3-56)$$

Then the Doppler vector of N elements associated with this phase shift can be defined as

$$\mathbf{d}_\emptyset = \begin{bmatrix} 1 \\ e^{j2\pi\emptyset} \\ e^{j2\pi2\emptyset} \\ \vdots \\ e^{j2\pi(N-1)\emptyset} \end{bmatrix} \quad (3-57)$$

To apply the GLRT tests, given in Section 3. 2. 1 and Section 3. 2. 2 we should estimate the reflection coefficients and velocity of the target first. So a cost function can be defined which is to be minimized as

$$J(\boldsymbol{\alpha}, \emptyset) = \|\mathbf{r}_k - \mathbf{D}_\emptyset \mathbf{A} \boldsymbol{\alpha}_k\|^2 \quad (3-58)$$

where \mathbf{D}_\emptyset is the $N \times N$ Doppler matrix which is defined as

$$\mathbf{D}_\emptyset = \text{diag}(\mathbf{d}_\emptyset) \quad (3-59)$$

Define a new matrix \mathbf{A}_d as:

$$\mathbf{A}_d = \mathbf{D}_\emptyset \mathbf{A} \quad (3-60)$$

Then the cost function which is to be minimized with respect to $\boldsymbol{\alpha}_k$ and \emptyset can be rewritten as

$$\min_{\emptyset} (\min_{\boldsymbol{\alpha}} \|\mathbf{r}_k - \mathbf{A}_d \boldsymbol{\alpha}_k\|^2) \quad (3-61)$$

We should first estimate $\boldsymbol{\alpha}_k$ by assuming that the velocity of the target or \mathbf{A}_d is known accordingly and then we should estimate the target velocity.

Consider the case where \mathbf{A} is full rank and $N \geq M_t$. It is well known that the estimate of $\boldsymbol{\alpha}_k$ which minimizes the cost function in (3-61) is the orthogonal projection of \mathbf{r}_k onto the vector space spanned by columns of \mathbf{A}_d .

Then the estimate of $\boldsymbol{\alpha}_k$ can be written directly as

$$\hat{\boldsymbol{\alpha}}_k = (\mathbf{A}_d^H \mathbf{A}_d)^{-1} \mathbf{A}_d^H \mathbf{r}_k \quad (3-62)$$

If $\hat{\boldsymbol{\alpha}}_k$ is replaced with $\boldsymbol{\alpha}_k$ in Equation (3-61), then the cost function turns into the form

$$\begin{aligned}
\min_{\hat{\alpha}_k} \|\mathbf{r}_k - \mathbf{A}_d \hat{\alpha}_k\|^2 &= \min_{\hat{\alpha}_k} \left\| \mathbf{r}_k - \mathbf{A}_d (\mathbf{A}_d^H \mathbf{A}_d)^{-1} \mathbf{A}_d^H \mathbf{r}_k \right\|^2 \\
&= \min_{\hat{\alpha}_k} \left\| \mathbf{r}_k - \mathbf{D}_\emptyset \mathbf{A} ((\mathbf{D}_\emptyset \mathbf{A})^H \mathbf{D}_\emptyset \mathbf{A})^{-1} (\mathbf{D}_\emptyset \mathbf{A})^H \mathbf{r}_k \right\|^2 \\
&= \min_{\hat{\alpha}_k} \left\| \mathbf{r}_k - \mathbf{D}_\emptyset \mathbf{A} (\mathbf{A}^H \mathbf{D}_\emptyset^H \mathbf{D}_\emptyset \mathbf{A})^{-1} \mathbf{A}^H \mathbf{D}_\emptyset^H \mathbf{r}_k \right\|^2 \quad (3-63)
\end{aligned}$$

By using the fact that

$$\mathbf{D}_\emptyset^H \mathbf{D}_\emptyset = \mathbf{D}_\emptyset \mathbf{D}_\emptyset^H = \mathbf{I} \quad (3-64)$$

the Equation (3-63) can be rewritten as

$$\begin{aligned}
\min_{\hat{\alpha}_k} \|\mathbf{r}_k - \mathbf{A}_d \hat{\alpha}_k\|^2 &= \min_{\hat{\alpha}_k} \left\| \mathbf{r}_k - \mathbf{D}_\emptyset \mathbf{A} (\mathbf{A}^H \mathbf{A})^{-1} \mathbf{A}^H \mathbf{D}_\emptyset^H \mathbf{r}_k \right\|^2 \\
&= \min_{\hat{\alpha}_k} \left\| (\mathbf{I} - \mathbf{D}_\emptyset \mathbf{A} (\mathbf{A}^H \mathbf{A})^{-1} \mathbf{A}^H \mathbf{D}_\emptyset^H) \mathbf{r}_k \right\|^2 \\
&= \min_{\hat{\alpha}_k} \left\| (\mathbf{D}_\emptyset \mathbf{D}_\emptyset^H - \mathbf{D}_\emptyset \mathbf{A} (\mathbf{A}^H \mathbf{A})^{-1} \mathbf{A}^H \mathbf{D}_\emptyset^H) \mathbf{r}_k \right\|^2 \\
&= \min_{\hat{\alpha}_k} \left\| \mathbf{D}_\emptyset (\mathbf{I} - \mathbf{A} (\mathbf{A}^H \mathbf{A})^{-1} \mathbf{A}^H) \mathbf{D}_\emptyset^H \mathbf{r}_k \right\|^2 \quad (3-65)
\end{aligned}$$

Since $\mathbf{D}_\emptyset \mathbf{D}_\emptyset^H = \mathbf{I}$, it only causes rotation of the vector $(\mathbf{I} - \mathbf{A} (\mathbf{A}^H \mathbf{A})^{-1} \mathbf{A}^H) \mathbf{D}_\emptyset^H \mathbf{r}_k$, and the norm of the rotated vector is preserved. So the equation in (3-65) can be written as

$$\min_{\hat{\alpha}_k} \|\mathbf{r}_k - \mathbf{A}_d \hat{\alpha}_k\|^2 = \min_{\hat{\alpha}_k} \left\| (\mathbf{I} - \mathbf{A} (\mathbf{A}^H \mathbf{A})^{-1} \mathbf{A}^H) \mathbf{D}_\emptyset^H \mathbf{r}_k \right\|^2 \quad (3-66)$$

In the above equation define

$$\mathbf{P}_a^c = \mathbf{I} - \mathbf{A} (\mathbf{A}^H \mathbf{A})^{-1} \mathbf{A}^H \quad (3-67)$$

\mathbf{P}_a^c denotes the matrix that causes projection of a vector onto a plane which is perpendicular to the plane spanned by the columns of \mathbf{A} .

Then the minimization problem becomes in the form

$$\min_{\hat{\alpha}_k} \|\mathbf{r}_k - \mathbf{A}_d \hat{\alpha}_k\|^2 = \min_{\hat{\alpha}_k} \left\| \mathbf{P}_a^c \mathbf{D}_\emptyset^H \mathbf{r}_k \right\|^2 \quad (3-68)$$

which is equal to the following maximization problem

$$\min_{\hat{\alpha}_k} \|\mathbf{r}_k - \mathbf{A}_d \hat{\alpha}_k\|^2 = \max_{\hat{\alpha}_k} \|\mathbf{P}_d \mathbf{D}_{\hat{\alpha}_k}^H \mathbf{r}\|^2 \quad (3-69)$$

The solution to the maximization problem in (3-69) can be found numerically.

3.3 Optimization of Space Time Codes [9],[28]

It has been stated that by involving the space time codes explicitly in the detector gives the opportunity to optimize these codes directly according to some performance metric. Optimization of the codes to achieve the best detection probability for all SNR values may not be a realistic purpose. So In [28], optimization of the codes for stationary targets according to some other criteria is investigated.

One of these criteria is Chernoff bound based code construction. Chernoff bound gives exponentially decreasing bounds on tail distributions of sums of independent random variables [30].

For the derivation of optimum codes it is assumed that the vectors α_k , $k = 1, \dots, M_t$ are independent and identically distributed zero mean complex Gaussian vectors with covariance matrix

$$\mathbf{E}\{\alpha_k \alpha_k^H\} = \sigma_a^2 \mathbf{I} \quad (3-70)$$

According to this Chernoff bound criterion the optimum code must satisfy the condition

$$\mathbf{C}^{-1/2} \mathbf{A} \mathbf{A}^H \mathbf{C}^{-1/2} = \begin{cases} \frac{\mu N}{\sigma_a^2} \mathbf{P}_{\mathbf{C}^{-1/2} \mathbf{A}} & , N \geq M_t \text{ Case} \\ \frac{\mu N}{\sigma_a^2} \mathbf{I} & , N \leq M_t \text{ Case} \end{cases} \quad (3-71)$$

where μ is a proportionality constant.

If the interfering disturbance is zero mean white Gaussian noise with covariance matrix $\mathbf{C} = \sigma_w^2 \mathbf{I}$, then the condition in (3-71) turns into the form

$$\mathbf{C}^{-1/2} \mathbf{A} \mathbf{A}^H \mathbf{C}^{-1/2} = \begin{cases} \frac{\mu N \sigma_w^2}{\sigma_a^2} \mathbf{P}_A & , N \geq M_t \text{ Case} \\ \frac{\mu N \sigma_w^2}{\sigma_a^2} \mathbf{I} & , N \leq M_t \text{ Case} \end{cases} \quad (3-72)$$

It can be easily seen from (3-72) that, if $M_t = M_r = N$, any orthonormal code set of length N satisfies the condition. That means orthogonal signals are optimum in the case of Chernoff bound based criteria.

CHAPTER 4

SIMULATION RESULTS

In this chapter, results of the simulations which have been performed in this thesis study are introduced. In this thesis, simulations are performed to present detection performance of different MIMO radar configurations. In Section 4. 1, the detection performance of Coherent MIMO Radar, in Section 4. 2 the detection performance of Statistical MIMO Radar, and in Section 4. 3 the detection performance of Space Time Coded MIMO radar is investigated. Throughout this chapter, detection performances of these MIMO radar systems are also compared with phased array radar.

4. 1 Detection in Coherent MIMO Radar

To show the detection performance of Coherent MIMO Radar, the detector in (2-68) is implemented. P_{fa} value is set to 10^{-2} and Monte Carlo simulations are run 10^5 times for the target absent case and 10^4 times for the target present case.

If the number of receive elements is held constant at the value of 5, and the number of transmit elements is increased, the P_d vs SNR curve in Figure 4-1 is obtained.

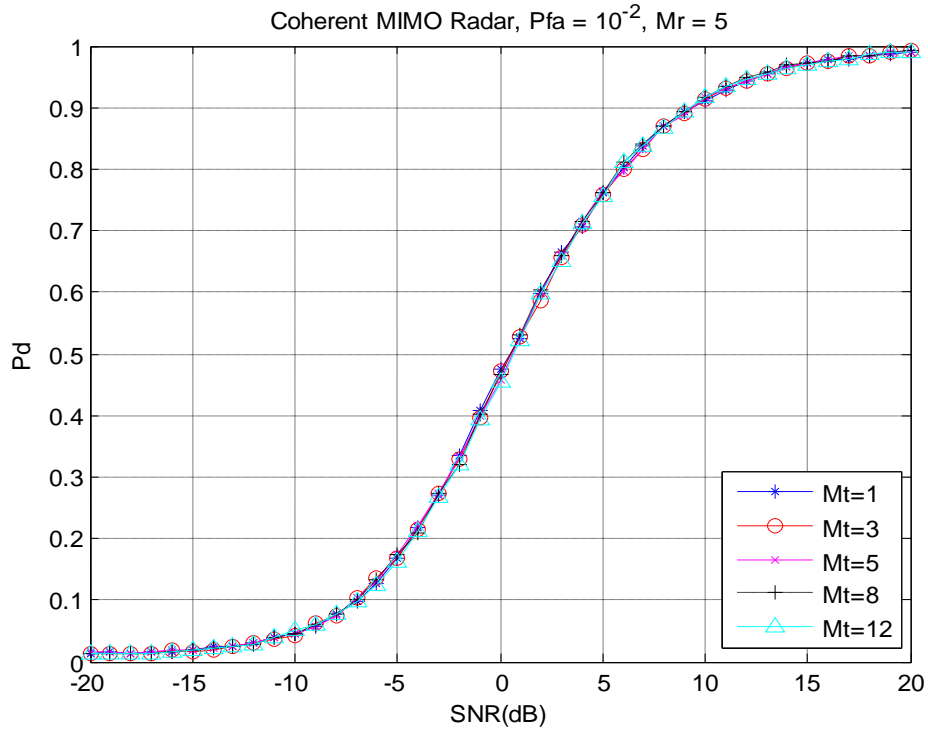


Figure 4-1 Coherent MIMO Radar, Changing M_t

The graphics in Figure 4-1 show that the detection performance does not change with increasing M_t . This is because the transmitted power is normalized and it does not change with the number of transmit elements, and also because the noise power and the signal power in the received signal after coherent summation increase at the same rate.

To compare with the detection performance of phased array radar, the detector in (2-19) is implemented. The resulting P_d vs SNR curve is represented in Figure 4-2.

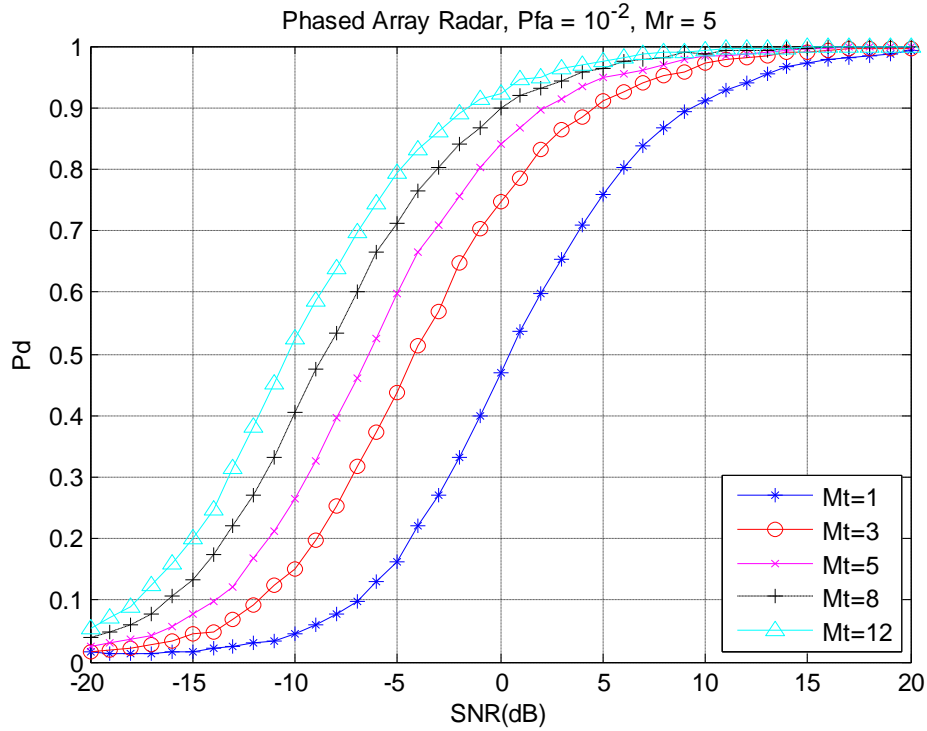


Figure 4-2 Phased Array Radar, Changing M_t

The detection performance of the phased array radar system enhances as the number of transmit antennas increases although the transmitted power is constant. This is due to the gain achieved as a result of the transmit beamforming. The gain increases as the number of transmit antenna increases although the noise power in the received signal remains constant.

When Figure 4-1 and Figure 4-2 is compared, it can be seen that the detection performance of both phased array radar and coherent MIMO radar is the same when $M_t = 1$, or in other words radars work at SIMO mode. But performance of phased array radar is better in other cases.

If the number of transmit elements is held constant at the value of 5 and the number of receive elements is increased, the P_d vs SNR curve in Figure 4-3 is obtained.

The detection performance of coherent MIMO radar enhances as the number of receiving antennas increase, because the total received energy increases. This is also valid for phased array radar system as can be seen in Figure 4-4.

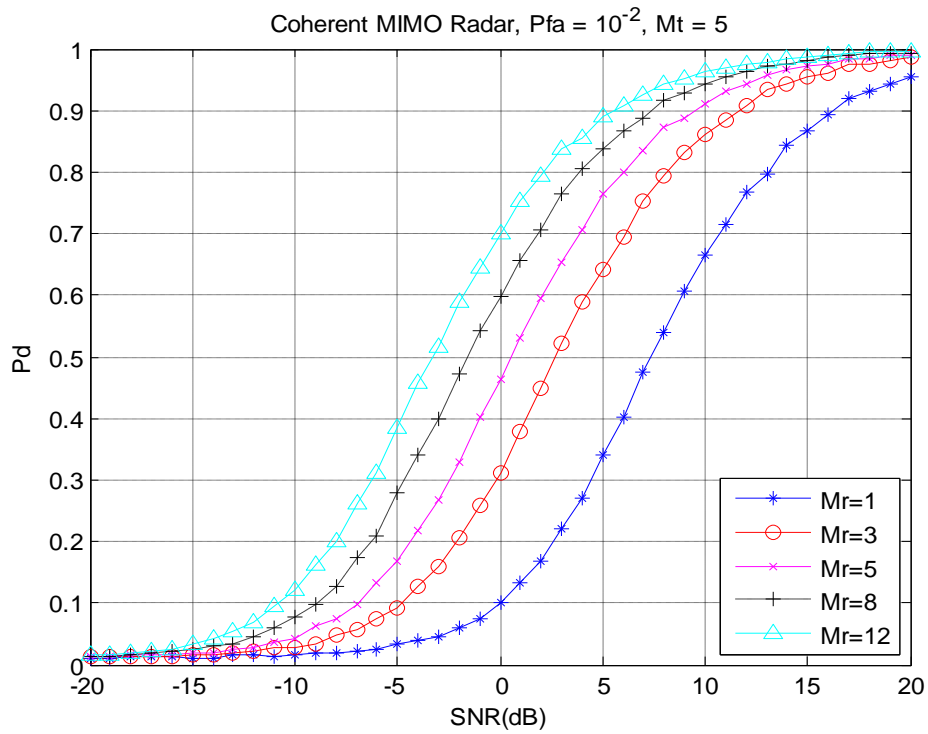


Figure 4-3 Coherent MIMO Radar, Changing M_r

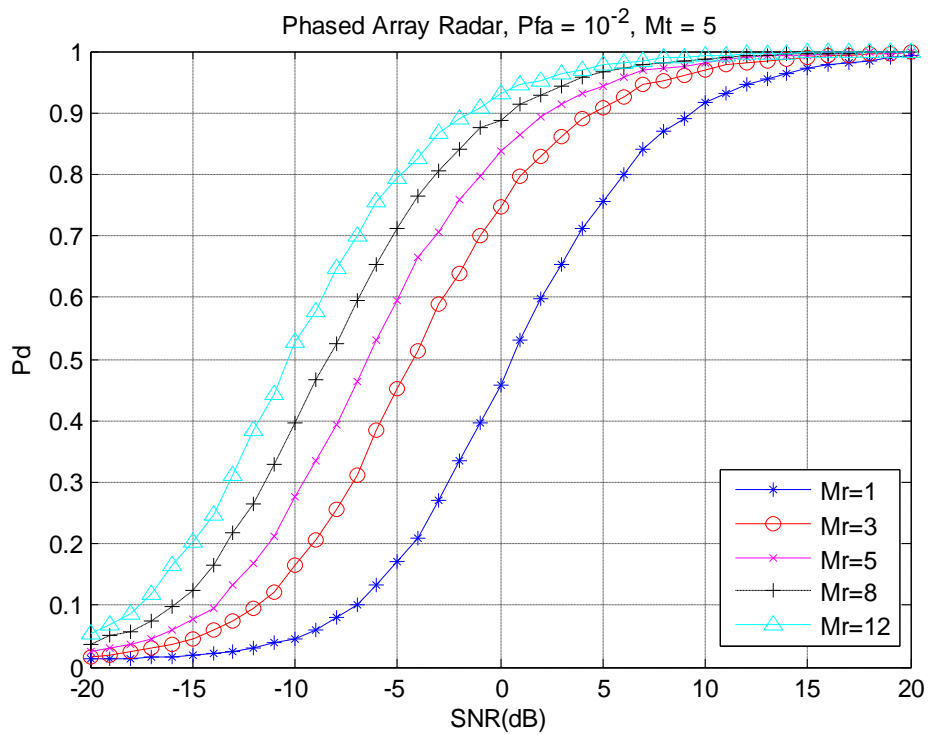


Figure 4-4 Phased Array Radar, Changing M_r

The detection performance of phased array radar system is better than the coherent MIMO radar system in every case. This is an expected result since total noise in the received signal is equal to $M_r \sigma_w^2$ in the phased array radar case whereas it is higher and equal to $M_t M_r \sigma_w^2$ in coherent MIMO radar case.

To see the performance difference clearly, the receiver operating curves of phased array radar and MIMO radar is given in Figure 4-5. This figure is obtained using the analytical expressions given in Equations (2-27) and (2-76) for $M_t = M_r = 2$. In the figure, the blue lines belong to coherent MIMO radar and the red lines belong to phased array radar. Again it can be seen from the figure that phased array radar outperforms coherent MIMO radar in every case.

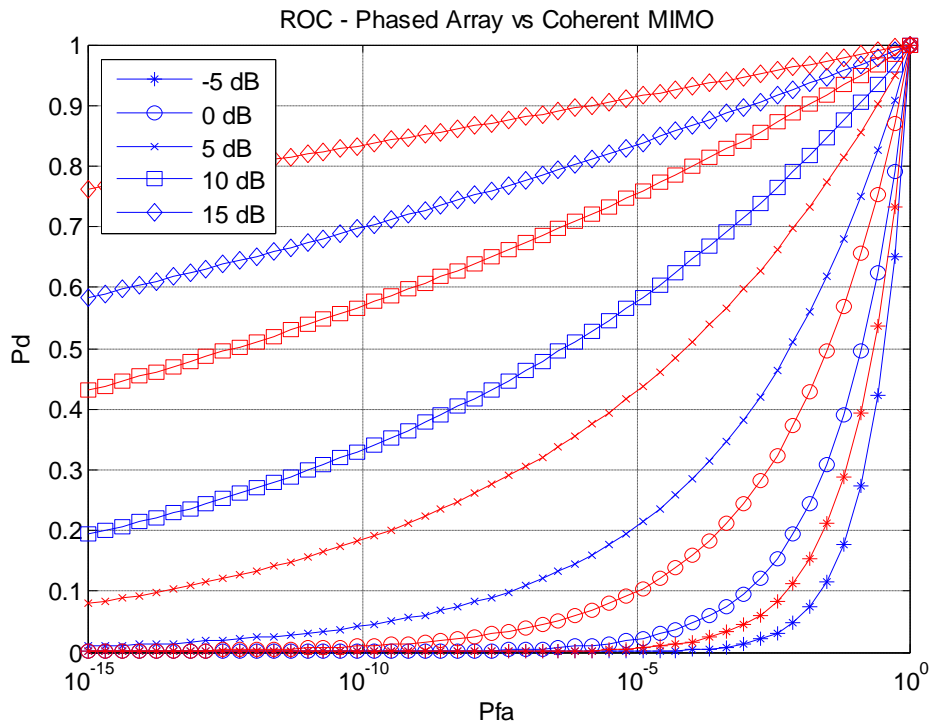


Figure 4-5 ROC of Coherent MIMO and Phased Array Radar

4.2 Detection in Statistical MIMO Radar

In this section detection performance of Statistical MIMO radar is examined.

To show the detection performance of Statistical MIMO Radar, the detector in (2-101) is implemented. P_{fa} value is set to 10^{-2} and Monte Carlo simulations are run 10^4 times for the target absent case and 10^3 times for the target present case.

If the number of receive elements is held constant at the value of 5, and the number of transmit elements is increased, the P_d vs SNR curve in Figure 4-6 is obtained.

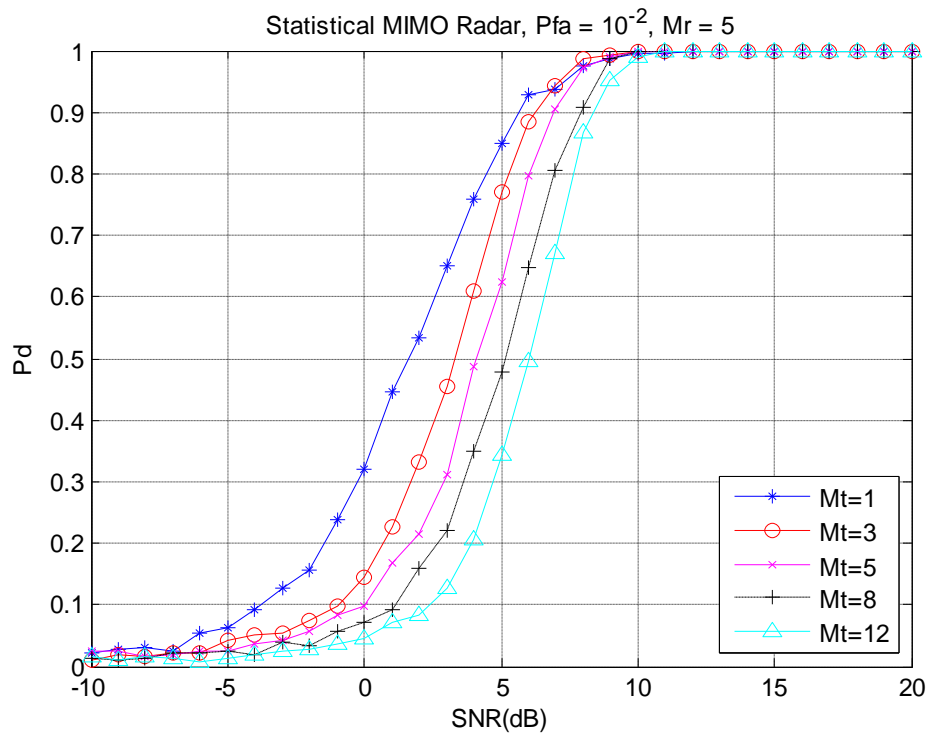


Figure 4-6 Statistical MIMO Radar, Changing M_t

It is interesting to see that the detection performance decreases as the number of transmit antennas increases. This is due to the normalization factor, $\sqrt{E_t/M_t}$, in the signal model. The detection performance depends heavily on the power of the received signal at the output of every matched filter. Since this power decreases as the number of transmitters increases, the detection performance is worse for greater

number of transmit antennas. Because of this decrease in the detection performance, using more widely separated receive antennas instead of increasing the number of spatially diverse transmit antennas seems more reasonable. If improved detection performance is the only benefit expected from a MIMO radar system, it is even better to give up waveform diversity and use a single transmit antenna and many spatially diverse receiving antennas.

If the number of transmit elements is held constant at the value of 5, and the number of receive elements is increased, the P_d vs SNR curve in Figure 4-7 is obtained. Similar to the case in Figure 4-3, P_d increases as the number of receive antennas increases since the total received power is increased.

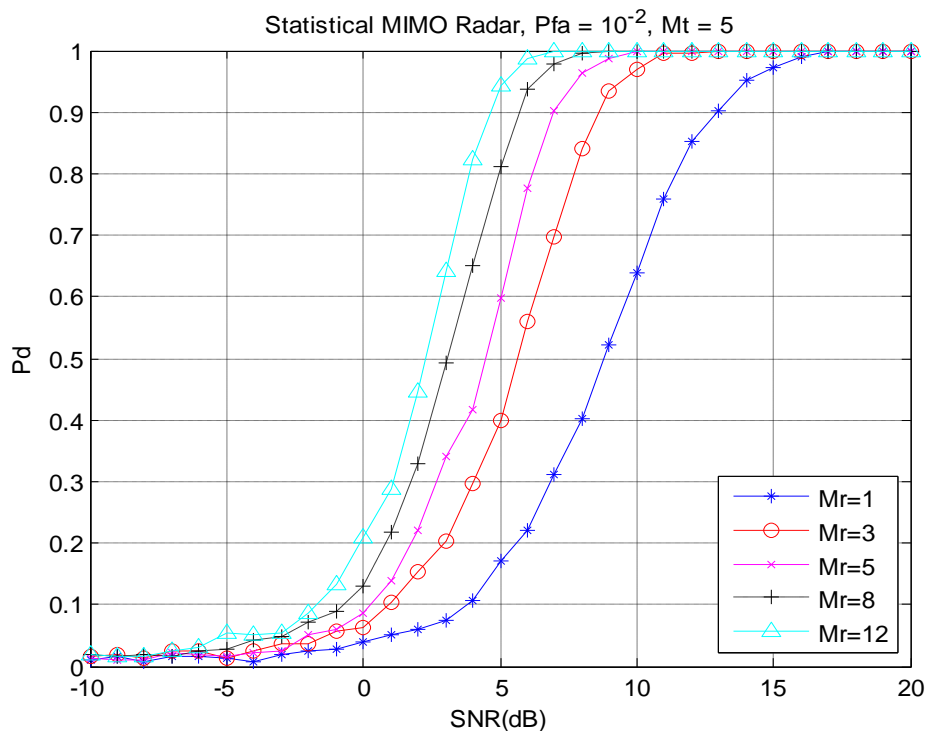


Figure 4-7 Statistical MIMO Radar, Changing Mr

The ROC of phased array radar versus statistical MIMO radar is given in Figure 4-8 and the ROC of statistical MIMO radar versus coherent MIMO radar is presented in Figure 4-9. These figures are obtained using the analytical expressions given in

Equations (2-27), (2-76) and (2-107) for $M_t = M_r = 2$. In both of the figures the blue lines belong to statistical MIMO radar and the red lines belong to phased array radar and coherent MIMO radar.

The results in Figure 4-8 show that at high SNR values and at high detection probabilities, the detection performance of statistical MIMO radar is better than phased array radar. Whereas, at low SNR values, phased array radar performs better than statistical MIMO radar. These results are consistent with the results given in [25]. The same comment also applies for the coherent MIMO statistical MIMO radar comparison case which is shown in Figure 4-9. But in this case the statistical MIMO radar outperforms coherent MIMO radar at lower SNR and P_{fa} values than phased array radar since detection performance of coherent MIMO radar is worse than phased array radar.

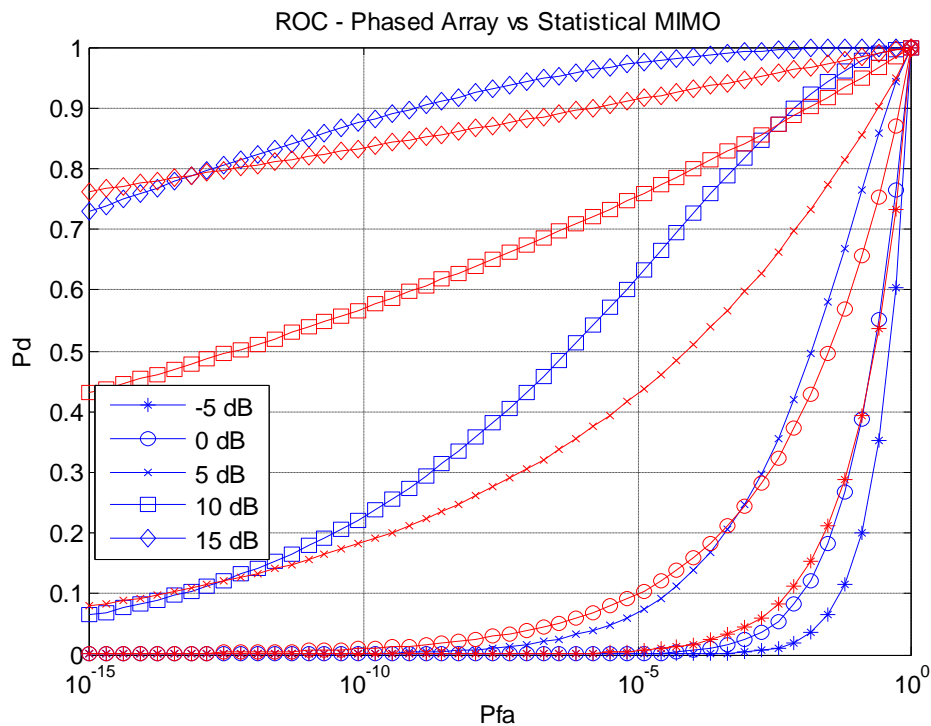


Figure 4-8 ROC of Statistical MIMO and Phased Array Radar, $M_t=2$, $M_r=2$

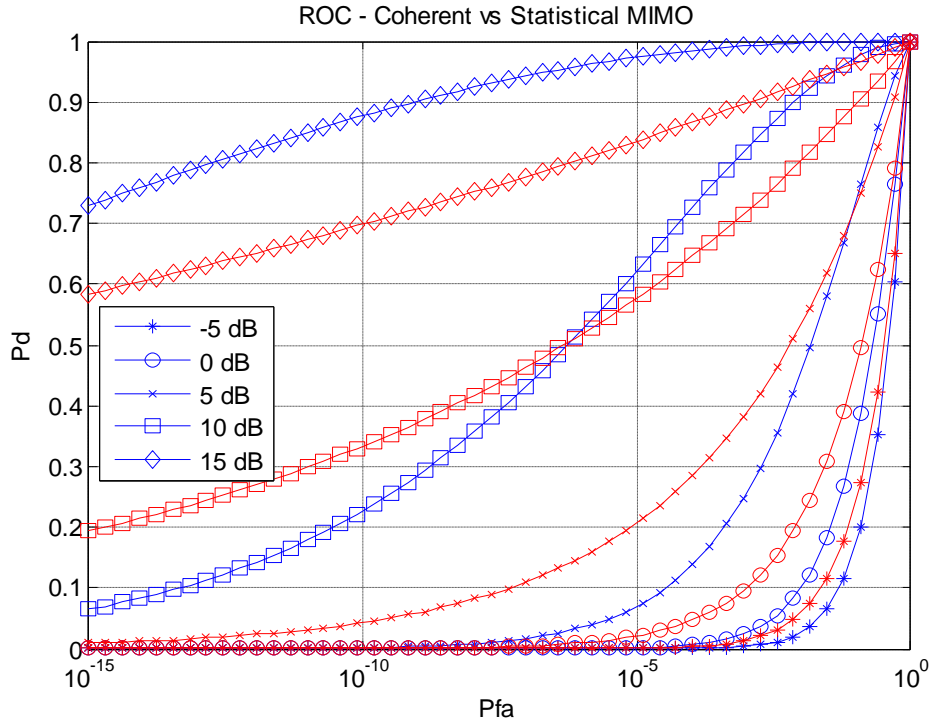


Figure 4-9 ROC of Statistical MIMO and Coherent MIMO Radar, $M_t=2$, $M_r=2$

4.3 Detection in STC MIMO Radar

In this section, simulations are performed to explore performance of detectors developed in Section 3. 2. To see the detection performance, P_{fa} value is set to 10^{-2} , and then Monte Carlo simulations are run 10^4 times for the target absent case and 10^3 times for the target present case.

In the simulations throughout this section, the code matrix is generated from Hadamard codes.

In order to be able to compare different MIMO radar configurations fairly, the transmitted signals are scaled so that the total transmitted energy does not change with the number of transmit elements. This is done by equating the norm of \mathbf{A} to 1 by dividing every \mathbf{A} by its Frobenious norm.

The simulations are conducted for the distribution of the noise at the receiver is equal to

$$w_k(j) \sim CN(0, \sigma_w^2) \quad j = 1, \dots, N \quad (4-1)$$

and the noise is assumed to be temporarily white besides being spatially white.

During simulations, the coefficients that represent RCS values whose values are estimated are also modeled as independent Gaussian random variables with distribution

$$\alpha_{k,m} \sim CN(0, 1) \quad k = 1, \dots, M_r, m = 1, \dots, M_t \quad (4-2)$$

The received signal is also scaled so that the total received signal increases directly proportional to N . The resultant signal model for the received signal can be written as

$$\mathbf{y}_k = \sqrt{NE_t} \mathbf{A} \boldsymbol{\alpha}_k + \mathbf{w}_k \quad (4-3)$$

As a result the SNR definition in this section is different from the definitions in previous sections and can be written as

$$SNR = \frac{NE_t}{\sigma_w^2} \quad (4-4)$$

4.3.1 Simulations for Stationary Target

4.3.1.1 MISO System

In this section the detection performance of MISO system with changing N and M_t values are investigated.

4.3.1.1.1 $N \geq M_t$ Case

In the first simulation the detector given in (3-35) is used. The length of the transmitted pulse sequence is held constant at 12 and the number of transmit antennas is increased. The resulting P_d vs SNR curve is given in Figure 4-10.

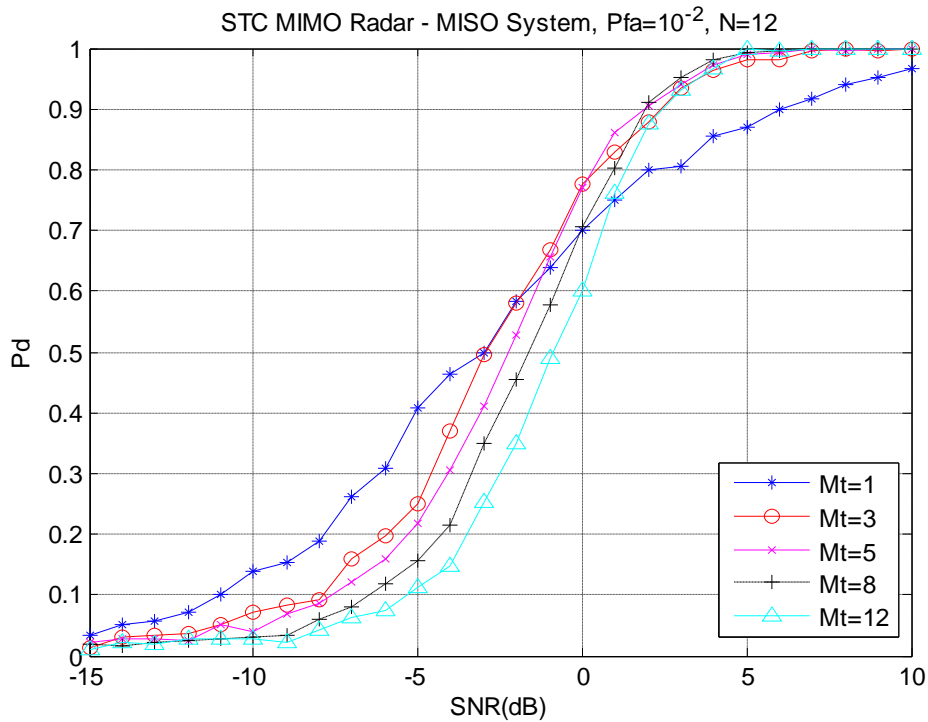


Figure 4-10 MISO Case, Full Rank, Changing M_t , Detector (3-35)

In our signal model received power is directly proportional to the number of pulses in a code word, not the number of transmitters. So when the number of pulses sent by a transmitter is constant the power of the received signal is constant. But as can be seen from the Figure 4-10, the detection performance decreases as the number of transmit antennas increases although the total noise power is constant. This is similar to the case given in Figure 4-6 for statistical MIMO radar.

The simulation is also carried out for a conventional single input single output radar system, which uses the same number of pulses as other MISO systems, with the same detector. Although the performance of the SISO system is better at low SNR values, MISO system outperforms the conventional system at high SNR and P_d values. This is due to the fact that the number of transmitters increases the angular diversity of the system and smoothes RCS fluctuations at high P_d values.

4.3.1.1.2 $N \leq M_t$ Case

In the second simulation, the detector in (3-47) is used. The length of the transmitted pulse sequence is held constant at 8 and the number of transmit antennas is increased. The resulting P_d vs SNR curve is given in Figure 4-11.

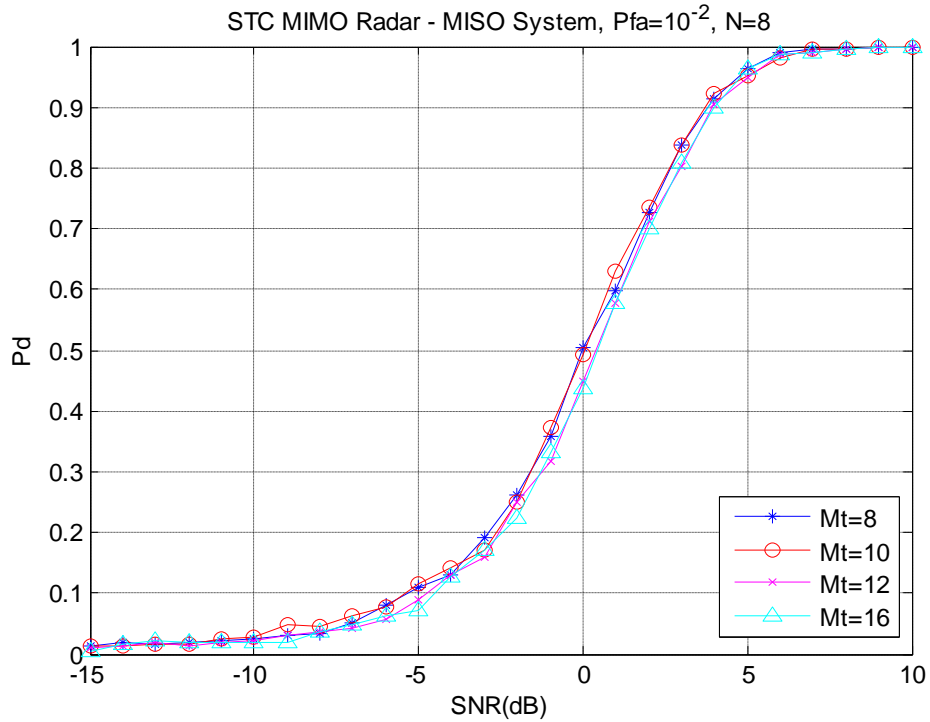


Figure 4-11 MISO Case, Full Rank, Changing M_t , Detector (3-47)

To increase the number of transmitters without increasing the number of linearly independent columns does not affect the detection probability as can be seen from Figure 4-11.

Another simulation is performed to see the effect of increasing M_t . But in this case, the number of transmitted pulses is kept equal to M_t . The detector in (3-47) is used in this simulation. Note that the detectors given in (3-47) and (3-35) are equivalent when $M_t = N$. The results are given in Figure 4-12.

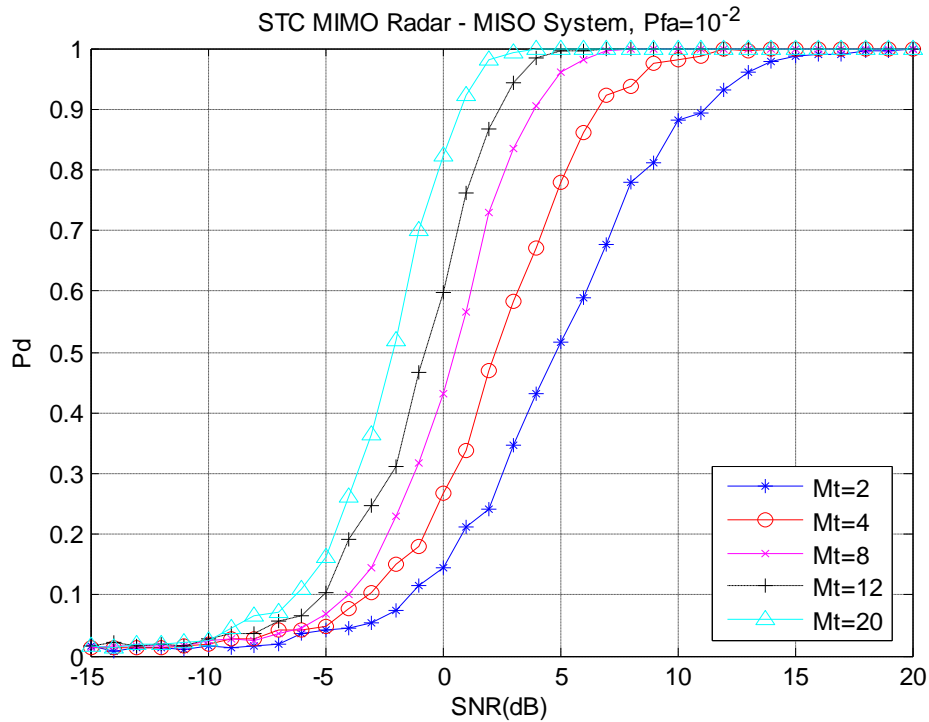


Figure 4-12 MISO Case, Full Rank, Changing N , $N=M_t$

As the transmitted power is increased as the number of pulses increases in our signal model, the detection performance is increased with increasing M_t .

The same simulation is performed again by modifying the transmitted signal model. In this case, the total transmitted power is held constant even when the total number of pulses is increased. The resulting graphics is given in Figure 4-13. The detection performance worsens as M_t increases since the signal power per pulse in the received signal is decreased in this case while the total transmit power remains constant. But again at high detection probabilities systems with more transmit antennas outperforms the systems with less antennas.

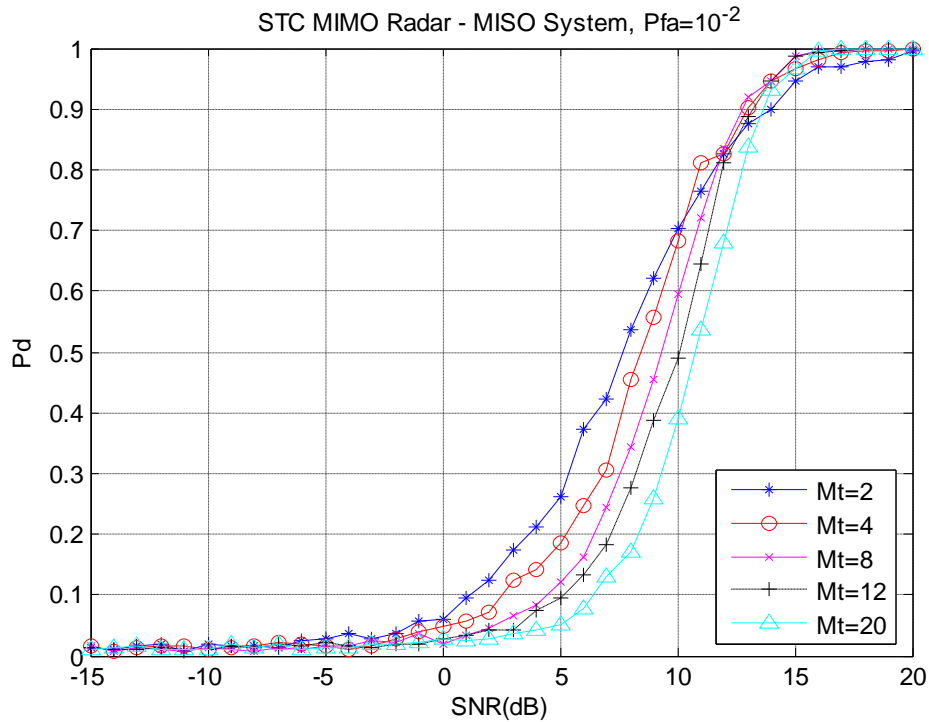


Figure 4-13 MISO Case, Full Rank, Transmit Power is Constant, Changing N , $N=M_t$

4.3.1.2 MIMO System

In this section the detection performance of MIMO system with changing N and M_r values are investigated.

4.3.1.2.1 $N \geq M_t$ Case

The simulation in Section 4.3.1.1.1 is repeated in this part by changing the number of receive antennas while keeping number of transmit antennas and the number of transmitted pulses constant. The simulation results are given Figure 4-14.

Although the number of transmitted signals and the total transmitted power is the same in every situation, the detection performance increases as the number of receive antennas increases since the total received energy is increased.

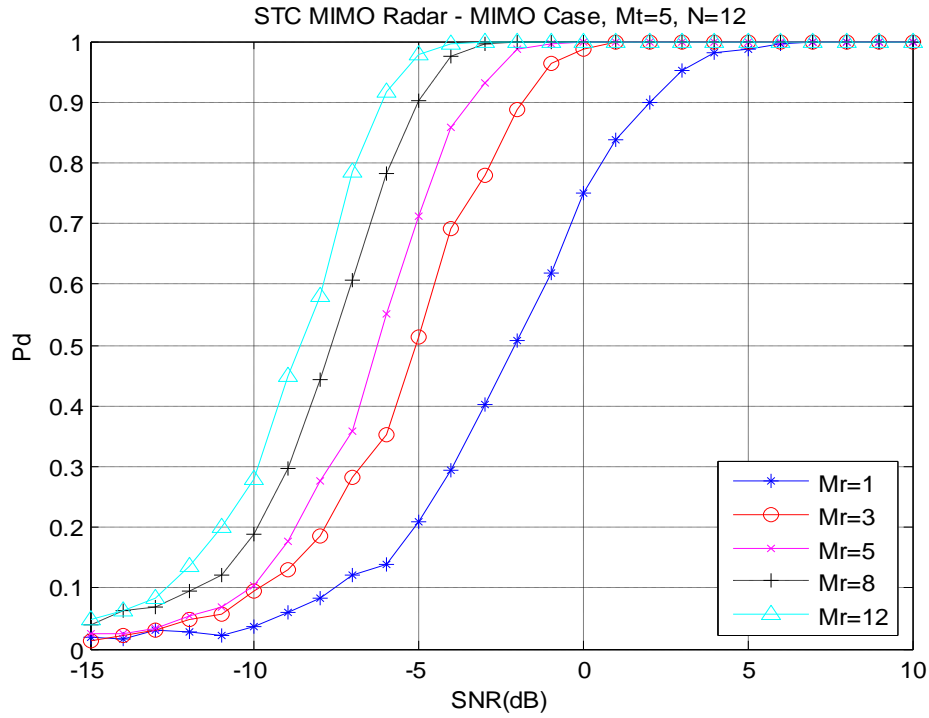


Figure 4-14 MIMO Case, Full Rank, Changing M_r , Detector (3-35)

Note that in the above figure the case when $M_r = 1$ corresponds to the case when $M_t = 5$ on Figure 4-10.

The preceding simulation is repeated by the same M_t , M_r and N values but using the detector given in (3-47) in this case. The resulting P_d vs SNR curve is given in Figure 4-15. When Figure 4-14 and Figure 4-15 are compared, it is seen that the detector given in (3-47) performs worse than the detector in (3-35) when $N \geq M_t$.

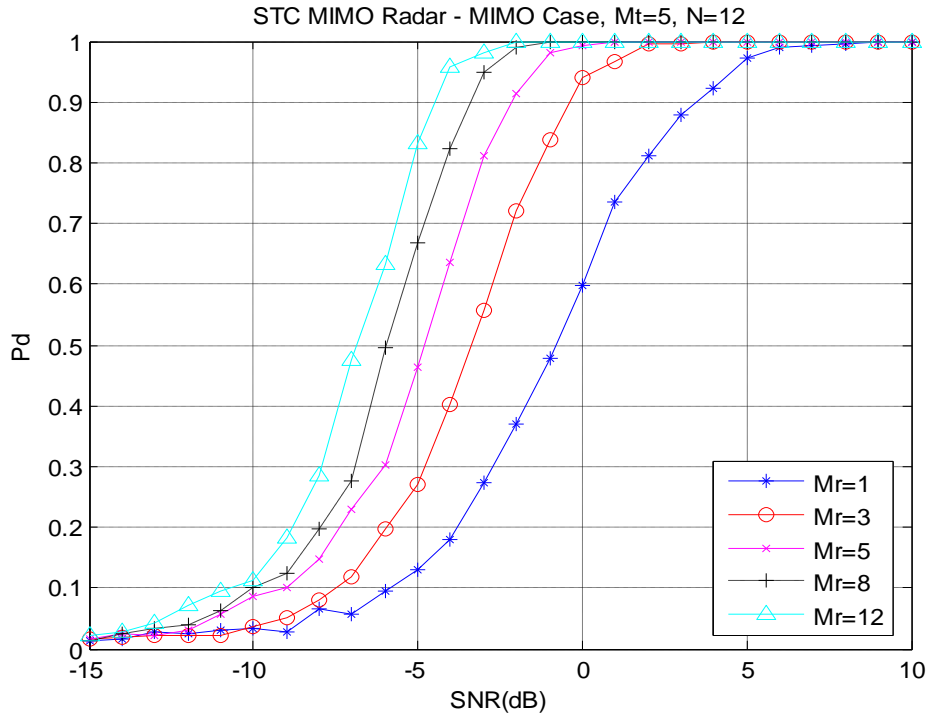


Figure 4-15 MIMO Case, $N \geq M_t$, Changing M_r , Detector (3-47)

To compare the noncoherent detector in (2-101) of statistical MIMO radar and detector in (3-35), a simulation is performed when $M_t = M_r = 2$ and $N = 4$ and P_d vs SNR curves are obtained at different P_{fa} values. The resulting graphics is presented in Figure 4-16. The detection performance of STC MIMO detector seems better, because the transmitted power increases as the number of pulses increases in STC MIMO radar although it remains constant in statistical MIMO radar signal model. So another simulation is performed by normalizing the transmitted power. The result of this simulation is given in Figure 4-17. The figure shows that there is no difference between the performances of those detectors when the interfering signal is only white Gaussian noise.

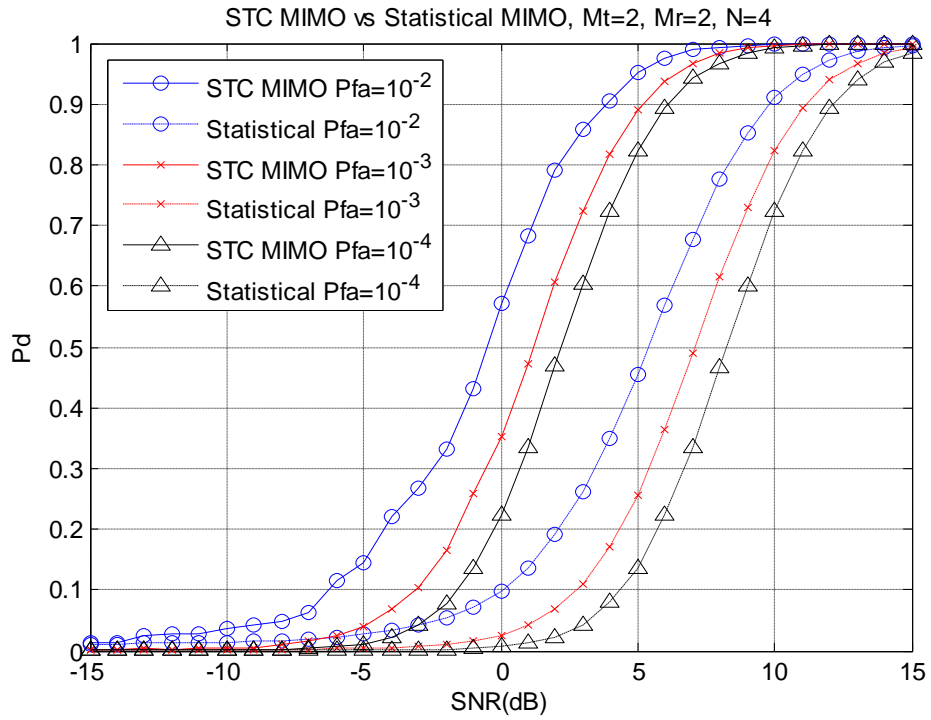


Figure 4-16 The Detector in (2-101) vs the Detector in (3-35)

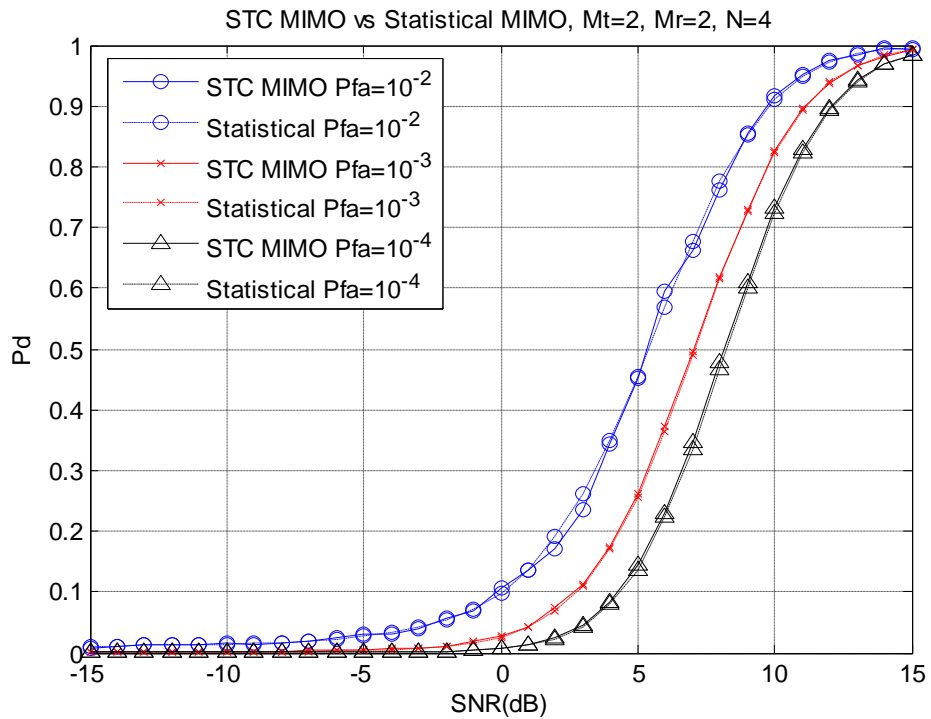


Figure 4-17 The Detector in (2-101) vs the Detector in (3-35), Normalized Power

4.3.1.2.2 $N \leq M_t$ Case

In this simulation the detector given in (3-47) is used. The length of the transmitted pulse sequence is held constant at 8, and the number of transmit antennas is held constant at 8. Then the number of receive antennas is increased. The resulting P_d vs SNR curve is given in Figure 4-18. As expected detection performance enhances as the number of receiving antennas is increased.

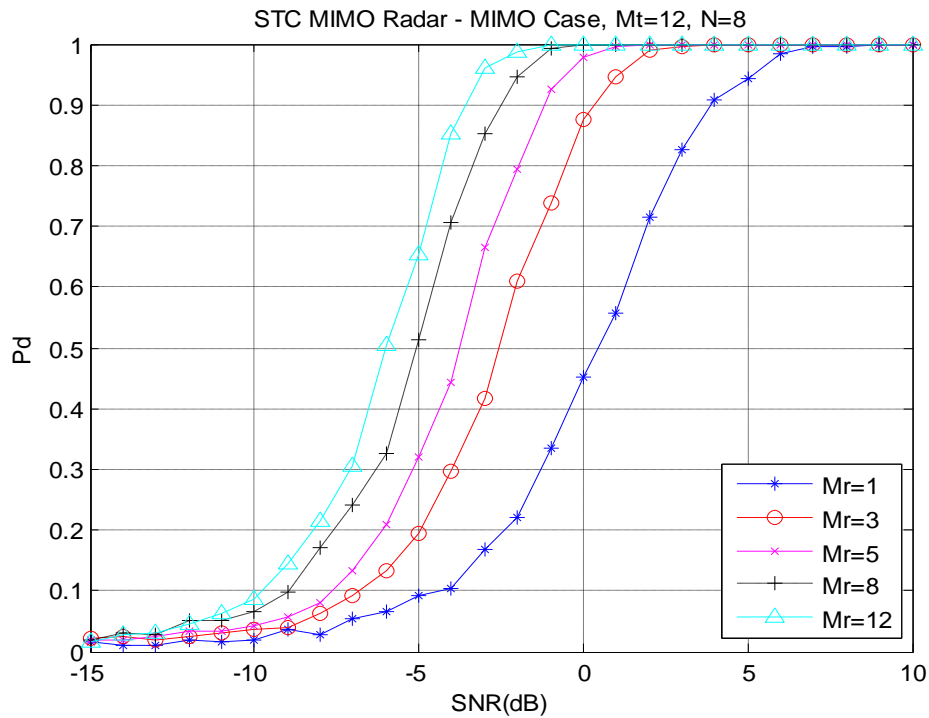


Figure 4-18 MIMO Case, Full Rank, Changing M_r , Detector (3-47)

To compare the noncoherent detector in (2-101) of statistical MIMO radar and detector in (3-47), again a simulation is performed when $M_t = M_r = 4$ and $N = 2$. The transmit power of STC MIMO radar system again is normalized with respect to N and P_d vs SNR curves are obtained at different P_{fa} values. The resulting graphics is given in Figure 4-19. Although the transmit power of STC MIMO system does not increase with N , it outperforms the statistical MIMO radar detector.

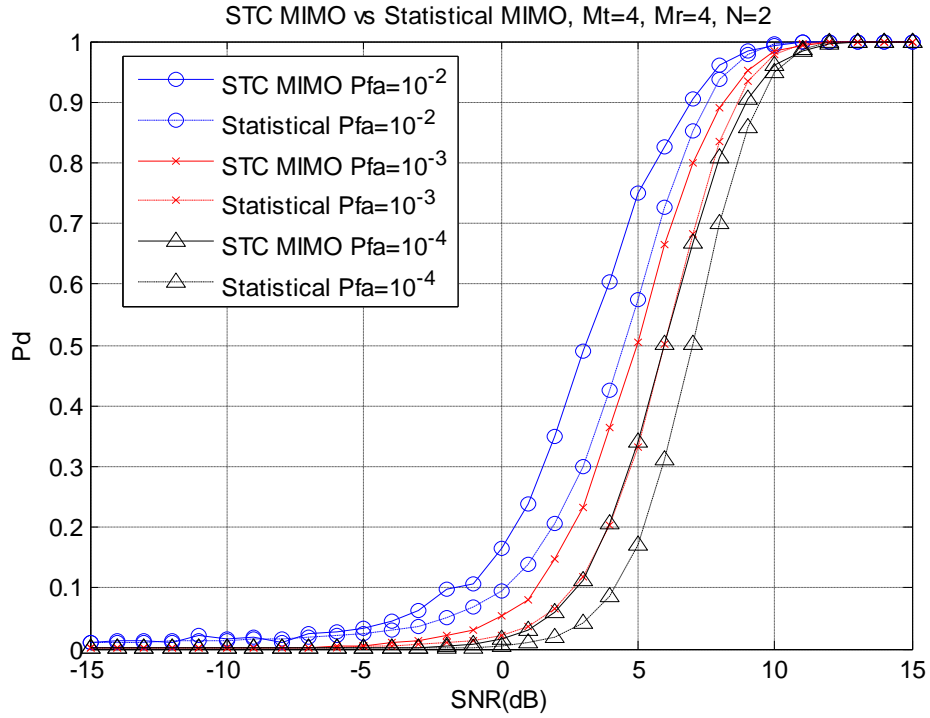


Figure 4-19 The Detector in (2-101) vs the Detector in (3-47), Normalized Power, $M_t = 4, M_r = 4, N = 2$

The same simulation is also performed for $M_t = M_r = N = 4$ again. In this case the performances of both detectors are the same as in Figure 4-20. It can be concluded here that the performance of MIMO radar can be enhanced by using both orthogonal and linearly dependent signals together.

Lastly, in this section a simulation is performed to see the effects of coded and uncoded signal transmission on the detection. The simulation is performed for different N values when $M_t = M_r = 8$. The angular diversity is assumed to exist in the uncoded case too. The results are shown in Figure 4-21. It can be seen from the figure that the orthogonal signals enhances detection performance noticeably especially at high SNR and detection rates. It can be also seen from the figure that the detection performance of uncoded signals are poorer.

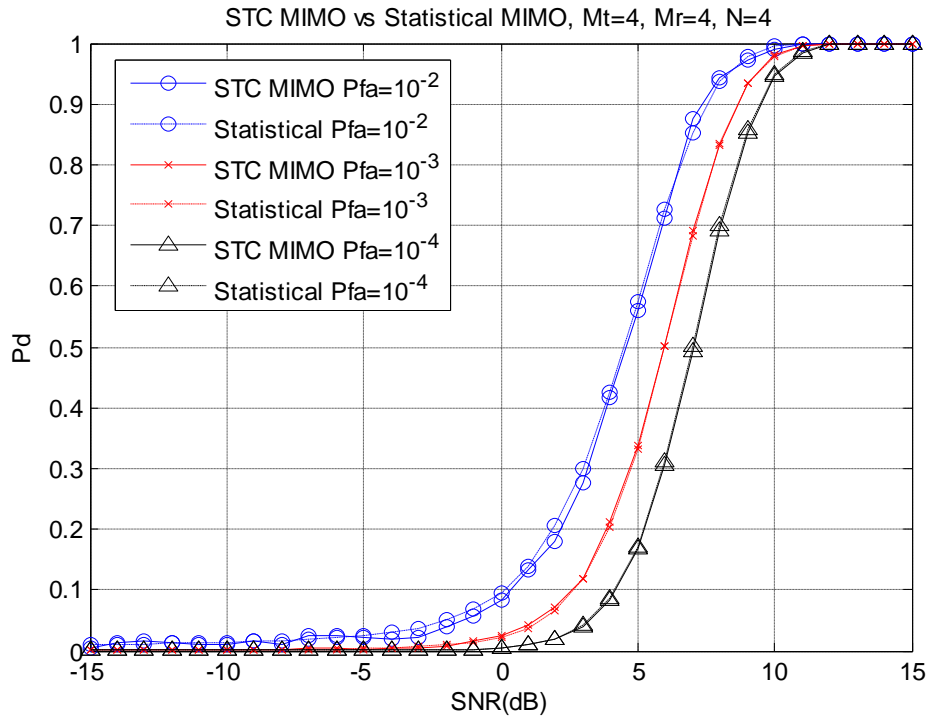


Figure 4-20 The Detector in (2-101) vs the Detector in (3-47), Normalized Power, Mt = 4, Mr = 4, N = 4

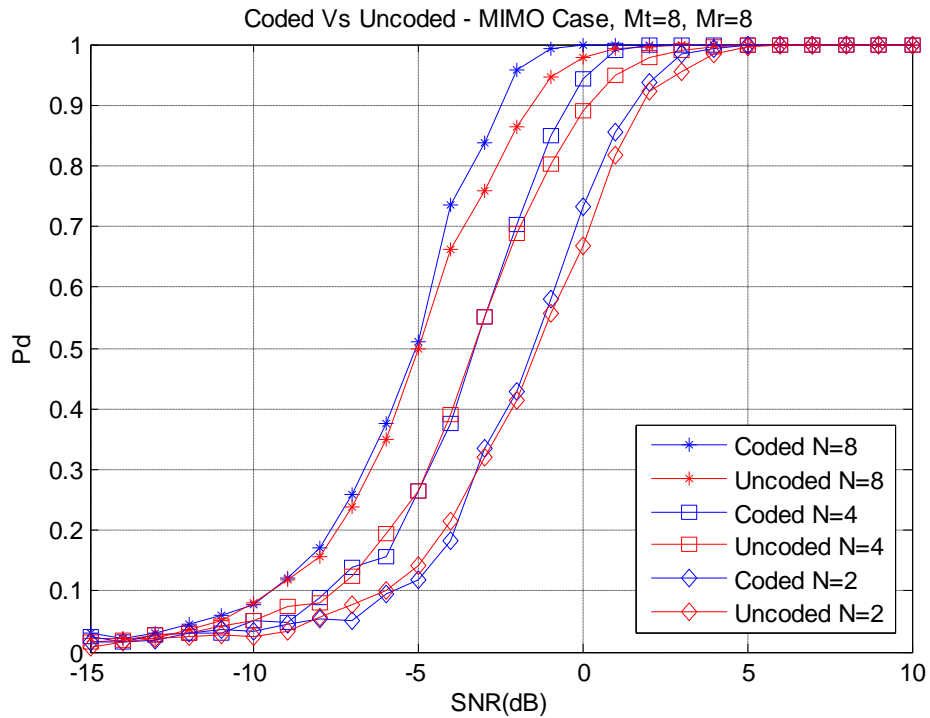


Figure 4-21 Detection Performance of Coded and Uncoded Signals

4.3.2 Simulations for Moving Target

Simulations for moving target are performed for MISO system. During the simulations it is assumed that all transmit receive pairs experience the same Doppler shift.

Firstly, the effect of changing N on the detection performance, when transmitted power is normalized, is investigated. The resulting graphics is given in Figure 4-22.

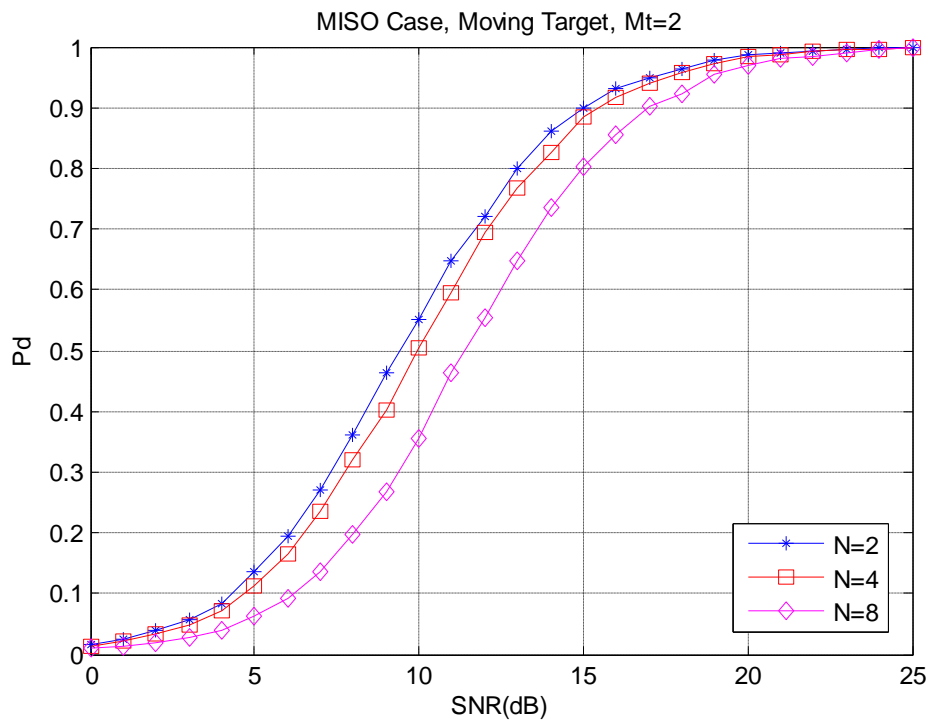


Figure 4-22 Moving Target, Changing N , $M_t=2$

As can be seen from the graph, the detection performance degrades as the number of transmitted pulses increases.

Secondly, the detection performance of the system, while the number of transmit antennas is changing, is explored. In this case, the number of transmitted pulses is held constant at $N = 8$. The result of the simulation is given in Figure 4-23.

Generally, it can be said that the detection performance enhances as the number of transmit antennas increases. This enhancement is clearer in high detection probabilities. But this enhancement does not increase at same rate and becomes saturated after the number of transmit antennas approaches six.

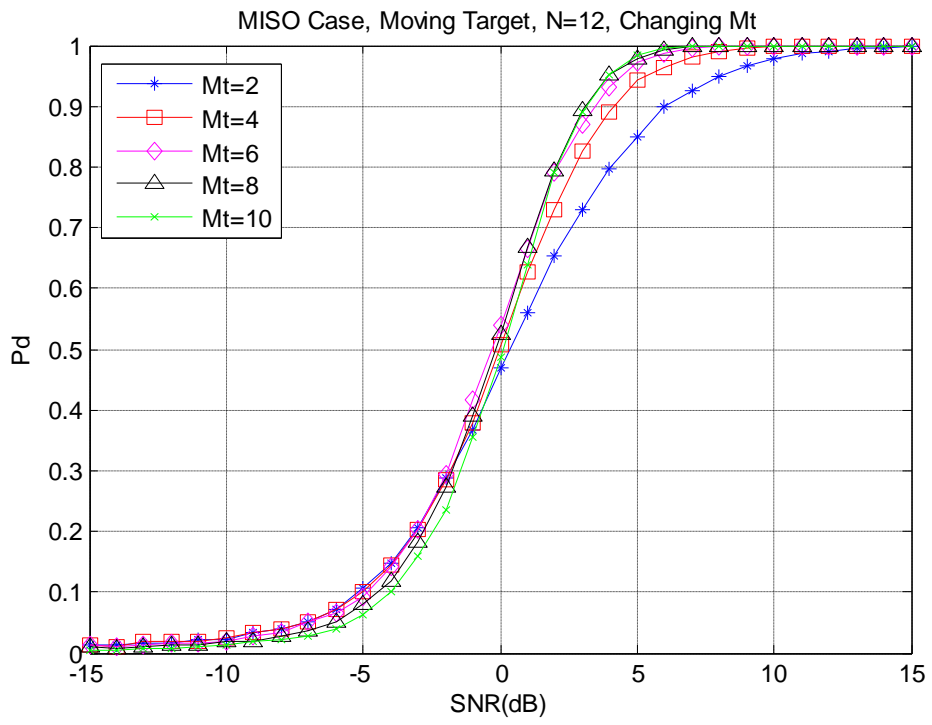


Figure 4-23 Moving Target, Changing Mt, N=8

CHAPTER 5

CONCLUSION AND FUTURE WORK

In this thesis study, an overview of MIMO radar is presented and some of the improvements that can be achieved by the use of MIMO radar systems are examined.

MIMO radar can be defined simply as a multi antenna radar system which transmits linearly independent or orthogonal waveforms. According to the separation between the transmit and receive elements MIMO radar can be classified into two categories namely, Coherent MIMO radar and Statistical MIMO radar.

Coherent MIMO radar is the replacement of phased array radar in MIMO radar world. Coherent MIMO radar have closely spaced antennas at both at the transmitter and receiver and it is assumed that every transmit receive pair sees the same RCS. The improvements achieved by coherent MIMO radar are results of waveform diversity. One of these improvements is higher angular resolution and better rejection of the jamming sources because of virtual extended array aperture. Better detection and parameter estimation performance can also be achieved by using data dependent adaptive array techniques. None of these achievements is possible in a phased array radar system since the transmitted and received signals are highly correlated in phased array radar systems. Another area that the MIMO radar performs better than phased array radar is parameter identifiability. The number of targets that can be uniquely identified by a MIMO radar is M_t times more than its phased array counterpart. It is also shown that even transmit beamforming can be possible for MIMO radar systems although the transmitted signals are orthogonal.

Statistical MIMO radar is in fact a type of multistatic radar system. Its transmit and receive antennas are widely separated ensuring that the signals coming to receivers are uncorrelated. This angular diversity is used as the source of performance improvement in MIMO radar. This angular diversity is used to increase detection probabilities at high SNR values and also to better the performance of moving target detection. It is also shown that the direction of arrival performance can be enhanced by using widely separated transmitters and closely spaced receivers. But in some sources this system is called MISO instead of MIMO. Although there is a big amount of research in the area of Statistical MIMO radar, there are still doubts to classify it as a new radar system. Some researchers state that the ideas in statistical MIMO radar is not new and the theory developed related to detection in statistical MIMO radar were originally developed in old publications related to multistatic radar systems.

In this thesis, detection performances of phased array radar, coherent MIMO radar and statistical MIMO radar were also compared. Similar studies exist in the literature that compare statistical MIMO radar and phased array radar. In this study, the detector for coherent MIMO radar is also developed and compared with other radar systems. The detection performance of phased array radar systems is better than the coherent MIMO radar's, since there is a lack of coherent processing gain in coherent MIMO radar systems. Statistical MIMO radar performs better than both phased array and coherent MIMO radar at high detection rates because angular diversity enables RCS fluctuation smoothing. But at low detection probabilities coherent MIMO radar performs better than statistical MIMO like phased array systems. So at high SNR values and mid level detection probabilities it may be better to use coherent MIMO radar and use its other advantages like transmit beamforming to reduce the effects of this disadvantage.

Another detector that includes the space time codes of the transmitted signals explicitly is also investigated in this thesis study. It is shown in the related publication that the use orthogonal codes is one of possible choices that satisfies a condition derived from Chernoff bound and is optimum with this respect. Using this detector several simulations are performed to see the performance limits of it under different scenarios.

It can be concluded that coherent MIMO radar provides performance enhancements in several fields whereas statistical MIMO provides performance enhancements in only limited number of fields. But these improvements may be very important for some applications. Using hybrid systems like phased-MIMO radar systems may overcome this gap and enables to use the best sites of different MIMO radar configurations.

For further study, different waveforms can be designed that satisfies the best detection performance under different clutter conditions. The performance of different detectors may also be investigated under diverse conditions.

REFERENCES

- [1] M. Skolnik, “*Introduction To Radar Systems*”, 3rd ed. McGraw-Hill, 2001
- [2] M.A. Richards, “*Fundamentals of Radar Signal Processing*”, McGraw-Hill, 2005
- [3] V.S. Chernyak, “*Fundamentals of Multisite Radar Systems : Multistatic Radars and Multiradar Systems*”, Gordon and Breach Science Publishers, 1998
- [4] S.M. Kay, “*Fundamentals Of Statistical Signal Processing Detection Theory*”, Prentice Hall, 1998
- [5] C.C. Cook, M. Bernfeld, “*Radar Signals: An Introduction To Theory and Application*”, Artech House, 1993
- [6] N. Levanon, E. Mozeson, “*Radar Signals*”, Wiley, 2004
- [7] T. Johnsen, K.E. Olsen, “*Bi- and Multistatic Radar*”, *Nato Documents, RTO-EN-SET-086, Jul. 2006*
- [8] IEEE Aerospace and Electronic Systems Society, *IEEE Std 686-2008 IEEE Standard Radar Definitions*, 2008
- [9] J. Li, P. Stoica, “*MIMO Radar Signal Processing*”, Wiley, 2009
- [10] E. Fishler, A. Haimovich, R. Blum, D. Chizhik, L. Cimini and R. Valenzuela, “*MIMO Radar: An Idea Whose Time Has Come*”, *Proceedings of IEEE International Conference on Radar*, pp. 71-78, Apr. 2004
- [11] D.W. Bliss and K.W. Forsythe, “*Multiple-Input Multiple-Output (MIMO) Radar and Imaging: Degrees of Freedom and Resolution*”
- [12] J. Li and P. Stoica , “*MIMO Radar – Diversity Means Superiority*”, *Proceedings of the 14th Annular Workshop on Adaptive Sensor Array Processing, MIT Lincoln Laboratory, Lexington, MA, Jun. 2006*
- [13] B. Liu, Z. He, J. Zeng and B. Liu, “*Polyphase Orthogonal Code Design for MIMO Radar Systems*,
- [14] H. Deng, “*Polyphase Code Design For Orthogonal Netted Radar Systems*”, *IEEE Transactions on Signal Processing*, vol. 52, pp. 3126-3135, Nov. 2004

- [15] J. Li, P. Stoica, L. Xu and W. Roberts, "On Parameter Identifiability Of MIMO Radar", *IEEE Signal Processing Letters*, vol. 14, no. 12, pp. 968-971, Dec. 2007
- [16] J. Li and P. Stoica, "MIMO Radar With Colocated Antennas", *IEEE Signal Processing Magazine*, vol. 24, no. 5, pp. 106-114, Sep. 2007
- [17] P. Stoica and J. Li, "On Probing Signal Design For MIMO Radar", *IEEE Transactions on Signal Processing*, vol. 55, no. 8, pp. 4151-4161, Aug. 2007
- [18] D.R. Fuhrman and G.S. Antonio, "Transmit Beamforming For MIMO Radar Systems Using Partial Signal Correlation", *Proc. 38th Asilomar Conf. Signals, Syst. Comput.*, vol. 1, pp. 295-299, Nov.2004
- [19] D.R. Fuhrman and G.S. Antonio, "Transmit Beamforming For MIMO Radar Systems Using Signal Cross-Correlation", *IEEE Transactions on Aerospace Electronic Systems*,
- [20] F.C. Robey, S. Coutts, D. Weikle, J.C. McHarg, K. Cuomo, "MIMO Radar Theory And Experimental Results", *Proceedings of the 38th Asilomar Conference on Signals, Systems and Computers*, vol. 1, pp. 300-304, Nov.2004
- [21] I. Bekkerman and J. Tabrikian, "Target Detection and Localization Using MIMO Radars and Sonars", *IEEE Transactions on Signal Processing*, vol. 54, no. 10, pp. 3873-3883, Oct. 2006
- [22] L. Xu, J. Li, P. Stoica, "Radar Imaging via Adaptive MIMO Techniques", *Proceedings of 14th European Signal Processing Conference*, Sep. 2006
- [23] N.H. Lehman, E. Fishler, A.M. Haimovich, R.S. Blum, D. Chizhik, L.J. Cimini, R. Valenzuela, "Evaluation Of Transmit Diversity In MIMO-Radar Direction Finding", *IEEE Transactions On Signal Processing*, vol. 55, no. 5, pp. 2215-2225, May 2007
- [24] E. Fishler, A. Haimovich, R. Blum, L. Cimini, D. Chizhik and R. Valenzuela, "Performance of MIMO Radar Systems: Advantages of Angular Diversity", *Proceedings of 38th Asilomar Conference on Signals, Systems and Computers*, vol. 1, no .xx, pp. 305-309, Nov. 2004
- [25] E. Fishler, A. Haimovich, R. Blum, L. J. Cimini, D. Chizhik and R. Valenzuela, "Spatial Diversity in Radars – Models and Detection Performance", *IEEE Transactions on Signal Processing*, vol. 54, no. 3, pp. 823-838, Mar. 2006
- [26] A. M. Haimovich, R. S. Blum and L. J. Cimini, "MIMO Radar with Widely Separated Antennas", *IEEE Signal Processing Magazine*, vol. 25, no. 1, pp. 116-129, Jan. 2008

- [27] A.Hassanien and S. Vorobyov, “*Phased-MIMO Radar: A Tradeoff Between Phased-Array and MIMO Radars*”, *IEEE Transactions on Signal Processing*, vol. 58, no. 6, pp. 3137-3151, Jun. 2010
- [28] A. De Maio and M. Lops, “*Design Principles Of MIMO Radar Detectors*”, *IEEE Transactions on Aerospace and Electronic Systems*, vol. 43, no. 3, pp. 886-898, Jul. 2007
- [29] V. Chernyak, “*On the Concept of MIMO Radar*”, *IEEE Radar Conference 2010*
- [30] “*Chernoff Bound*”, http://en.wikipedia.org/wiki/Chernoff_bound
- [31] A.Yazici, A. C. Hamurcu and B. Baykal, “*A Practical Point of View: Performance of Neyman-Pearson Detector for MIMO Radar in K-Distributed Clutter*”, *Proceedings of IEEE/SP 15th Workshop on Statistical Signal Processing*, pp. 273-276, 2009
- [32] C. Y. Chong, F. Pascal, J.P. Ovarlez, M. Lesturgie, “*MIMO Radar Detection in Non-Gaussian and Heterogeneous Clutter*”, *IEEE Journal of Selected Topics in Signal Processing*, vol.4, no.1, pp. 115-126, Feb. 2010
- [33] G. Cui, L. Kong, X. Yang, J. Yang, “*Two-Step GLRT Design of MIMO Radar in Compound-Gaussian Clutter*”, *IEEE Radar Conference 2010*